UNIVERSITÀ CATTOLICA DEL SACRO CUORE
Sede di Piacenza

Scuola di Dottorato per il Sistema Agro-alimentare

Doctoral School on the Agro-Food System

cycle XXVIII

S.S.D: AGR/12

Studies on inoculum dynamics of *Guignardia bidwellii*, causal agent of grape black-rot

Candidate: Giovanni Onesti
Matr. n°: 4110926

Academic Year 2014/2015

UNIVERSITÀ
CATTOLICA
del Sacro Cuore

Scuola di Dottorato per il Sistema Agro-alimentare

Doctoral School on the Agro-Food System

cycle XXVIII

S.S.D: AGR/12

Studies on inoculum dynamics of *Guignardia bidwellii*, causal agent of grape black-rot

Coordinator: Ch.mo Prof. Antonio Albanese

Candidate: Giovanni Onesti
Matriculation n.: 4110926

tutor: Prof. Vittorio Rossi

Academic Year 2014/2015

Content Index

Chapter 1

Chapter 1

INTRODUCTION

Grapevine is affected all over the word by several diseases caused by fungi that can result in substantial losses of production and vine quality (Ramsdell and Milholland, 1988). Downy and powdery mildews, grey mould, and Phomopsis cane and leaf spot are the most important diseases in several grape-growing areas (Ramsdell and Milholland, 1988). Black-rot is also economically important in some viticultural areas with mild and moist conditions in spring and early summer, where it can cause yield loses up to 80% and reduce wine quality (Ellis *et al.*, 1986; Ferrin and Ramsdell, 1977, 1978; Funt *et al.*, 1990; Ramsdell and Milholland, 1988; Scribner, 1886; Magarey *et al.*, 1993).

The pathogen

Taxonomy

Black-rot is caused by the ascomycete *Guignardia bidwellii* (Ellis) Viala and Ravaz (anamorph: *Phyllosticta ampleicida* (Englem.)). Viala and Ravaz (1892) introduced *Guignardia* as a replacement name for *Laestadia* Auersw, which was a later homonym of *Laestadia* Kunth ex Lessing. Viala and Ravaz applied the new name to *Sphaeria bidwellii* (≡ *G. bidwellii*) only, not to *L. alnea*, the type species of *Laestadia* Auersw (Bissett, 1986). Later, Petrak (1957) concluded that *G. bidwellii* and related species could be accommodated in the genus *Botryosphaeria*, and Barr (1970, 1972) classified *Guignardia* and *Phyllosticta* as *Botryosphaeria*.

Recently, Schoch *et al.* (2006) have considered, based on molecular analyses, that *Phyllosticta* and *Guignardia* belongs to the Botryosphaeriales. Crous *et al.* (2006) and Liu *et al.* (2012) also classified them in the Botryosphaeriaceae family. Wikee *et al.* (2013) performed a phylogenetic study combining molecular and morphological data of 160 *Phyllosticta* strains and considered that they should belong to the Phyllostictaceae family. In the Mycobank (accessed in October 2015, www.mycobank.org), *G. bidwellii* is currently classified as follows: kingdom Fungi, division Ascomycota, sub-division Pezizomycotina, class Dothideomycetes, order Botryosphaeriales, family Botryosphaeriaceae. Currently, there are 344 epithets listed under *Guignardia* in Index Fungorum (accessed in October 2015, www.indexfungorum.org).

The genus *Phyllosticta*, introduced by Persoon (1818), is mostly composed by pathogens of a broad range of hosts and is responsible for numerous diseases including leaf and fruit spots (Wikee *et al.*, 2013). *Phyllosticta* asexual states have been mainly linked to *Guignardia* species via cultural studies or observation of co-occurrence of both states in close proximity on the host (Van der Aa, 1973; Van der Aa and Vanev, 2002; Motohashi *et al.*, 2009). Another, *Leptodothiorella* is also known as the asexual state of

some *Phyllosticta* species (Wulandari *et al.*, 2009; Su and Cai, 2012; Zhang *et al.*, 2013). The principal characteristic of *Phyllosticta* species is the production of pycnidia containing aseptate, hyaline conidia that are usually covered by a mucoid layer and bearing a single apical appendage (Van der Aa, 1973). *Phyllosticta* was first monographed by Van der Aa (1973), who described and illustrated 46 species. After that, Van der Aa and Vanev (2002) revised all species names described in *Phyllosticta*, and provided a list of 190 accepted epithets.

According to the Amsterdam Declaration on fungal nomenclature (Hawksworth *et al.*, 2011) and the new International Code of Nomenclature for algae, fungi and plants (Melbourne Code, McNeill *et al.*, 2011), a single-name nomenclatural system is being adopted for all fungi. In the case of the causal agent of black-rot, the oldest name, *Phyllosticta ampelicida*, was chosen instead of that of *Guignardia bidwellii* (Glienke *et al.*, 2011; Sultan *et al.*, 2011; Wikee *et al.*, 2011, 2013; Wong *et al.*, 2012). However, several authors in the last years continued to name the pathogen as *G. bidwellii* (Rex *et al.*, 2011; Sosnowski *et al.*, 2012; Wicht *et al.*, 2012; Molitor *et al.*, 2012; Miessner *et al.*, 2011; Hoffman *et al.*, 2002; Northover, 2008; Northover and Travis, 1998). In this Thesis, the pathogen is called *Guignardia bidwellii*, because of the relevance of the sexual stage into the fungus life cycle (Hewitt and Pearson, 1988; Emele *et al.*, 1999; Ullrich *et al.*, 2009; Gessler and Jermini, 2009). Moreover, *G. bidwellii* have been the prevalent name in the literature published from 2000 to 2015: 13 papers were indexed in the Web of Science containing the name *Guignardia bidwellii* in the title, versus only 6 containing *Phyllostica ampelicida*. In the same period, two PhD Thesis used the name *G. bidwellii* (Northover, 2008; Molitor, 2009).

Biological characteristics

G. bidwellii forms two main spore types: ascospores from ascocarps and conidia from pycnidia. Spermatia and pycnosclerotia are also produced by *G. bidwellii*. The fruiting bodies for ascospore production (ascocarps), have been referred as either pseudothecia (Northover, 2008; Hoffman *et al.*, 2004; Ullrich *et al.*, 2009) or perithecia (Janex-Favre *et al.*, 1996; Luttrell, 1946; Jailloux, 1992; Crous *et al.*, 2006; Ellis, 2008; Kong, 2012). Luttrel (1981) pointed out the difficulties of distinguishing the wall of stromal tissue in a small, globoid pseudothecium from the wall formed by the peridium in a simple perithecium. The term perithecia is used in this Thesis. Perithecia of *G. bidwellii* are rounded, ranging from 61-199 μm in diameter, black, separate, with a flat or papillate ostiole at the apex. Perithecia formation on berries surfaces starts with the differentiation of a conical carpocentrum in the centre of a stromatic primordial structure. The carpocentral cells are arranged in palisadic, parallel rows and later, in the lower part of these, ascogonial cells differentiate. When the ascogonial apparatus is completely developed comprises several curved ascogonial filaments. From the lower part, where are

located fertile cells, take place the formation of numerous asci form in the ascal locule. Finally, at the time of maturity, asci produce ascospores (Janex-Favre *et al.*, 1996). Ascospores are produced within bitunicate asci (Ramsdell and Milholland, 1988; Janex-Favre *et al.*, 1996). *G. bidwellii* perithecia lack paraphyses. Ascospores are unicellular, hyaline, oblong, and rounded at the ends, 10.6 to 18.4 µm in length and 4.8-9.0 µm width, with hyaline mucilaginous apical caps (Northover, 2008)(Figure 1B). The production of ascomata *in vitro* (Jailloux, 1992) has demonstrated the homothallism of *G. bidwellii*.

Pycnidia are rounded, ranging from 59 to 196 µm in diameter, appearing black, solitary, erumpent, and with an ostiole at the apex (Ramsdell and Milholland, 1988; Janex-Favre *et al.*, 1993). Pycnidia formation starts when cell multiply within the superficial myceliar layer. Division of the cells form a surrounding stroma and structural character of the pycnidia primordium become evident (Figure 1D). From the cells of pycnidial cavity start the formation of the radiating future conidiogenous filaments and from the tips of these the production of conidia take place by a septum division; it begins while the cavity is still closed (Janex-Favre *et al.*, 1993). Conidia are 7.1 to 14.6 µm length and 5.3 to 9.3 µm width, and are surrounded by a mucilaginous sheath which extends 5 to 8 µm from the apical end, to form a solitary appendage of 5 to 8 µm (Kuo and Hoch, 1995; Sivanesan and Holliday, 1981). The function of the appendage is unknown; it may be involved in the spore attachment to a substrate (Kuo and Hoch, 1996). A scar is located at the proximal end of the spore at the former point of attachment to the conidiogenous cell (Kuo and Hoch, 1995)(Figure 1A).

Spermatia form in spermogonia. They are bacilliform-shaped and measure 5.9 × 1.7 µm (Ullrich *et al.*, 2009). The development of the spermogonium does not differ from that of the pycnidium, at least in the early stages (Reddick, 1911). The spermogonium is often developed in a stroma together with the pycnidium, separated only by a thin membranous wall. Scribner and Viala (Scribner and Viala, 1888) indicated that the development rate of the spermogonium is slower than that of the pycnidium, so spermatia are commonly found later in the season (Ullrich *et al.*, 2009). The function of spermatia is still unknown (Ullrich *et al.*, 2009): some authors have hypothesized that they act as sex cells (Alexopoulos *et al.*, 1996; Reddick, 1911), but there is no evidence supporting this hypothesis.

Pycnosclerotia form conidia after a long period of incubation and probably serve as survival structure during winter (Reddick, 1911; Caltrider, 1961).

In vitro, *G. bidwellii* forms colonies of greenish mycelium surrounded by a band of white mycelium (Kong, 2012). *G. bidwellii* hyphae are hyaline, 2 to 6 µm wide, varicose, and contain numerous buds from which ramifications originate (Kong, 2012). Mycelium growth rate ranges 1 to 2 mm per day and appears speckled and irregular (Figure 1C). Under natural conditions, the mycelium is hyaline with granular content, frequently septate, very irregular in diameter and producing gnarled lateral branches (Reddick,

1911). The mycelium has both intercellular and intracellular growth, and it doesn't form haustoria (Reddick, 1911). Old mycelium becomes brownish in color. The mycelium forming fruiting bodies turns yellow, then brown and later becomes very dark (Reddick, 1911).

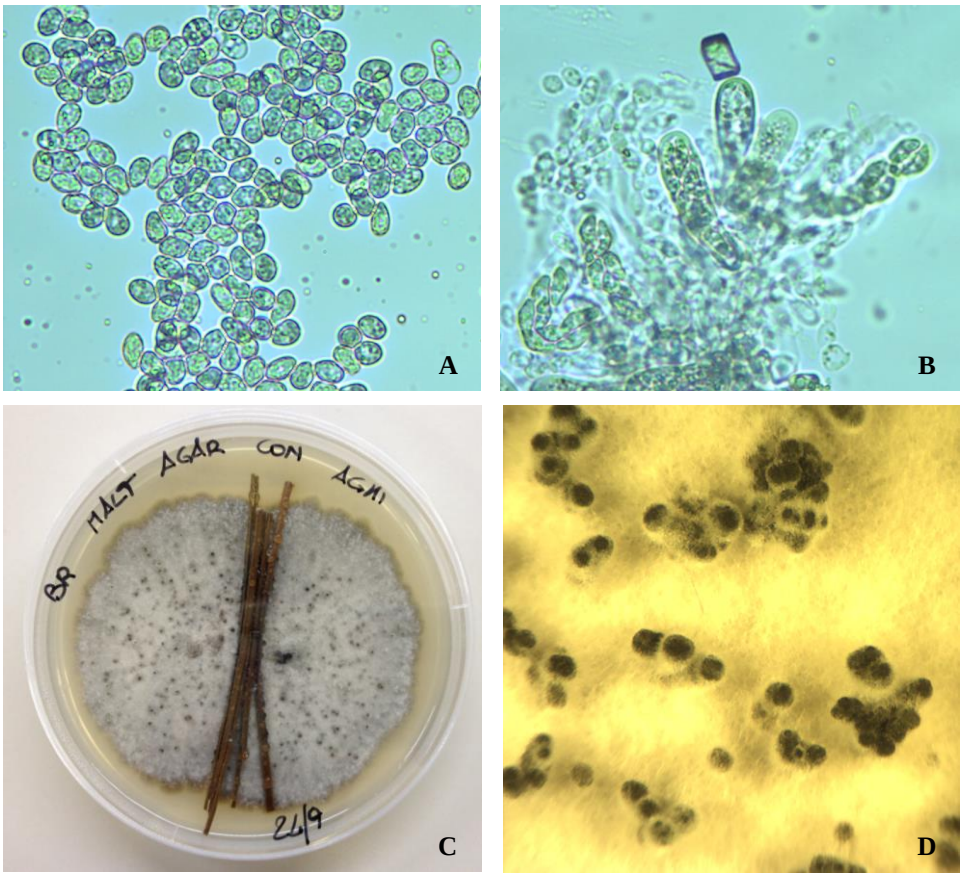

Figure 1. A, conidia of *Guignardia bidwellii* (×200 magnification); **B**, ascocarps and ascospores deriving from perithecia developed on rotted berries in the vineyard (×200 magnification); **C**, 21 days-old colonies bearing pycnidia developed on malt extract agar (MEA) with sterile pine needles incubated at 25°C and 12-h photoperiod; **D**, detail of pycnidia developed on MEA.

Origins and geographical distribution.

Guignardia bidwellii probably originated in the wild grapes from which became established at colonial times in the vineyards of the eastern United States (Andersen, 1956). Then, the fungus has been spread all over the word (Reddick, 1911; Ramsdell and Milholland, 1988); actually is possible to see the world wide spread of black-rot from the Plantwise web page (accessed in October 2015, www.plantwise.org). In Europe, it was firstly detected in France in 1885 due to the import of infected American filloxera-resistant rootstock material at the end of the 19th century (Scribner, 1886; Jermini and Gessler, 1996; Northover, 2008; Harms *et al.*, 2005). After this first introduction, the fungus progressively spread to other grape-growing countries (Besselat and Bouchet, 1984; Mauri and Kobel, 1988). The pathogen has been reported in France (Hesler and Whetzel, 1917) Germany (Maixner and Holz, 2003), Italy (Rinaldi and Mugnai, 2012), Switzerland (Pezet and Jermini, 1989; Siegfried *et al.*, 1993), and Spain (Magrama, 2010). In Italy, *G. bidwellii* has been detected for the first time in Tuscany by Ugolino Martinelli (1891). Later, Corte (1975) detected the pathogen in the "Cinque terre" area (Liguria; north-west), Rui (1989) in the vineyards of the western Friuli Venezia Giulia (north-east). More recently, severe attacks of black-rot were signalled in Friuli Venezia Giulia by Clabassi *et al.* (2000), and in Veneto by Costacurta *et al.* (2004). The disease is considered endemic in Friuli (Bigot G., personnel communication) and Tuscany (Rinaldi and Mugnai, 2012).

Pathogenesis

Different genera in the family of Vitacee can be affected by *G. bidwellii*: *V. vinifera* (domestic grape) *V. arizonica* (Canyon grape), *V. labrusca* (American grape), and *Vitis rotundifolia* (muscadine grape) are cultivated hosts of this pathogen. The host range also includes: *Ampelopsis* (wild grape), *Cissus* (ornamental vine), *Parthenocissus quinquefolia* (Virginia creeper) and *P. tricuspidata* (Boston ivy) (Eyres *et al.*, 2006).

G. bidwellii conidia germinate readily when attached to a hydrophobic surface like that of the host plant (Kuo and Hoch, 1996). Infection of the expanding green tissue occurs through the direct penetration of the plant cuticole by melanized appressoria produced by the conidia (Kuo and Hoch, 1995). *G. bidwellii* is a hemibiotroph, which is able to overstep the resistance barriers of the host plants and remain latent inside their tissues, usually in the subcuticular anticlinal cell wall region (Ullrich *et al.*, 2009). After a period of 12 to 14 days, the host tissue is killed by the pathogen growth and the lesions appears on the leaves (Luttrell, 1946); approximately 3 to 5 days after, the pycnidia start to appear on the lesion surface and the sporulation takes place on the dead tissue (Roussel and Bouard, 1971).

The mecanisms involved in the plant resistance against black-rot infection have not been studied in deep. For leaves, the success of infection depends on the ontogenic

resistance of the host; indeed, it as been aknowledge for a long time that infection of black-rot only occours in growing leaves (Luttrell, 1946; Prunet, 1898; Reddick, 1911; Scribner and Viala, 1888). Kuo and Hoch (1996) observed that fully expanded leaves inoculated with the pathogen did not develop symptoms, whereas expanding leaves expressed the typical black-rot symptoms. Ullrich *et al.* (2009) confirmed that young leaves growing on a shoot (position 2, 3 and 4 from the tip) were susceptible to the infection and showed typical disease symptoms, whereas very young (position 1 from the shoot tip) and older leaves (position 5 and older from the tip) were not or only scarcely infected. The difference in leaf susceptibility did not relate to conidial germiantion and appressorium formation, because both took place on young and old leaves (Kuo and Hoch, 1996; Ullrich *et al.*, 2009). However, the subcuticular growth of the hyphae originated by the appressoria in mature leaves was lower and very limited compared to the growth observed in the expanding leaves (Kuo and Hoch, 1996; Ullrich *et al.*, 2009). In asymptomatic leaves, Ullrich *et al.* (2009) observed the production of *G. bidwellii* dense hyphal nets without forming haustoria or the haustoria did not penetrate or visually damaged the epidermal or mesophyll cells. A limitation of the hyphal growth in the space between the cuticle and the epidermal cells was also observed. The physiological causes for limited hyphal growth in mature tissues are not known. Ullrich *et al.* (2009) discussed that morphological active defence factors of the host tissue, like thickness of the cuticle (as in mature leaves), may affect the success of penetration.

Clusters also manifest an age-related or ontogenic resistance, which seems to act differently in different vine grape variety (Molitor *et al.*, 2012; Hoffman *et al.*, 2002; Ferrin and Ramsdell, 1977, 1978). Results from different experiments showed that berries became highly susceptible at mid-bloom (Ferrin and Ramsdell, 1977, 1978; Hoffman *et al.*, 2002) and remain susceptible until 2 to 10 weeks later, depending on the variety and the experiment, when they become resistant (Ferrin and Ramsdell, 1977, 1978; Hoffman *et al.*, 2002). Scribner and Viala (1888) indicated that berries become resistant at veraison (Ferrin and Ramsdell, 1978).

Grape berries acquire resistance to other pathogens during ripening (Salzman *et al.*, 1998) and it has been suggested that an osmotin-like protein may be involved in this resistance (Tattersall *et al.*, 1997). Salzam *et al.* (1998) established that thaumatin-like protein and chitinases, which are effective antifungal proteins against isolates of the grape berry pathogens, accumulate synchronously at stages of ripening when the fruits become resistant to black-rot.

Life cycle

An exhaustive review of the *G. bidwellii* life cycle is performed in Chapter 2 (Rossi *et al.*, 2014) of this Thesis. This revision also includes the current knowledge on the pathogen epidemiology.

Disease control

It has been for long time assumed that successful protection of vineyards against *G. bidwellii* was guaranteed by a combination of cultural practices and calendar-based application of fungicides against downy and powdery mildews, without any additional application (Harms *et al.*, 2005; Molitor and Berkelmann-Loehnertz, 2011).

Cultural practices have been proposed to reduce the canopy wetness duration in the vineyard, which include planting vines in sites with good air circulation and sun exposure, and the use of training systems allowing good air movement through the canopy and prevent the excess of shading, which also provide a better spray penetration and coverage (Harms *et al.*, 2005; Myers, 2006). Other cultural practices were recommended for reducing the primary inoculum dose; specifically, the removal of mummified clusters during winter pruning (Gadoury, 1993). Becker and Pearson (1993) observed a reduction of the cluster severity by 25 to 35% when the mummies were removed from the trellis. Emele *et al.* (1999) and Hoffman *et al.* (2004) also observed an increase of fruit infection when mummies were retained in the trellis, compared to the plots where mummies were dropped to the ground. For this reason, the burying of the infected mummies in soil has been recommended, especially in vineyards that chronically suffer from black-rot epidemics or that are being managed organically (Myers, 2006; Sosnowski *et al.*, 2012). To reduce the inoculum dose in a viticultural areas, abandoned vineyards should be eradicated or managed (Harms *et al.*, 2005; Gessler and Jermini, 2009).

Fungicide types and timings affected the treatment efficacy against black-rot (Ramsdell and Milholland, 1988; Emele *et al.*, 1998; Hoffman *et al.*, 2002). The most critical period for *G. Bidwellii* control was from 10 cm shoot length until berries are pea-sized (Ramsdell and Milholland, 1988). Emele *et al.* (1998) recommended fungicide spray at two-weeks intervals from 4 weeks pre-bloom to 8 weeks post-bloom, and observed that the first 4 weeks after bloom are the critical period for the control. Hoffmann *et al.* (2004) evaluated different strategies of fungicide applications in New York vineyards severely affected by black-rot, observing complete control of the pathogen when treatments were performed at 25 cm shoot length, immediate pre-bloom, and 2 and 4 weeks post-bloom. Gessler and Jermini (2009) affirmed that two well-timed sprays with an appropriate fungicide were sufficient to fully control the diseases on bunches and avoid yield losses. Harms *et al.* (2005) observed that fungicide applications beginning between five to seven leaves unfolded until bunch closure provided a good disease control. Gadoury (1995) recommended to protect the bunches until the natural acquisition of ontogenic resistance because that greatly reduced or prevented any late-season development of black-rot. Indeed, Ramsdell and Milholland (1988) suggested that no fungicide protection was necessary when berries accumulated more than 5% of sugar.

In organic vineyards, liquid copper formulations, or copper-sulfur compounds such as Bordeaux mixture, were used for preventing black-rot and, at the same time, suppressions powdery and downy mildews, and Phomopsis leaf and cane spot (Dufour, 2006). Copper and sulfur compounds have preventative activity and must be present on the plant surfaces before an infection period. Luttrell (1946) observed that four treatments with Bordeaux mixture, two before blooming, one after the fruit set and the last one when the fruits were at half-growth were enough for avoiding yield losses. Bigot *et al.* (2014) observed that a fungicide composed by copper hydroxide (14%) and copper oxychloride (14%), applied with a calendar-based strategy controlled black-rot by 90%.

Hoffman and Wilcox (2003) evaluated the post-infection activity of myclobutanil and azoxystrobin in an *in vitro* experiment with artificially inoculated seedlings. They observed a complete control of lesion formation when myclobutanil was applied until 6 days post-inoculation, whereas for azoxystrobin the post-infection efficacy was 60%. Harms et el. (2005) observed 77% to 98% efficacy for dithiocarbamates (mancozeb and metiram), 95% to 100% efficacy for strobilurines (azoxystrobin, kresoxim, pyraclostrobin and trifloxystrobin), and 91% to 100% for the azoles (fluquinconazol, mycobutanil, penconazol, tebuconazol).

Empirical rules and prediction models

Different methods have been developed for better scheduling fungicide applications against black-rot (Devaut, 1992; Ellis *et al.*, 1986; Maurin *et al.*, 1991; Spotts, 1977). Spotts (1977) established wetness duration-temperature guidelines for predicting infection on leaves by conidia. Ellis *et al.* (1986) programmed a microprocessor to predict black-rot infection periods based on the work of Spotts (1977), and observed a reduction in the number of fungicide treatments by using this software in Ohio, US.

Maurin *et al.* (1991) developed a forecasting model (mainly based on the results of Spotts, 1977) to protect grapevines against black-rot infections in France. The model uses data of relative humidity, rainfall and temperature to predict the black-rot risk level. The model was able to predict the periods with favorable conditions for disease development over two testing seasons.

Gadoury *et al.* (1993) developed a set of simple rules to define the criteria for black-rot infection based on (i) any amount of rain for spore dispersal and (ii) infection occurrence due to wetness duration and temperature (not specified). The program provided good control of the disease with reduction in the fungicide number by 40% in New York, US.

Smith (2009) developed an advisory system based on Spotts (1977) results and the susceptibility of vines in relation to their growth stage. The system was evaluated in Oklahoma for recommendation of preventative and curative fungicide sprays; its use reduced the number of fungicide treatments by approximately 45% on the average. Smith

(2012) further improved the system by developing a quadratic equation to calculate the number of wetness hours (as relative humidity >85%) necessary for black-rot infection as a function of the daily temperature; no validation data were indicated.

Objectives of the Thesis

In recent years, the use of decision support systems (DSS) to target fungicide sprays have started to be a commonly sustainable tool for the protection of vineyards and the environment (Rossi *et al.*, 2012). Viticulture management have seen a drop out of a calendar-based control of mildews with a consequent reduction in fungicide applications by 30 to 40% (Caffi *et al.*, 2012, 2010). This reduction in fungicide applications means that, when there is no risk of mildew infection and no fungicides were applied, vineyards are not protected against black-rot. A model for black-rot could therefore help growers to manage fungicide sprays so as to control both mildews and black-rot.

The models developed so far to predict black-rot development have some limitations; particularly, they: (i) are focused on conidial infection and disregard ascosporic ones; (ii) do not consider the presence and abundance of the inoculum over the season; (iii) do not carefully consider the inoculum dispersal; (iv) do not incorporate the variation in host susceptibility; and (v) do not provide a quantitative estimation of the infection risk. However, substantial information exists in the literature regarding the biology and epidemiology of black-rot, with potential value for modelling. The aim of this Doctoral work was: (i) perform a system analysis of the literature data regarding epidemiology and biology of *G. bidwellii* and define out the lack of knowledge (Rossi *et al.*, 2014), (ii) develop a mechanistic, weather driven model for prediction of black-rot infections based on literature data (Rossi *et al.*, 2014), (iii) validate the model against independent data (Rossi *et al.*, 2014); (iv) conduct experiments in controlled environment and in the vineyard in order to improve the model by filling the main gaps in our knowledge, specifically: the dispersal of *G. bidwellii* ascospores and conidia in relation to weather data (Chapter 4); the effect of environment on production of pycnidia and cirri, and on conidial germination (Chapter 5); and the production course of conidia as influenced by repeated washing events and dry periods (Chapter 6), Finally, how the new findings on biology and epidemiology of *G. bidwellii* rising from the present Thesis can be used to improve the model are discussed in the Conclusion (Chapter 7).

LITERATURE CITED

Aa H.A. van der, 1973. Studies in *Phyllosticta* I. Studies in Mycology 5, 1−110.

Aa, H.A. van der, Vanev, S., 2002. A revision of the species described in *Phyllosticta*. Centraalbureau voor Schimmelcultures, Utrecht, The Netherlands.

Alexopoulos, C.J., Mims, C.W., Blackwell, M., 1996. Introductory Mycology, Fourth edition. John Wiley and Sons, New York, NY, USA.

Andersen, 1956. Diseases of grapes: black-rot, in: Disease of Fruit Crops. pp. 355–364.

Barr, M.E., 1970. Some amerosporous ascomycetes on Ericaceae and Empetraceae. Mycologia 62, 377–394.

Barr, M.E., 1972. Preliminary studies on the Dothideales in temperate North America. Contributions from the University of Michigan Herbarium 9, 523–638.

Becker, C., Pearson, R., 1993. Evaluation of cultural control strategies for managing Black-rot (*Guignardia bidwellii*) of grapes. Plant Dis. 83, 1377.

Besselat, B., Bouchet, J., 1984. Black-rot: situation inquiétante dans certains vignobles. Phytoma - défense des Cultures 33–35.

Bigot, G., Freccero, A., Mugnai, L., Baleani, M., Bossio, D., Cotromino, M., Faccini, F., Reggiori, F., 2014. Airone fungicida rameico: risultati sperimentali di efficacia su Black-rot (*Phyllosticta ampelicida/Guignardia bidwellii*) della vite in Friuli Venezia Giulia e Toscana, in: ATTI Giornate Fitopatologiche - Vol 2. pp. 339–346.

Bissett, J., 1986. *Discochora yuccae* sp. nov. with *Phyllosticta* and *Leptodothiorella synanamorphs*. Canadian Journal of Botany 64, 1720–1726.

Caffi, T., Legler, S.E., Rossi, V., Bugiani, R., Cattolica, U., Pathology, P., 2012. Evaluation of a warning system for early-season control of grapevine powdery mildew. Plant Disease 96, 104–110.

Caffi, T., Rossi, V., Bugiani, R., 2010. Evaluation of a Warning System for Controlling Primary Infections of Grapevine Downy Mildew. Plant Disease 94, 709–716.

Caltrider, P., 1961. Growth and sporulation of *Guignardia bidwellii*. Phytopathology 51, 860–863.

Clabassi, I., 2000. Black-rot, nouva ampelopatia in Friuli Venezia Giulia, in: Vitenda 2000. L'agenda Del Viticultore. A. Morando, M. Morando, and D. Morando (Eds.). Calosso, pp. 58–60.

Corte, A., 1975. Il marciume nero degli acini o "Black-rot" della vite in provincia di La Spezia. Informatore Fitopatologico 8, 15–20.

Costacurta, A., Lavezzi, A., Tomasi, D., Giorgessi, G., Antoniazzi, P., 2004. Black-rot o marciume nero. In: Guida per il viticoltore, 138–140. Informtore Agrarario, Legnaro (Pd).

Crous, P.W., Slippers, B., Wingfield, M.J., Rheeder, J., Marasas, W.F.O., Alan, J.L., Alves, A., Burgess, T., Barber, P., Groenewald, J.Z., 2006. Phylogenetic lineages in

the Botryosphaeriaceae. Studies in Mycology. 55, 235–253.

Devaut, T., 1992. Contribution a la modelisation des contaminations de la vigne par *Guignardia bidwellii* (Ellis) Viala e Ravaz agent responsable du Black-rot. Section de troisiéme cycle intércoles. Montpellier: Ecole nationale superieure agronomiqe.

Dufour, R., 2006. Grapes : Organic Production, ATTRA - National Sustainable Agriculture Information Service.

Ellis, M.A., 2008. Grape black-rot. In: Agriculture and Natural Resources. HYG-3004-08. The Ohio State University, US.

Ellis, M.A., Madden, L. V, Wilson, L.L., 1986. Electronic grape black-rot predictor for scheduling fungicides with curative activity. Plant Disease 70, 938–940.

Emele, L., Wilcox, W.F., Gadoury, D., Seem, R., 1999. Retaining overwintered mummies within the trellis increases grape black-rot severity. Phytopathology 89, S23.

Emele, L., Wilcox, W.F., Gadoury, D., Seem, R., 1998. Critical period for control of black-rot of grape. Phytopathology 88, 25–26.

Eyres, N., Wood, C., Taylor, A., 2006. Black-rot - *Guignardia bidwellii*. Department of Agriculture and the State of Western Australia. Note: 167, Replaces Factsheet 6/2000.

Ferrin, D.M., Ramsdell, D.C., 1978. Influence of conidia dispersal and environment on infection of grape by *Guignardia bidwellii*. Phytopathology 68, 892-895. doi:10.1094/Phyto-68-892

Ferrin, D.M., Ramsdell, D.C., 1977. Ascospore dispersal and infection of grapes by *Guignardia bidwellii*, the causal agent of grape black-rot disease. Phytopathology 67, 1501–1505.

Funt, R., Ellis, M., Madden, L., 1990. Economic analysis of protectant and disease-forescast-based fungicide spray programs for control of apple scab and grape black-rot in Ohio. Plant Disease 74, 638–642.

Gadoury, D., 1993. Integrating management decisions for several pests in fruit production. Plant Disease 77, 299–302.

Gadoury, D.M., 1995. Controlling fungal diseases of grapevines under organic management practices. In: Organic grape and wine production symposium. pp. 35–44.

Gessler, C., Jermini, M., 2009. Working Group "Integrated Protection and Production in Viticulture". Proceedings of the Meeting at Staufen im Breisgau (Germany), in: Black-rot - Downy Mildew Control in Small Vineyards in Southern Switzerland. Duso, C., Gessler, C., Kassemeyer, H., Maixner, M., Thiéry, D., Zahavi, T. (Eds.), pp. 139–142.

Glienke, C., Pereira, O.L., Stringari, D., Fabris, J., Kava-Cordeiro, V., Galli-Terasawa, L., Cunnington, J., Shivas, R.G., Groenewald, J.Z., Crous, P.W., 2011. Endophytic

and pathogenic *Phyllosticta* species, with reference to those associated with Citrus Black Spot. Persoonia 26, 47–56. doi:10.3767/003158511X569169

Harms, M., Holz, G., Hoffmann, C., Lipps, H., Silvanus, W., 2005. Occurrence of *Guignardia bidwellii*, the causal fungus of black-rot on grapevine, in the vine growing areas of Rhineland-Palatinate, Germany. BCPC Symp. Proc. 81, 127–132.

Hawksworth, D.L., Crous, P.W., Redhead, S.A., Reynolds, D.R., Samson, R.A., *et al.*, 2011. The Amsterdam declaration on fungal nomenclature. IMA Fungus 2, 105–112.

Hesler, L.R., Whetzel, H.H., 1917. Black-rot, caused by *Guignardia bidwellii* (Ellis) Viala and Ravaz., in: Manual of Fruit Diseases. Bailey, L.H. (Ed.), New York: Macmillan, pp. 462.

Hewitt, W.B., Pearson, R.C., 1988. Compendium of Grape Diseases. Pearson, R.C. and Goheen A. (Eds.), American Phytopathological Society Press, St. Paul, MN, USA.

Hoffman, L.E., Wilcox, W.F., 2003. Factors Influencing the Efficacy of myclobutanil and azoxystrobin for control of grape black-rot. Plant Disease 87, 273–281.

Hoffman, L.E., Wilcox, W.F., Gadoury, D.M., Seem, R.C., 2002. Influence of grape berry age on susceptibility to *Guignardia bidwellii* and its Incubation period length. Phytopathology 92, 1068–76. doi:10.1094/PHYTO.2002.92.10.1068

Hoffman, L.E., Wilcox, W.F., Gadoury, D.M., Seem, R.C., Riegel, D.G., 2004. Integrated control of grape black-rot: influence of host phenology, inoculum availability, sanitation, and spray timing. Phytopathology 94, 641–50. doi:10.1094/PHYTO.2004.94.6.641

Jailloux, F., 1992. *In vitro* production of the teleomorph of *Guignardia bidwellii*, causal agent of black-rot of grapevine. Canadian Journal of Botany 70, 254–257.

Janex-Favre, M.C., Parguey-Leduc, A., Jailloux, F., 1996. The ontogeny of perithecia in *Guignardia bidwellii*. Mycological Research 100, 875–880. doi:10.1016/S0953-7562(96)80038-4

Janex-Favre, M.C., Parguey-Leduc, A., Jailloux, F., 1993. The ontogeny of pycnidia of *Guignardia bidwellii* in culture. Mycological Research 97, 1333–1339.

Jermini, M., Gessler, C., 1996. Epidemiology and control of grape black-rot in Southern Switzerland. Plant Disease 80, 322–325.

Kong, G., 2012. Diagnostic methods for blackrot of grapes - *Guignardia bidwellii*, PaDIL - Plant Biosecurity Toolbox.

Kuo, K., Hoch, H.C., 1995. Visualization of the extracellular matrix surrounding pycnidiospores, germlings, and appressoria of *Phyllosticta ampelicida*. Mycologia 87, 759–771.

Kuo, K.C., Hoch, H.C., 1996. The parasitic relationship between *Phyllosticta ampelicida* and Vitis vinifera. Mycologia 88, 626–634.

Liu, J.K., Phookamsak, R., Doilom, M., Wikee, S., Li, Y.M., Ariyawansha, H., *et al.*,

2012. Towards a natural classification of Botryosphaeriales. Fungal Diversity 57, 149–210.

Luttrell, E., 1946. Black-rot of muscadine grapes. Phytopathology 36, 905–924.

Luttrel, E.S., 1981. Ascomycete systematics. The Luttrellian concept. Springer-Verlag New York Inc., Heidelberg, Berlin.

Magarey, R.D., Coffey, B.E., Emmett, R.W., 1993. Anthracnose of grapevines, a review. Plant Protection Quarterly. 8, 106–110.

Magrama, 2010. Patógenos de plantas descritos en España. Ministerio de Medio Ambiente y Medio rural y Marino. 854 pp.

Maixner, M., Holz, B., 2003. Risks by invasive species for viticulture. Schriftenreihe des Bundesministeriums fur Verbraucherschutz. Ernahrung und Landwirtschaft 498, 154–164.

Martinelli, U., 1891. Il black-rot sulle viti presso Firenze. Nuovo Giornale Botanico Italiano 23, 604–610.

Mauri, G., Kobel, U., 1988. Black-rot – A new severe grape disease in Ticino. Schweizer Zeitschrift für Obstund Weinbau (SZOW) Wädenswil 124, 473–475.

Maurin, G., Cartolaro, P., Clerjeau, M., Benac, G., 1991. Black-rot: vers une méthode de prévisions des risques. Phytoma 433, 39–42.

Mcneill, J., Barrie, F.R., Buck, W.R., Demoulin, V., Greuter, W., Hawkasworth D.L., Herendeen, P.S., Knapp S., Marhold K., Prado, J., Prud'homme van Reine W.F., Smith G.F., Wiersema J.H., 2011. International Code of Nomenclature for algae, fungi, and plants (Melbourne Code). Eds. Koeltz Scientific Books. ISBN 978-3-87429-425-6

Miessner, S., Mann, W., Stammler, G., 2011. Short Communication *Guignardia bidwellii*, the causal agent of black-rot on grapevine has a low risk for QoI resistance. Journal of Plant Disease and Protection 118, 51–53.

Molitor, D., 2009. Untersuchungen zur Biologie und Bekämpfung der Schwarzfäule (*Guignardia bidwellii*) an Weinreben.

Molitor, D., Berkelmann-Loehnertz, B., 2011. Simulating the susceptibility of clusters to grape black-rot infections depending on their phenological development. Crop Protection 30, 1649–1654. doi:10.1016/j.cropro.2011.07.020

Molitor, D., Fruehauf, C., Baus, O., Berkelmann-Loehnertz, B., 2012. A Cumulative Degree-Day-Based Model to Calculate the Duration of the Incubation Period of *Guignardia bidwellii*. Plant Disease 96, 1054–1059.

Motohashi, K., Inaba, S., Anzai, K., Takamatsu, S., Nakashima, C., 2009. Phylogenetic analyses of Japanese species of *Phyllosticta sensu stricto*. Mycoscience 50, 291–302.

Myers, A.L., 2006. Online guide to grapevine disease - Black rot. AHS Agricultural Research and Extension Center, Winchester, VA

Northover, P., 2008. Factors influencing the infection of cultivated grape (*Vitis* spp. section *Euvitis*) shoot tissue by *Guignardia bidwellii* (Ellis) Viala and Ravaz. The Pennsylvania State University.

Northover, P., Travis, J., 1998. Infection requirements of *Guignardia bidwellii* conidia on grapevine shoots. Phytopathology 88, S68.

Persoon, C.H., 1818. Traité sur les champignons comestibles, contenant l'indication des espèces nuisibles; a l'histoire des champignons. Belin-Leprieur, Paris, France.

Petrak, F., 1957. Über die Gattungen *Guignardia* Viala and Ravaz und *Discosphaerina v.* Höhnel. Sydowia 11, 435–445.

Pezet, R., Jermini, M., 1989. Le Black-rot de la vigne: Symptomes, epidemiologie et lutte. Revue Suisse Viticulture Arboriculture Horticulture 21, 27–34.

Prunet, A., 1898. Observations et expériences sur le black-rot II. Conditions internes du développement du black-rot. Rev. Vit. 9, 601–603.

Ramsdell, D.C., Milholland, R., 1988. Black-rot, in: Compendium of grape diseases. Pearson, R., Goheen, A. (Eds.), APS Press, St. Paul, pp. 15–17.

Reddick, D., 1911. The black-rot disease of grapes. Cornell University Agricultural Experiment Station Bulletin 293, 289-364.

Rex, F., Fechter, I., Hausmann, L., Töpfer, R., 2011. Etablierung einer methode zur phänotypisierung der schwarzfäule (*Guignardia bidwellii*) resistenz in der Weinrebe (*Vitis* spec.).

Rinaldi, P.A., Mugnai, L., 2012. Marciume nero degli acini, potenziale pericolo in viticoltura. Informatore Agrario 15, 68–71.

Rossi, V., Caffi, T., Salinari, F., Srl, H., 2012. Helping farmers face the increasing complexity of decision-making for crop protection. Phytopathologia Mediterranea. 51, 457–479.

Rossi, V., Onesti, G., Legler, S.E., Caffi, T., 2014. Use of systems analysis to develop plant disease models based on literature data : grape black-rot as a case-study. European Journal of Plant Pathology. 141, 427–444. doi:10.1007/s10658-014-0553-z

Roussel, C., Bouard, 1971. Maladies cryptomatiquae. In: Traite d'Ampelologie; Science e Tecnologiques de la Vigne. Dunod, Paris.

Rui, D., 1989. "Ultimissime" sul black-rot della vite. Informatore Agrario 39, 67–69.

Salzman, R.A, Tikhonova, I., Bordelon, B.P., Hasegawa, P.M., Bressan, R. a, 1998. Coordinate accumulation of antifungal proteins and hexoses constitutes a developmentally controlled defense response during fruit ripening in grape. Plant Physiology 117, 465–72.

Schoch, C.L., Shoemaker, R.A., Seifert, K.A., Hambleton, S., Spatafora, J.W., Crous, P.W., 2006. A multigene phylogeny of the Dothideomycetes using four nuclear loci. Mycologia 98, 1041–1052.

Scribner, F., 1886. Report on the fungus diseases of the grapevine. US Dep. Agric. Bot. Div. Sect. Plant Pathol. Bull. 2 GPO. Washington DC.

Scribner, F.L., Viala, P., 1888. Black-rot (*Laestadia bidwellii*). United States Department of Agriculture, Botany Division, Vegetable Pathology Bulletin 7.

Siegfried, W., Pezet, R., Jermini, M., 1993. Marciume nero o Black-rot. Agroscope Changins-Wädenswil ACW.

Sivanesan, A. and Holliday, P., 1981. CMI Descriptions of Pathogenic Fungi and Bacteria, No. 710. Wallingford, UK: CAB International.

Smith, D.L., 2009. Grape pathology research update: Black-Rot advisory. Le Vigneron 4, 7-8.

Smith, D.L., 2012. Mesonet grape black-rot advisor. Eds. Oklahoma State University Albert Sutherland.

Sosnowski, M.R., Emmett, R.W., Wilcox, W.F., Wicks, T.J., 2012. Eradication of black-rot (*Guignardia bidwellii*) from grapevines by drastic pruning. Plant Pathology 61, 1093–1102. doi:10.1111/j.1365-3059.2012.02595.x

Spotts, R.A., 1977. Effect of Leaf wetness duration and temperature on the infectivity of *Guignardia bidwellii* on grape leaves. Phytopathology 77, 1378-1381. doi:10.1094/Phyto-67-1378

Su, Y.Y., Cai, L., 2012. Polyphasic characterisation of three new *Phyllosticta* spp. Persoonia 28, 76–84.

Sultan, A., Johnston, P.R., Park, D., Robertson, A.W., 2011. Two new pathogenic ascomycetes in *Guignardia* and *Rosenscheldiella* on New Zealand's pygmy mistletoes (Korthalsella: Viscaceae). Studies in Mycology 68, 237–247.

Tattersall, D.B., van Heeswijck, R., Bordier Hoj, P., 1997. Identification and characterization of a fruit-specific, thaumatin-like protein that accumulates at very high levels in conjunction with the onset of sugar accumulation and berry softening in grapes. Plant Physiology 114, 759–769.

Ullrich, C.I., Kleespies, R.G., Enders, M., Koch, E., 2009. Biology of the black-rot pathogen, *Guignardia bidwellii*, its development in susceptible leaves of grapevine *Vitis vinifera*. Journal Für Kulturflanzen 61, 82–90.

Viala, P., Ravaz, L., 1892. Sur la dénomination botanique (*Guignardia bidwellii*) du black-rot. Bulletin de la Société Mycologique de France 8: 63.

Wicht, B., Petrini, O., Jermini, M., Gessler, C., Broggini, G. a. L., 2012. Molecular, proteomic and morphological characterization of the ascomycete *Guignardia bidwellii*, agent of grape black-rot: a polyphasic approach to fungal identification. Mycologia 104, 1036–1045. doi:10.3852/11-242

Wikee, S., Udayanga, D., Crous, P.W., Chukeatirote, E., McKenzie, E.H.C., *et al.*, 2011. *Phyllosticta* – an overview of current status of species recognition. Fungal Diversity 51, 43–61.

Wikee, S., Lombard, L., Nakashima, C., Motohashi, K., Chukeatirote, E., Cheewangkoon, R., McKenzie, E.H.C., Hyde, K.D., Crous, P.W., 2013. A phylogenetic re-evaluation of *Phyllosticta* (Botryosphaeriales). Studies in Mycology. 76, 1–29. doi:10.3114/sim0019

Wong, M.H., Crous, P.W., Henderson, J., Groenewald, J.Z., Drenth, A., 2012. *Phyllosticta* species associated with freckle disease of banana. Fungal Diversity 56, 173– 187.

Wulandari, N., To-Anun, C., Hyde, K.D., Duong, L., Gruyter, J., *et al.*, 2009. *Phyllosticta citriasiana* sp. nov., the cause of Citrus tan spot of Citrus maxima in Asia. Fungal Diversity 34, 23–39

Zhang, K., Zhang, N., Cai, L., 2013. Typification and phylogenetic study of *Phyllosticta ampelicida* and *P. vaccinii*. Mycologia 105, 1030–1042.

Chapter 2

Chapter 2

Use of systems analysis to develop plant disease models based on literature data: grape black-rot as a case-study[1]

ABSTRACT

The available knowledge on black-rot of grape was retrieved from literature, analyzed, and synthesized to develop a mechanistic model of the life cycle of the pathogen (*Guignardia bidwellii*) based on the systems analysis. Three life-cycle compartments were defined: (i) production and maturation of inoculum in overwintered sources (i.e., ascospores from perithecia and conidia from pycnidia in berry mummies and cane lesions); (ii) infection caused by ascospores and conidia; and (iii) disease onset and production of secondary inoculum. An analysis of published, quantitative information was conducted to develop a mechanistic model driven by weather and vine phenology; equations were developed for ascospore and conidial maturation in overwintered fruiting bodies, spore release and survival, infection occurrence and severity, incubation and latency periods, onset of lesions, production of pycnidia, and infectious periods. The model was then evaluated for its ability to represent the real system and its usefulness for understanding black-rot epidemics by using three typical epidemics. Finally, weaknesses in our knowledge are discussed. Additional research is needed concerning the influence of wetness duration and temperature on infection by ascospores, production dynamics of pycnidia and conidia in black-rot lesions, and the dynamics of conidia exudation from pycnidia.

Keywords: epidemiology, disease modeling, model validation, *Guignardia bidwellii.*

INTRODUCTION

Systems analysis has become a useful tool for conceptualizing pathosystems and for developing plant disease models since its first use in plant pathology in the early 1970s by Zadoks (1971). Model building based on systems analysis involves the development of a conceptual model that describes the system (both conceptually and mathematically) (Kranz and Hau, 1980) and a set of driving models that account for changes in the system caused by the external variables (Rossi *et al.*, 2010). The development of driving models

[1] Rossi V., Onesti G., Legler S.E., Caffi T., 2015. *European Journal of Plant Pathology* 141: 427–444.

requires the acquisition of data on relationships between life cycle components and the external, influencing variables, and the mathematical formalization of these relationships through rules, thresholds, and equations (Rossi *et al.,* 2010). Acquisition of the necessary data requires the execution of specific experiments carried out with and without control of environmental conditions, i.e., in the laboratory and in the field (Kranz and Hau, 1980). Experiments performed in the laboratory (with control of temperature, wetness duration, relative humidity, etc.) allow researchers to consider pathogen response over the entire range of the considered environmental variable, with little or no interference from uncontrolled factors (Rotem, 1988). However, results obtained in controlled studies must be evaluated under natural conditions (Aust and Kranz, 1988), making the development of driving models a long and costly process.

The literature contains substantial information concerning quantitative relationships between weather variables and pathogens; although this information has potential value for modeling (Kranz and Hau, 1980), it is usually difficult to use because it was obtained with different, not directly comparable methods, was not described with sufficient detail, or was not properly analyzed. The paper of Magarey *et al.* (2005) is an example of how previously published information can be used to develop and test mathematical relationships between weather variables (e.g., temperature and wetness duration) and epidemiological parameters of plant diseases (e.g., occurrence of infection).

The renewed interest in black-rot of grape and the need for improved control strategies makes this disease a useful case-study for using the systems analysis to develop a model based on literature data, to reveal possible weaknesses in the current knowledge and to address further research efforts accordingly.

Black-rot, caused by the ascomycete *Guignardia bidwellii* (Ellis) Viala and Ravaz (anamorph: *Phyllosticta ampelicida* (Englem.) van der Aa), originated in eastern North America and now occurs in parts of Europe, South America, and Asia where humidity is high in spring and early summer (Ramsdell and Milholland, 1988). In Europe, black-rot was first described at the end of the 19th century (Scribner, 1886), and its occurrence was sporadic. For example, the presence of black-rot was documented in the 1930s in Germany (Mueller, 1934; Luestner, 1935) but no major epidemics occurred until 2002 (Harms *et al.*, 2005). Currently, black-rot has become well established in the northern wine-growing areas of Germany where it now represents one of the major fungal diseases (Harms *et al.,* 2005). In Italy, the disease was first noticed in 1974 in the area of La Spezia (North-West Italy) and subsequently became endemic in some vine-growing areas. In Friuli (North-East Italy), the disease was first detected in 1985 (Clabassi, 2000) and occurred frequently in the early 1990s. It nearly disappeared from 2001 to 2007 but then increased again in importance (Bigot G., personnel communication); in 2011, black-rot caused severe epidemics in Friuli and in other Italian areas (Rinaldi and Mugnai 2012). Black-rot poses a serious threat to both grape yield (losses range from 5 to 80%)

and wine quality (Scribner, 1886; Ellis *et al.,* 1986; Ferrin and Ramsdell, 1977; Ferrin and Ramsdell 1978; Ramsdell and Milholland, 1988; Funt *et al.,* 1990).

Control of black-rot requires fungicide applications between bud break and "berry touch"(Ramsdell and Milholland, 1988; Emele *et al.,* 1998; Doufor, 2006; Carisse *et al.,* 2009), which is when vineyards also require protection against downy and powdery mildews. Selection of fungicides in mildew spray programs that are also effective against *G. bidwellii* (i.e., strobilurins, triazoles, and dithiocarbamates) ensures control of black-rot without any additional applications (Molitor and Berkelmann-Loehnertz, 2011). Nevertheless, Roussel (1971) advised French growers that treatments against downy mildew and black-rot cannot be scheduled on a calendar basis without considering the differences between the two diseases. Currently, the transition from a calendar-based control of mildews to targeted sprays based on plant disease models, and the consequent reduction in fungicide applications by 30-40% (Caffi *et al.,* 2010; Caffi *et al.,* 2012), means that vines will not be protected against black-rot when there is no risk of mildews. A model for black-rot should therefore help growers manage fungicide sprays so as to control both mildews and black-rot.

Simple models for black-rot of grape have been developed (Ellis *et al.,* 1986; Devaut, 1990; Maurin *et al.,* 1992) based on the length of the wetness period and the temperature conditions required for infection (Spotts, 1977). These models, however, have some limitations: they do not consider the presence and abundance of inoculum or the variations in host susceptibility, and they do not provide quantitative estimates of risk.

The aim of this study was to: (i) collect the published knowledge on black-rot of grape; (ii) analyze and synthesize that knowledge to conceptualize a model of the life cycle of *G. bidwellii* according to the systems analysis; (iii) carry out an analysis of the quantitative information to develop a mechanistic, dynamic, weather-driven model; (iv) evaluate the model for its ability to represent the real system and its usefulness for understanding black-rot epidemics; and finally (v) determine gaps in our knowledge that need further research.

MATERIALS AND METHODS

Literature search

A protocol was developed following Zins (1999) and Okoli and Schabram (2010) for retrieving published papers and other information sources that contain data of interest for the systems analysis of the life cycle of *G. bidwellii*. To be considered, the papers had to satisfy the following criteria: (i) they had to contain original data on the biology, ecology, or epidemiology of the black-rot pathogen; (ii) they had to contain original data on the pathogenic interaction between *G. bidwellii* and *Vitis* spp.; and (iii) they had to be

published in journals, proceedings, or in other forms including reports or web-sites from competent authorities/organizations. The literature search was carried out in the CAB Abstracts database (http://www.cabdirect.org), the AGRIS database, and the World Wide Web. Papers were searched by using combinations of the following keywords: (i) *Guignardia bidwellii* OR *Phyllosticta ampelicida* OR their synonyms as listed in CAB (2007); (ii) black-rot OR other common names as listed in CAB (2007); (iii) life cycle OR germination OR appressoria OR infection OR incubation OR latency OR latent period OR pycnidia OR conidia OR pycnidiospore OR pseudothecia OR perithecia OR ascospore OR perennation OR overwintering OR model OR prediction OR simulation. The literature search was first performed in the selected database (e.g., the CAB Abstracts database). Each paper found was then reviewed on the basis of the information in the title and abstract: if the paper met the eligibility criteria, it was considered of potential interest; otherwise, it was discarded. If a publication was considered to be of potential interest, the full paper was retrieved and reviewed. Further papers were selected from the "References" section of the papers found; these papers were then retrieved and reviewed.

Systems analysis and model development

Information from selected papers was used to draw the relational diagram of the system as described by Leffelaar and Ferrari (1989) and Rossi *et al.* (2010). The data retrieved in text, Tables, or figures of selected papers were used to develop the mathematical equations describing the system both quantitatively and dynamically. In these equations, the system's variables were the dependent variables while external factors (e.g., weather data, vine growth stage, time) were the independent ones. Original data (i.e., data in the paper) expressed as a function of time (e.g., number of days or calendar dates) were expressed as a function of thermal time, i.e., in degree-days, a temperature-derived variable widely used in plant disease epidemiology (Lovell *et al.*, 2004). When temperature data were not indicated in the paper, the daily temperature records were downloaded from the GSOD (Global Surface Summary of Day) database of NOAA (National Oceanic and Atmospheric Administration), which contains over 8000 worldwide stations (http://www.ncdc.noaa.gov/cdo-web/); data from the station nearest to the experimental site were used. Equations were selected based on the shape of data, and equation parameters were estimated using the non-linear regression procedure of SPSS (ver. 18, SPSS Inc.), which minimizes the residual sums of squares using the Marquardt algorithm. The magnitude of the standard errors of the model parameters, R^2 adjusted for the degree of freedom, the number of iterations taken by the Marquardt algorithm to converge on parameter estimates, and the magnitude and distribution of residues of predicted versus observed data were considered to evaluate the goodness-of-fit. Lower and upper temperature thresholds for calculating degree-days were determined by using

the same procedure, i.e., by evaluating the goodness-of-fit of equations calculated with different temperature thresholds.

Model evaluation

The model was evaluated for its defined purpose (Madden, 2007), i.e., its ability to represent the real system and its usefulness for understanding black-rot epidemics. Three disease epidemics that developed in North Italy and that represent typical epidemic patterns were considered: (i) a light epidemic that occurred in a vineyard in Piacenza in 2010; (ii) a severe epidemic on both leaves and clusters (with repeated infections during the season) that occurred in a vineyard in Udine in 2010; and (iii) a severe epidemic with symptoms that rapidly appeared on leaves only in a vineyard in Piacenza in 2012.

Running the model requires the setting of initial parameters concerning the amount of primary inoculum in the vineyard. Lacking data on the actual inoculum dose in the three vineyards, these parameters were set as the proportional contribution of each inoculum source to the total inoculum, so that the total inoculum was equal to 1. The model also requires periodical inputs as hourly weather data of air temperature, relative humidity, leaf wetness, and rainfall, which were measured by weather stations in the vineyards. Hourly weather data were used instead of daily data in order to better describe the environmental effects on the pathosystem (Rossi *et al.*, 2010). Dates of bud break of vines and other growth stages, which were collected by visiting the vineyards once or twice each week (depending on the period), are also requested as model inputs. During these visits to the vineyards, the BBCH scale (Lorenz *et al.,* 1995) was used to estimate the prevalent growth stage (i.e., the growth stage of >50% of vines) on a random sample of 100 plants.

Model output was then compared with actual disease severity. The latter was estimated as the percentage of affected leaves or clusters (disease incidence) when the disease symptoms were light, and as the percentage of affected leaf area or berries (disease severity) when the epidemic was severe (>30% incidence). Because black-rot usually first appears on isolated plants and then spreads from these foci, the vineyards were carefully inspected to detect the first seasonal onset of disease, and the disease incidence or severity was estimated in the foci.

RESULTS

Systems analysis of the *G. bidwellii* life cycle

A relational diagram of the life cycle of *G. bidwellii* is shown in Figure 1, and the acronyms are explained in Table 1. The meta-synthesis of the literature review which led to model development is provided in Supplementary material 1.

The main stages of the life cycle are the state variables (boxes) of the system (Figure 1). The system starts with three state variables that correspond to the seasonal dose of the three overwintering forms of inoculum: perithecia (SDASC) and pycnidia (SDCOC) produced in mummified fruit within the vine or on ground, and pycnidia (SDCOM) produced in lesions on infected shoots that are retained as canes or spurs. Ascospores and conidia progressively form and mature within the fruiting bodies, which represent the second set of state variables (ASCMAT and CONMAT). Spring rains trigger the release of ascospores into the air, and splashing rain drops disperse conidia within the vine or to neighboring vines; air-borne ascospores and splash-borne conidia are then the third set of state variables (SPOREL ascospores and SPOREL conidia). Either spore type may lands on vine surfaces (fourth set of state variables: SPODOSE ascospores and SPODOSE conidia) and cause infection on leaves, shoots, blossoms, and fruit, which results in the next state variable, i.e., the infection sites. Black-rot symptoms appear after an incubation period as visible lesions (state variable) and the lesions produce pycnidia after a latency period (state variable). Lesions caused by an infection and pycnidia formed on those lesions do not appear simultaneously; these delays in lesion appearance and pycnidia production are represented by grids that are inserted into the symbols (on the relational diagram) for lesions and for pycnidia within lesions (Figure 1). Pycnidia in lesions continue to produce conidia throughout the season and feed the state variable “conidia in pycnidia”(CONMAT); these conidia extrude, disperse, and infect new host tissue, thereby causing secondary infections.

The flow from one stage to the next (arrows in the relational diagram of Figure 1) is regulated by rates (valves) and while switches (diamonds) which are in turn influenced by external variables, auxiliary variables or constants (short segments and circles). The external variables are weather variables (temperature, T in °C; wetness duration, WD in hours; rainfall, R in mm) or the growth stage of the vine (expressed as the stage of the BBCH scale). Therefore, the system’s dynamics are regulated by the external variables through a framework of mathematical equations that constitute the model. Three examples on how the literature data were used to develop the model equations are provided in Supplementary material 2.

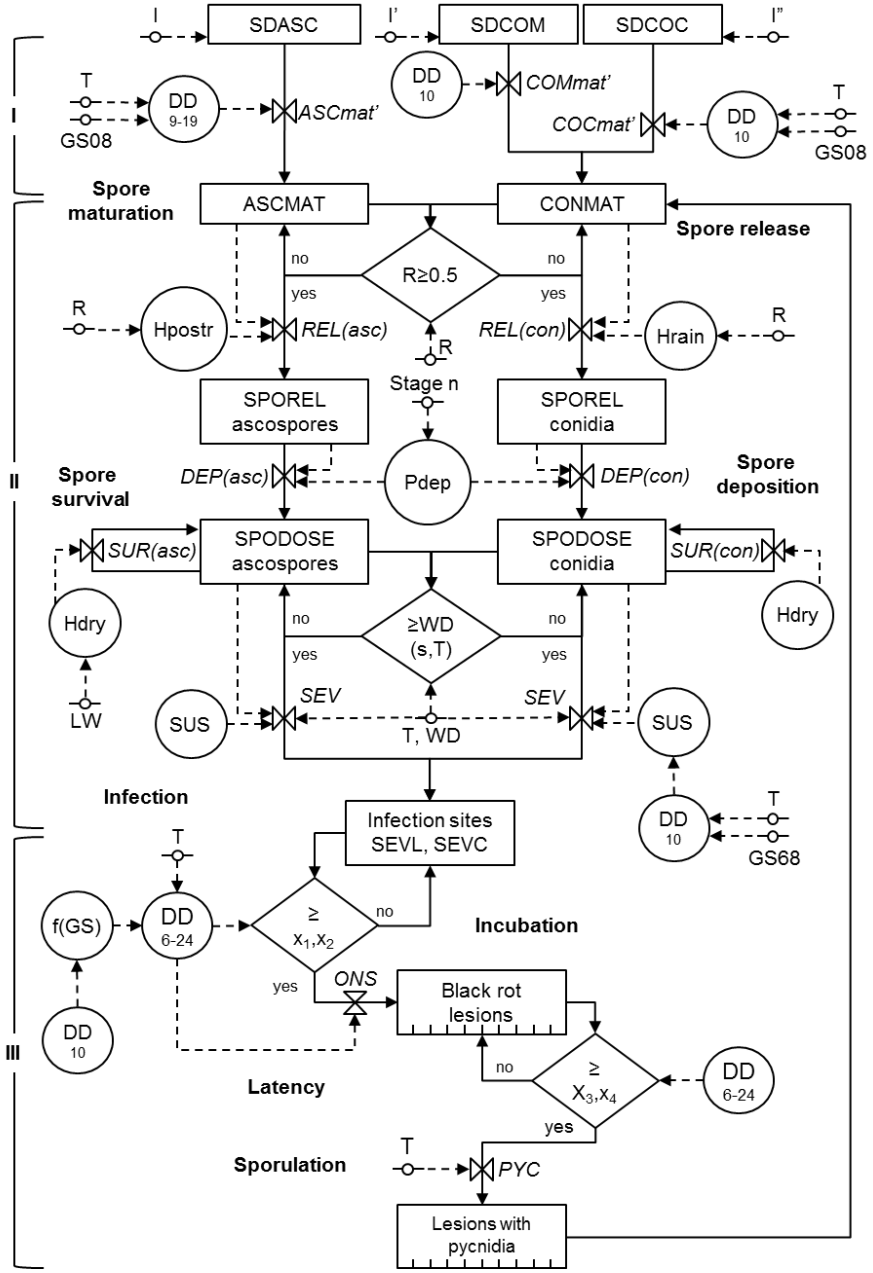

Figure 1. Relational diagram of the life cycle of *Guignardia bidwellii*. Legend: □ state variable; —► flux and direction of states; ---► flux and direction of information; —○— parameter; ○ intermediate variable; ◇ switch; >|< valve in a flux (rate) (see Table 1 for acronym explanations).

Table 1. List of variables, rates, and parameters used in the model.

Acronym	Description	Unit
ASCMAT	Mature ascospores in perithecia	0 to I
ASCmat	Cumulative proportion of mature ascospores	0 to I
ASCmat'	Ascospore maturation rate	0 to 1
COCMAT	Mature conidia in pycnidia in cane lesions	0 to I"
COCmat	Cumulative proportion of mature conidia in cane lesions	0 to I"
COCmat'	Conidial maturation rate in cane lesions	0 to 1
COMMAT	Mature conidia in pycnidia in mummies	0 to I'
COMmat	Cumulative proportion of mature conidia in mummies	0 to I'
COMmat'	Conidial maturation rate in mummies	0 to 1
CONMAT	Total mature conidia (COMMAT + COCMAT)	0 to (I'+I")
DD_{10}	Cumulative degree-days (T ≥10°C)	°C
$DD_{6\text{-}24}$	Cumulative degree-days (6≤ T ≤24°C)	°C
$DD_{9\text{-}19}$	Cumulative degree-days (9≤ T ≤19°C)	°C
DEP(s)	Deposition rate of s= ascospores or conidia	0 to 1
f(GS)	Correction factor for incubation length in clusters	N
GS	Growth stage of the plant based on the BBCH scale	-
Hdry	Duration of the dry period (i.e., hours with LW = 0)	N hours
Hpostr	Hours after start of spore release	N hours
Hrain	Consecutive hours of rain after start of spore release	N hours
i	Counter of hours	N
I, I', I"	Seasonal dose of ascospores, conidia from mummies and cane lesions	I+I'+I"=1
j	Counter of days	N
LW	Presence of leaf wetness in a hour (yes/not)	1/0
ONS	Relative lesion onset	0 to 1

ONS'	Rate of black-rot lesion onset	0 to 1
Pdep	Empirical probability of spores to deposit on the plant surface	0 to 1
PYC	Relative pycnidia production	0 to 1
PYC'	Rate of pycnidia production in fertile lesions	0 to 1
R	Hourly rainfall	mm
REL(s)	Release rate of s = ascospores or conidia	0 to 1
s	Spore type: ascospores or conidia	-
SDASC	Seasonal dose of ascospores from mummies	0 to I
SDCOC	Seasonal dose of conidia from cane lesions	0 to I"
SDCOM	Seasonal dose of conidia from mummies	0 to I'
SEV	Relative infection severity	0 to 1
SEV'	Rate of infection severity	0 to 1
SEVC(s)	Infection severity on clusters by s = ascospores or conidia	0 to I or (I'+I")
SEVL(s)	Infection severity on leaves by s = ascospores or conidia	0 to I or (I'+I")
SPODOSE(s)	Dose of viable spores (s = ascospores or conidia) on plant surface	0 to I or (I'+I")
SPOREL(s)	Spores (s = ascospores or conidia) released in air currents or rain splashes	0 to I or (I'+I")
SUR(s)	Survival rate of s= ascospores or conidia	0 to 1
SUS	Relative susceptibility to infection of clusters	0 to 1
T	Hourly air temperature	°C
Teq	Equivalent of temperature	0 to 1
Tm	Mean temperature of a period	°C
Tmax	Maximum temperature for infection or production of pycnidia	°C
Tmin	Minimum temperature for infection or production of pycnidia	°C

Topt	Optimum temperature for infection	°C
Tw	Average temperature of the wet period	°C
WD	Duration of the wet period	N hours
WD(s,T)	WD requirement for infection at temperature T for spore s	N hours
WDmin	Minimum duration of the wet period for infection	N hours
X_1 to X_4	Thresholds for $DD_{6\text{-}24}$	°C

Model description

Based on the relational diagram in Figure 1, the system has three main steps, which correspond to three model compartments: (I) production and maturation of inoculum in overwintered sources; (II) infection caused by ascospores and/or conidia; and (III) disease onset and production of secondary inoculum.

The 1st model compartment accounts for production of inoculum by overwintered sources. Ascospores from 1-year-old rotted berries (mummies) that overwintered in the vineyard (on the ground or in the trellis) are the major form of primary inoculum, although conidia produced from overwintered mummies and cane lesions may also contribute to primary infections. At the start of a grape-growing season, the abundance of perithecia (in mummies) and pycnidia (both in canes and mummies) determines the seasonal dose of ascospores and conidia, named SDASC, SDCOC and SDCOM, respectively (Figure 1 and Table 1). In this compartment, the system progresses with the maturation of ascospores and conidia within the fruiting bodies (Figure 1).

Ascospores from mummies. The model calculates the cumulative proportion of mature ascospores in perithecia on each day j, ASCMAT(j), as:

$$ASCMAT(j) = I \times ASCmat'(j) \quad (1)$$

where: ASCMAT(j) ranges from 0 (no ascospores have matured until day j) to I (all seasonal ascospores have matured), with I = estimate of the seasonal ascospore dose, expressed as the estimated contribution of ascospores to the total inoculum of the vineyard (on a 0 to 1 scale); *ASCmat'*(j) = rate of ascospore maturation, as the first order derivative of the following equation:

$$ASCmat(j) = \exp(-5.31 \times \exp(-0.99 \times DD_{9\text{-}19}(j) / 100) \quad (2)$$

where: ASCmat(j) = cumulative proportion of mature ascospores on j^{th} day; $DD_{9\text{-}19}(j)$ = cumulative degree-days on day j, calculated from bud break (stage 08 of the BBCH scale) using 9°C and 19°C as cardinal temperatures, as follows: when T(j) ≤9, T(j) = 0; when 9≤

T(j) ≤19, T(j) = T(j)-9; when T(j) >19, T(j) = 10. Estimates and standard errors of equation parameters were: 5.31±0.43, 0.99±0.04. Equation 2 was developed and parameterized using the data of Ferrin and Ramsdell (1977) and Jermini and Gessler (1996), with $R^2 = 0.97$ (Figure 2A) (see supplementary material 2 for details).

Conidia from mummies. The model calculates the cumulative proportion of mature conidia in mummies on each day j, COMMAT(j), as:

$$COMMAT(j) = I' \times COMmat'(j) \quad (3)$$

where: COMMAT(j) ranges from 0 (no conidia have been produced until day j) to I'(all seasonal conidia from mummies have been produced), with I' = estimate of the seasonal dose of conidia from mummies, expressed as the estimated contribution of conidia from mummies to the total inoculum of the vineyard (on a 0 to 1 scale); *COMmat'*(j) = first order derivative of the following equation:

$$COMmat(j) = 1 / (1 + \exp(6.12-0.76 \times DD_{10}(j) / 100)) \quad (4)$$

where: COMmat(j) = cumulative proportion of mature conidia in mummies on j^{th} day; $DD_{10}(j)$ = cumulative degree-days on day j, calculated from bud break (stage 08) using 10°C as the minimum temperature, as follows: when T(j) ≤10°, T(j) = 0; when T(j) >10, T(j) = T(j)-10. Estimates and standard errors of equation parameters were: 6.12±1.21, 0.76±0.14. Equation 4 was developed and parameterized using the data of Ferrin and Ramsdell (1978) and Hoffman *et al.* (2004), with $R^2 = 0.97$ (Figure 2B).

Conidia from cane lesions. The model calculates the cumulative proportion of mature ascospores in cane lesions on each day j, COCMAT(j), as:

$$COCMAT(j) = I'' \times COCmat'(j) \quad (5)$$

where: COCMAT(j) ranges from 0 (no conidia have been produced until day j) to I''(all seasonal conidia from canes have been produced), with I'' = estimate of the seasonal dose of conidia from canes, expressed as the estimated contribution of conidia from canes to the total inoculum of the vineyard (on a 0 to 1 scale, so that I + I' + I'' = 1); *COCmat'*(j) = first order derivative of the following equation:

$$COCmat(j) = (1 -0.75 \times 0.65^{DD10\ (j)/100}) \quad (6)$$

where: COCmat(j) = cumulative proportion of mature conidia in cane lesions on j^{th} day; $DD_{10}(j)$ = cumulative degree-days on day j, calculated as in equation 4. Estimates and standard errors of equation parameters were: 0.75±0.07, 0.65±0.06. Equation 6 was

developed and parameterized using the data of Becker and Pearson (1996) (R^2 = 0.84; Figure 2C).

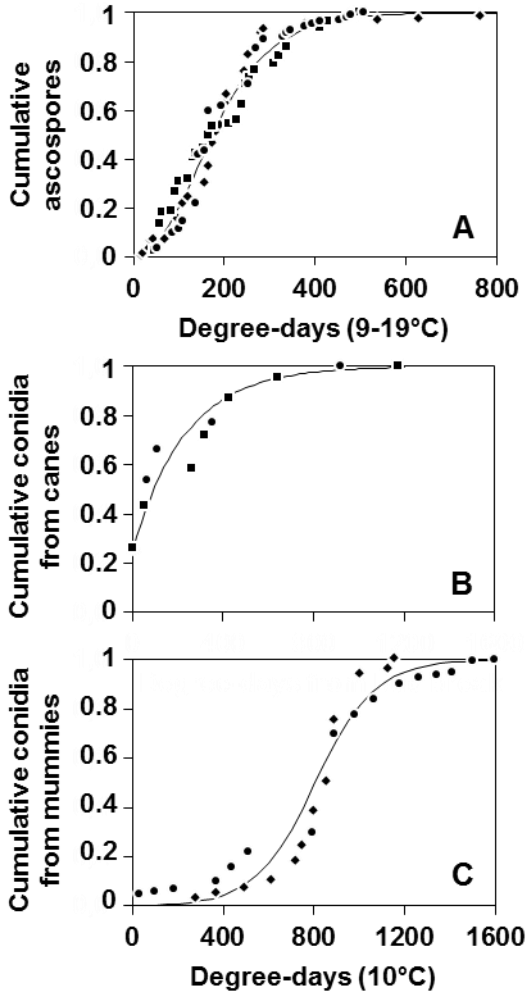

Figure 2. Cumulative proportion of mature ascospores (**A**), conidia from overwintered mummies (**B**), and conidia from canes (**C**) of *Guignardia bidwellii*. Time is expressed in degree-days between 9 and 19°C (**A**) or base 10°C (**B** and **C**) accumulated after bud break. In **A**, dots show the data of Hoffman *et al.* (2002) for 1974 (◆) and 1975 (■) (MI, US) and of Jermini and Gessler (1996) for 1990 (●) (Switzerland); the line shows the fit of data by equation 2, R^2 = 0.97. In **B**, dots show the data of Ferrin and Ramsdell (1978) for 1974 (●) (MI, US) and of Hoffman *et al.* (2002) for 1998 (◆) (NY, US); the line shows the fit of data by equation 4, R^2 = 0.97. In **C**, dots show the data of Becker and Pearson (1996) for 1990 (●) and 1991 (■) (Dresden, NY, US); the line shows the fit of data by equation 6, R^2 = 0.84.

The 2nd model compartment considers infection caused by ascospores and conidia (Figure 1). Primary infection can be caused by both ascospores and conidia from the overwintered sources. The chain of events that leads to infection include: (i) spore release, dispersal, and deposition on the host surface; (ii) spore survival; and (iii) infection of susceptible host tissue. Therefore, the system has the following state variables: air-borne ascospores and splash-borne conidia (SPOREL); viable ascospores

and conidia on the host surface (SPODOSE); and infection sites on leaves and clusters (SEVL and SEVC, respectively) (Figure 1).

Spore release and deposition. Both ascospores and conidia are assumed to be released when R ≥0.5 mm in 1 h, which is a release event. The total amount of ascospores or conidia released in any release event, SPOREL(s) (where s = ascospores or conidia), is equal to ASCMAT or CONMAT (i.e., COMMAT + COCMAT) at the time of spore release, under the assumptions that all the mature ascospores or conidia are released during a release event.

The model considers that mature ascospores and conidia are released progressively after the rain at a release rate, *REL*(s), which is calculated for each hour i as follows:

$$REL(\text{s=ascospores,i}) = 1 - 0.195 \times 0.57^{\text{Hpostr (i)}} \quad (7)$$

$$REL(\text{s=conidia,i}) = 1/(1 + \exp(3.96 - 2.83 \times \text{Hrain(i)})) \quad (8)$$

where: *REL*(s) ranges from 0 (there is no spore release) to 1 (all mature spores are released); Hpostr and Hrain = total number of hours and number of consecutive hours of rain after the start of the ascospore and conidia release (i.e., when R(i) ≥0.5), respectively. Estimates and standard errors of equation parameters were: 0.195±0.007, 0.57±0.02, for equation 7; 3.96±0.27, 2.83±0.19, for equation 8. Equations 7 and 8 were developed and parameterized using the data of Jermini and Gessler (1996) and Spotts (1980), respectively, with $R^2 = 0.99$ for both equations (Figure 3A and B).

The model assumes that the released ascospores and conidia are deposited on the host surface at a deposition rate, *DEP*(s,i), which ranges from 0 (no spores have been deposited) to 1 (all released spores have been deposited). *DEP*(s) is calculated hourly by multiplying *REL*(s,i) by Pdep, the empirical probability that spores will land on the host surface as a function of vine growth stage. Pdep ranges from 0 to 1, and it increases by 0.07 for each leaf unfolded; when Pdep >1, Pdep = 1.

Spore survival. The survival rate, *SUR*(s), of ascospores or conidia in dry periods is calculated in each hour i, as follows:

$$SUR(\text{s,i}) = 1 / (1 + \exp(-\alpha(\text{s}) + \gamma(\text{s}) \times \text{Hdry(i)})) \quad (9)$$

where: *SUR*(s) ranges from 0 (no spores have survived) to 1 (all spore are alive); Hdry = number of hours of dryness; α(s), γ(s) = equation parameters for ascospores (α = 2.94±0.57, γ = 0.18±0.05) and conidia (α = 4.45±1.88, γ = 0.18±0.08). Equation 9 was developed and parameterized using the data of Ferrin and Ramsdell (1977) for ascospores, and the data of Spotts (1977) for conidia ($R^2 = 0.97$, Figure 3C and $R^2 = 0.99$, Figure 3D, respectively).

Therefore, in any i^{th} hour after spore release, the proportion of viable spores, SPODOSE(s), is calculated as:

$$\text{SPODOSE}(s,i) = \text{SPOREL}(s,i) \times \textit{REL}(s,i) \times \textit{DEP}(s,i) \times \textit{SUR}(s,i) \qquad (10)$$

Infection. Occurrence of infection (i.e., an infection period) is calculated for ascospores and conidia by fitting the data of Ferrrin and Ramsdell (1977), Spotts (1977), Weber (1987), Northover (2008), and Molitor (2009) to the general model of Magarey *et al.* (2005) (Figure 3E and F). A potential infection period starts with 1 h of wetness, and infection occurs when:

$$\text{WD} \geq \text{WD}(s,T) \qquad (11)$$

where: WD = cumulative number of hours with wetness; WD(s,T) = wetness duration requirement (in hours) for infection at temperature T for the kind of spore s, calculated as:

$$\text{WD}(s,T) = \text{WDmin}(s) / f(s,T) \qquad (12)$$

$$f(s,T) = (Tw - \text{Tmin}(s)) / (\text{Topt}(s) - \text{Tmin}(s)) \times ((\text{Tmax}(s) - Tw) / (\text{Tmax}(s) - \text{Topt}(s)))^{(\text{Tmax}(s) - \text{Topt}(s)) / (\text{Topt}(s) - \text{Tmin}(s))}$$

where: WDmin(s) = minimum wetness duration requirement for infection by the spore type s at any temperature (i.e., 5 h for ascospores, 6 h for conidia); Tw = mean temperature during the wet period; Tmin(s) = minimum temperature for infection by ascospores (7°C) or conidia (7°C); Tmax(s) = maximum temperature for infectionby ascospores (31°C) or conidia (33°C); Topt(s) = optimal temperature for infection by ascospores (24°C) or conidia (25°C); when $\text{Tmin} \leq Tw \leq \text{Tmax}$; $f(s,T) = 0$.

When infection has occurred, infection severity on leaves, SEVL(s) with $0 < \text{SEVL}(s) \leq 1$, is calculated in each i^{th} hour over the WD, as follows:

$$\text{SEVL}(s,i) = \text{SPODOSE}(s,i) \times \textit{SEV'}(i) \qquad (13)$$

where: *SEV'*(i) = first order derivative of the following equation:

$$\text{SEV}(s,i) = (4.47 \times \text{Teq}(i)^{1.18} \times (1-\text{Teq}(i)))^{1.35} \times \exp(-4.70 \times \exp(-0.062 \times \text{WD}(i))) \qquad (14)$$

where:SEV(i) = relative infection severity; Teq(i) = equivalent of temperature, calculated as: Teq(i) = (Tw(i)-Tmin) / (Tmax-Tmin); with Tw, Tmin and Tmax as in equation 12; estimates and standard errors of equation parameters were: 4.47±0.24, 1.18±0.07,

1.35±0.16, 4.70±0.48, 0.062±0.006. Equation 14 was developed and parameterized using the data of Molitor (2009), with $R^2 = 0.93$ (see Supplementary material 2 for details).

Leaf infection severity of any infection period is then calculated by summing SEVL(s = ascospores) and SEVL(s = conidia).

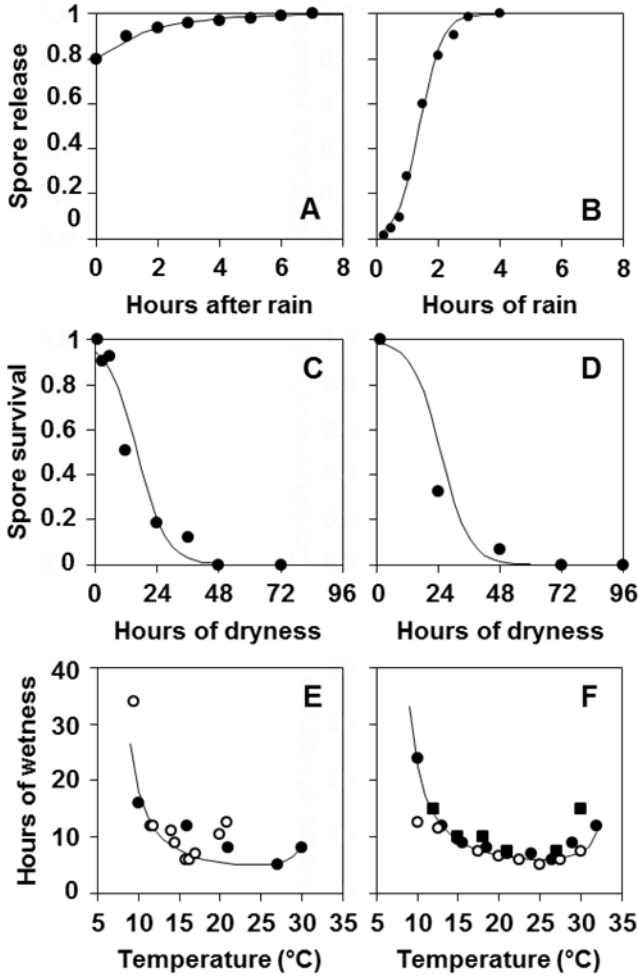

Figure 3. Dynamics of *Guignardia bidwellii* spore release (**A**, ascospores; **B**, conidia) and survival (**C**, ascospores; **D**, conidia), and minimum number of hours of wetness for infection by ascospores (**E**) or conidia (**F**) at different temperatures. In (**A**), dots show the data of Jermini and Gessler (1996), and the line shows the fit of data by equation 7, $R^2 = 0.99$. In (**B**), dots show the data of Spotts (1980), and the line shows the fit of data by equation 8, $R^2 = 0.99$. In (**C**), dots show the data of Ferrin and Ramsdell (1977), and the line shows the fit of data by equation 9, $R^2 = 0.97$. In (**D**), dots show the data of Spotts (1980), and the line shows the fit of data by equation 9, $R^2 = 0.99$. In (**E**), dots show the data of Ferrin and Ramsdell (1977) (●) and Weber (1987) (○); the line is calculated by equation 12. In F, dots show the data of Spotts (1980) (●), Molitor (2009) (○), and Northover (2008) (■); the line is calculated by equation 12.

Host susceptibility. The equation of Molitor and Berkelmann-Loehnertz (2011) is used as follows:

$$SUS = 0.995 \times \exp(-0.5 \times (((DD_{10} - 144.4) / 110.7)^2)) \quad (15)$$

where: SUS = relative susceptibility of clusters when infection occurs (see equation 12), with $0 > SUS \leq 1$; DD_{10} = cumulative degree-days when infection occurs, calculated as in equation 4 and accumulated starting from when 80% of flower caps have fallen (stage 68 of the BBCH scale). Equation 15 is then multiplied by SEVL(s) to determine infection severity on clusters, SEVC(s).

The 3rd model compartment considers disease onset and production of secondary inoculum (Figure 1). After the occurrence of an infection period, relatively small, brown, circular lesions develop on infected leaves, and within a few days tiny black spherical pycnidia protrude from them. Infected berries first appear light or chocolate brown but quickly turn darker brown, with masses of black pycnidia developing on the surface. Finally, infected berries shrivel and turn into hard, black, raisin-like bodies, i.e., the mummies.

Pycnidia produce conidia (i.e., the secondary inoculum), which can infect leaves and fruit (i.e., secondary infections) repeatedly throughout the spring and summer during favorable weather conditions. The chain of events that leads to secondary infection includes: (i) appearance of black-rot lesions after an incubation period; (ii) appearance of pycnidia on lesions after a latency period; and (iii) production of pycnidia over the infectious period of a lesion. The system has two state variables: visible lesions in the form of black-rot symptoms and lesions bearing pycnidia without and with pycnidia. Conidia produced within these pycnidia directly feed the state variable "conidia in pycnidia"at the beginning of compartment II (Figure 1).

Incubation and latency periods. The black-rot symptoms of any infection period, which form a cohort of lesions, are predicted to appear in the following time windows:

$$175 \leq DD_{6\text{-}24} \leq 305 \text{ for leaves} \quad (16)$$

$$175 \times f(GS) \leq DD_{6\text{-}24} \leq 305 \times f(GS) \text{ for clusters} \quad (17)$$

where: $DD_{6\text{-}24}$ = degree-days accumulated from the day when infection has occurred using 6°C and 24°C as cardinal temperatures (see equation 12), as follows: when $T(j) \leq 6$, $T(j) = 0$; when $6 \leq T(j) \leq 24$, $T(j) = T(j)-6$; when $T(j) > 24$, $T(j) = 18$; f(GS) = is a correction factor that increases the incubation length based on the growth stage of clusters at the time of infection and is calculated from the data of Molitor *et al.* (2012) as follows:

$$f(GS) = 1+1/(1+ \exp(7.10-2.23\times DD_{10} / 100)) \quad (18)$$

where: DD_{10} = cumulative degree-days calculated as in the equation 15; estimates and standard errors of equation parameters were: 7.10±0.20, 2.23±0.06.

Lesions in a cohort of lesions (i.e., those that originate from the same infection period) appear at the rate *ONS'*, calculated as the first derivative of the following equation:

$$ONS(j) = \exp(-316.15 \times \exp(-2.91 \times DD_{6\text{-}24} / 100)) \quad (19)$$

where: ONS(j) = relative lesions onset, which ranges from 0 (no lesions appear) to 1 (all lesions have appeared); estimates and standard errors of equation parameters were: 316.15±23.96, 2.91±0.35. Equation 19 was developed and parameterized using the data for berries of Hoffman *et al.* (2002), with $R^2 = 0.91$ (Figure 4A). The model assumes no difference in the rate of lesion appearance on leaves and berries.

Production of pycnidia on a cohort of lesions is predicted to occur in the following time windows:

$$262 \leq DD_{6\text{-}24} \leq 392 \text{ for leaves} \quad (20)$$

$$262 \times f(GS) \leq DD_{6\text{-}24} \leq 392 \times f(GS) \text{ for clusters} \quad (21)$$

which is 1.5 times the duration of the incubation window in equations 16 and 17 (see Supplementary material 2). The start of infectiousness when 262 degree-days had accumulated after leaf infection, with $6 \leq T \leq 24$°C, is similar to the value of 245 degree-days found by Northover (1998), with $7 \leq T \leq 26$°C.

Production of pycnidia in lesions. The rate of pycnidia production by a cohort of lesions, *PYC'*, is calculated as the first order derivative of the following equation:

$$PYC(j) = (4.71 \times Teq^{1.26} \times (1\text{-}Teq))^{3.584} \times (1 + \exp(12.09\text{-}3.96 \times DD_{6\text{-}24}(j) / 100)) \quad (22)$$

where: PYC = relative pycnidia production, which ranges from 0 (no pycnidia produced) to 1 (maximum production of pycnidia); Teq = equivalent of temperature, calculated as Teq = (Tm-Tmin) / (Tmax-Tmin), with Tm = mean temperature of the period of pycnidia production, Tmin = 10°C, Tmax = 35°C; $DD_{6\text{-}24}(j)$ = cumulative degree-days on day j, calculated as in equation 17, in the time window defined by equation 21 or 22; estimates and standard errors of equation parameters were: 4.71±0.32, 1.26±0.11, 3.584±1.025, 12.09±2.41, 3.96±0.79. Equation 22 was developed and parameterized using the data of Caltrider (1961), Galet (1977), and Northover (2008) for the effect of temperature (R^2 =

0.75) (Figure 4C) and the data of Northover (1998) for the dynamics over the degree-days ($R^2 = 0.88$) (Figure 4B).

Pycnidia on leaf and berry lesions are the source of inoculum from secondary infections. The kinetics of conidia release by a single cohort of pycnidia is not known. The model assumes that pycnidia extrude conidia during four consecutive wetness periods of at least 4 h each; 29, 28, 22, and 21% of the conidia are extruded in the 1st to 4th period (Northover, 1998).

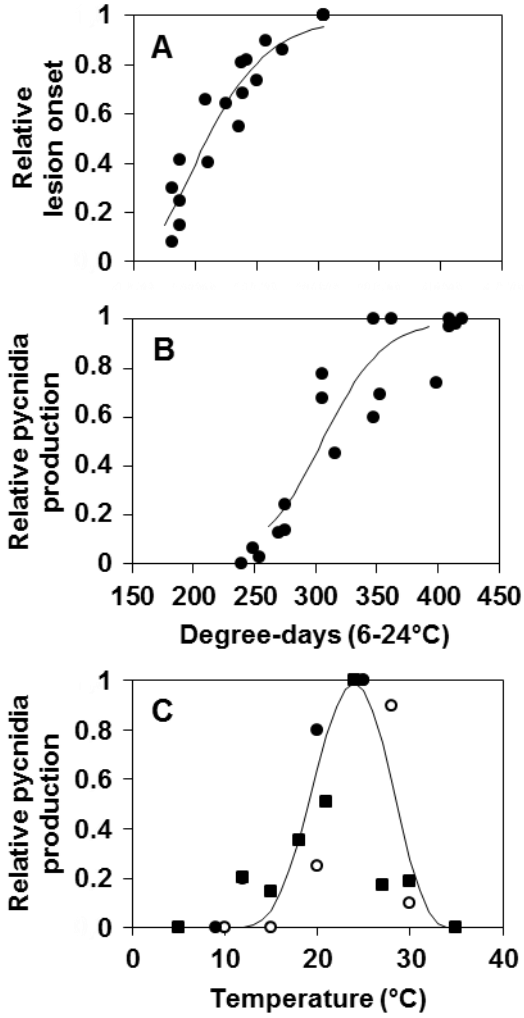

Figure 4. Progress of black-rot lesion onset over time after infection by *Guignardia bidwellii* (**A**), production of pycnidia over time after infection (**B**), and effect of temperature on production of pycnidia (C). In (A) and (B), time is expressed in degree-days between 6 and 24°C accumulated after infection. In (A), dots show the data of Hoffman *et al.* (2004), and the line shows the fit of data by the second term of equation 18, $R^2 = 0.91$. In (B), dots show the data of Northower (1998), and the line shows the fit of data by equation 21, $R^2 = 0.88$. In (**C**), dots show the data of Caltrider (1961) (○), Galet (1977) (●), and Northover (2008) (■); the line shows the fit of data by the first term of equation 22, $R^2 = 0.75$.

Model evaluation

To initiate the model, the parameters I, I', and I" were set at 0.7, 0.2, and 0.1, respectively. Because some mummies were present in the vineyards at bud break and canes showed no visible black-rot lesions, it was assumed that 70% of the primary inoculum consisted of ascospores from mummies, 20% consisted of conidia from mummies, and 10% consisted of conidia from canes.

In the Piacenza vineyard in 2010, the average temperature between bud break (early April) and the beginning of ripening (BBCH 81, early July) was 18.6°C with 240 mm of rain; a dry period occurred between 20 May and 14 June (Figure 5A), when vines were between "early blooming"(BBCH 63) and "berries beginning to touch" (BBCH 77) (Figure 5B). Black-rot was not severe; less than 3% of leaves were affected at the end of May, and an additional 1% were affected in early July, with no symptoms on berries. The model simulated eight infection periods in the Piacenza vineyard (Figure 5D); the first infection period occurred on 4-5 April and the last one on 20-21 June. These infection periods were not severe except for those on 3-5 May and 16 June. Because the vines were at "inflorescences swelling" (BBCH 55) on 3-5 May and "majority of berries touching" (BBCH 79) on 16 June (Figure 5B), the clusters were not susceptible to infection on these dates. In the former period (3-5 May), the inoculum dose was predicted to be high and mostly represented by ascospores (Figure 5C), but there were only 13 h of wetness at 15.3°C, which made infection possible by only a small part of the inoculum. Symptoms caused by this infection were predicted to appear in the last 10 days of May, as really occurred, and were to predicted to produce pycnidia between late May and early July (Figure 5D). The infection period on 16 June also had a high inoculum dose, consisting of both ascospores and conidia (most conidia were produced on sporulating lesions of the previous infection) because the previous dry period made the accumulation of spores possible in the fruiting bodies (Figure 5C); a period of 14 h at 19.1°C made infection possible, but with low severity. Lesions were predicted to appear in early July (Figure 5D), as was observed in the vineyard.

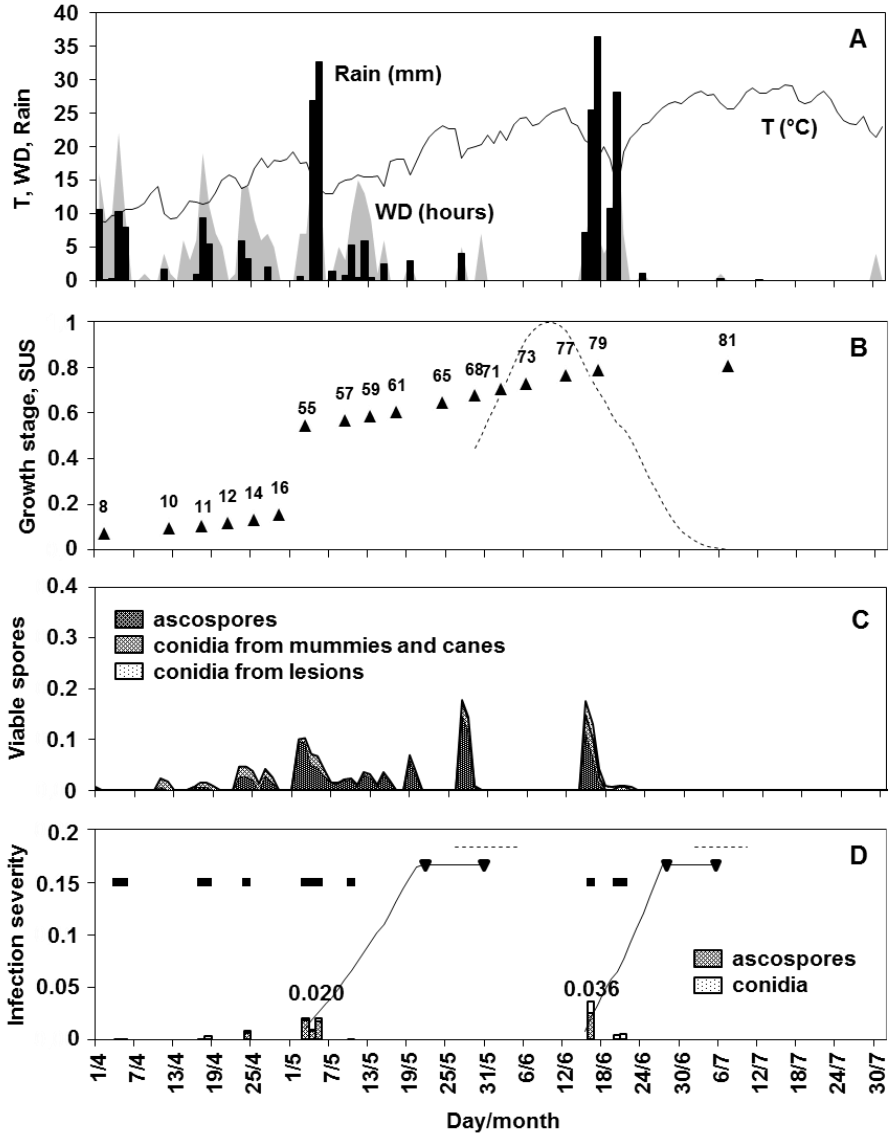

Figure 5. Model output for the Piacenza vineyard in 2010. (**A**) Air temperature (line), rainfall (bars), and leaf wetness duration (area). (**B**) Growth stages of the vines based on the BBCH scale (triangles) and relative susceptibility of clusters based on equation 15. (**C**) Viable ascospores, conidia from overwintered mummies or canes, and conidia from black-rot lesions. (**D**) Infection events (dots), relative severity of infections by ascospores or conidia (bars), progress of incubation (line), period of lesion onset (line between overturned triangles), and pycnidia production on lesions (dotted line); values are relative severity data for significant infection clusters.

In the Udine vineyard in 2010, 260 mm of rain fell with regular distribution between April and July; the average temperature was 18.4°C (Figure 6A). Black-rot appeared in the last 10 days of May on leaves and then progressed over the season on both leaves and clusters, with severe epidemics and >60% yield loss. The model predicted 20 infection periods in the Udine vineyard; most were clustered in four periods, which were predicted to have a significant effect on the black-rot epidemic (Figure 6D). In the first infection cluster, between 2 and 6 May, when vines were in the pre-blooming stage (BBCH55 to 57) (Figure 6B), there were four infections; the most severe were on 4 May (14 h of wetness at 15.6°C) and on 5 May (15 h of wetness at 13.8°C). In that period, 70% of the hours were wet, and there was 61 mm of rainfall. In addition, about 30% and 10% of the seasonal dose of ascospores and conidia, respectively, were available from the overwintered sources (Figure 6C). In the second infection cluster, 9 to 15 May, four additional infections occurred, with 33 h of wetness at 13.8°C between 12 and 13 May. All of the above-mentioned infections were estimated to produce visible lesions between 21 May and 5 June and pycnidia between 27 May and 10 June (Figure 6D). In the third infection cluster, 29 to 31 May, both primary and secondary inoculum were predicted to be present, which caused infection in two periods, one with 14 h of wetness at 16.1°C and the other with 10 h of wetness at 16.7°C. Vines were at the "end of blooming"(BBCH 68) (Figure 6B), and therefore these infections were expected to involve the clusters and to begin producing visible lesions between 11 and 20 June; pycnidia were predicted to appear on 17 to 26 June (Figure 6D). The last infection cluster occurred between 13 to 21 June, and was predicted to cause severe infections on clusters (as really occurred) because: (i) berries were in a highly susceptible stage (Figure 6B); (ii) abundant (mainly secondary) inoculum was present (Figure 6C); and (iii) there were four infection periods (Figure 5D), including one with 31 h of wetness at 15°C, and one with 27 h of wetness at 19.8°C.

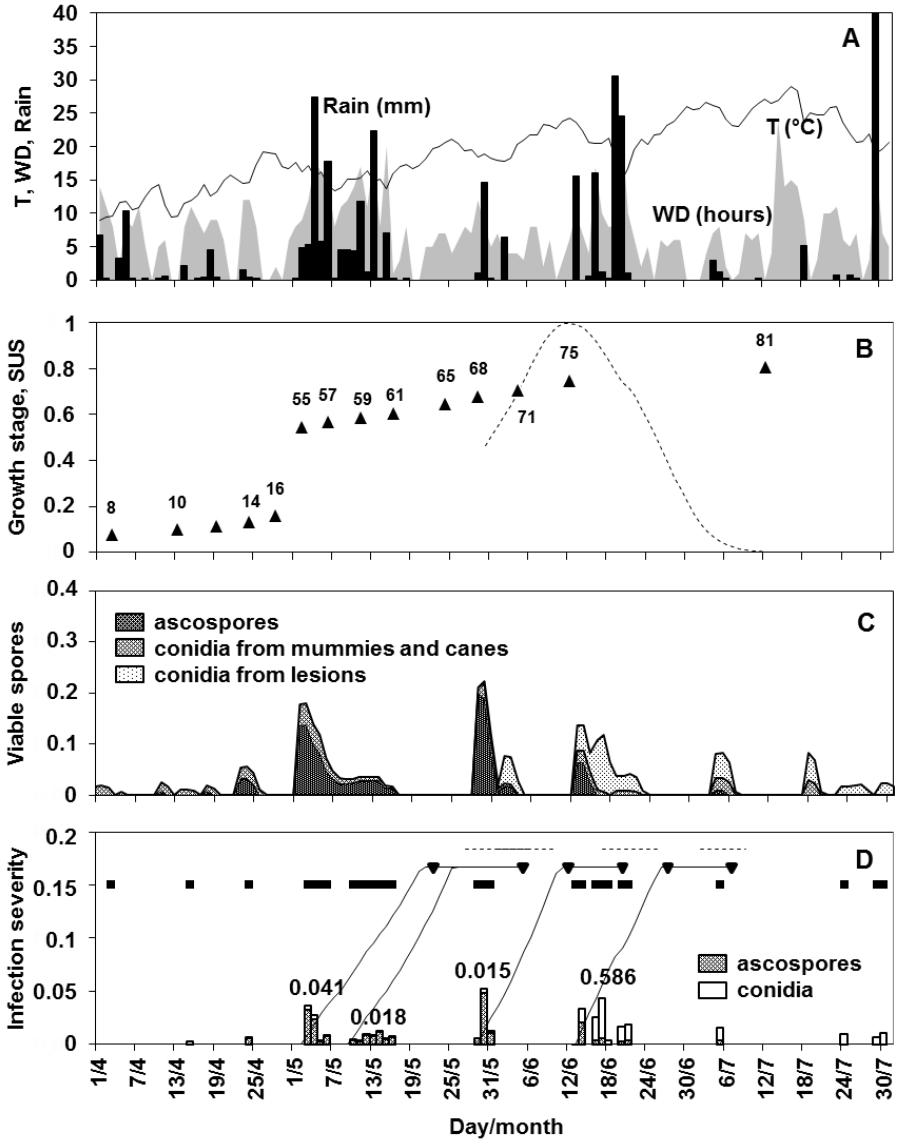

Figure 6. Model output for the Udine vineyard in 2010. (**A**) Air temperature (line), rainfall (bars), and leaf wetness duration (area). (**B**) Growth stages of the vines based on the BBCH scale (triangles) and relative susceptibility of clusters based on equation 15. (**C**) Viable ascospores, conidia from overwintered mummies or canes, and conidia from black-rot lesions. (**D**) Infection events (dots), relative severity of infections by ascospores or conidia (bars), progress of incubation (line), period of lesion onset (line between overturned triangles), and pycnidia production on lesions (dotted line); values are relative severity data for significant infection clusters.

In the Piacenza vineyard in 2012, the average temperature of the considered period was 19.3°C; 317 mm of rain occurred, mostly in April and between mid-May and mid-June (Figure 7A). Black-rot symptoms appeared on leaves in a narrow period of time in the first week of June; no further lesions developed on leaves or berries. Ten infection periods were calculated by the model (Figure 7D), but only one (on 20 and 21 May) was significant, when about 30% of the seasonal ascospore dose and 5% of the conidia from overwintered sources were available because a previous period with no rain favored the recovery of the fruiting bodies (Figure 7C). During this infection period (which lasted 27 h and had an average temperature of 12.9°C and repeated rainfall), vines were at "the beginning of blooming" (Figure 7B). Disease symptoms were predicted to appear between 2 and 11 June (Figure 7D), as really occurred in the vineyard. No further infection was predicted until late July even though both primary and secondary inoculum was present (Figure 7C) and rain fell (Figure 7A), because the duration of leaf wetness was too short. In agreement with model output, no further black-rot symptoms were observed on leaves or berries.

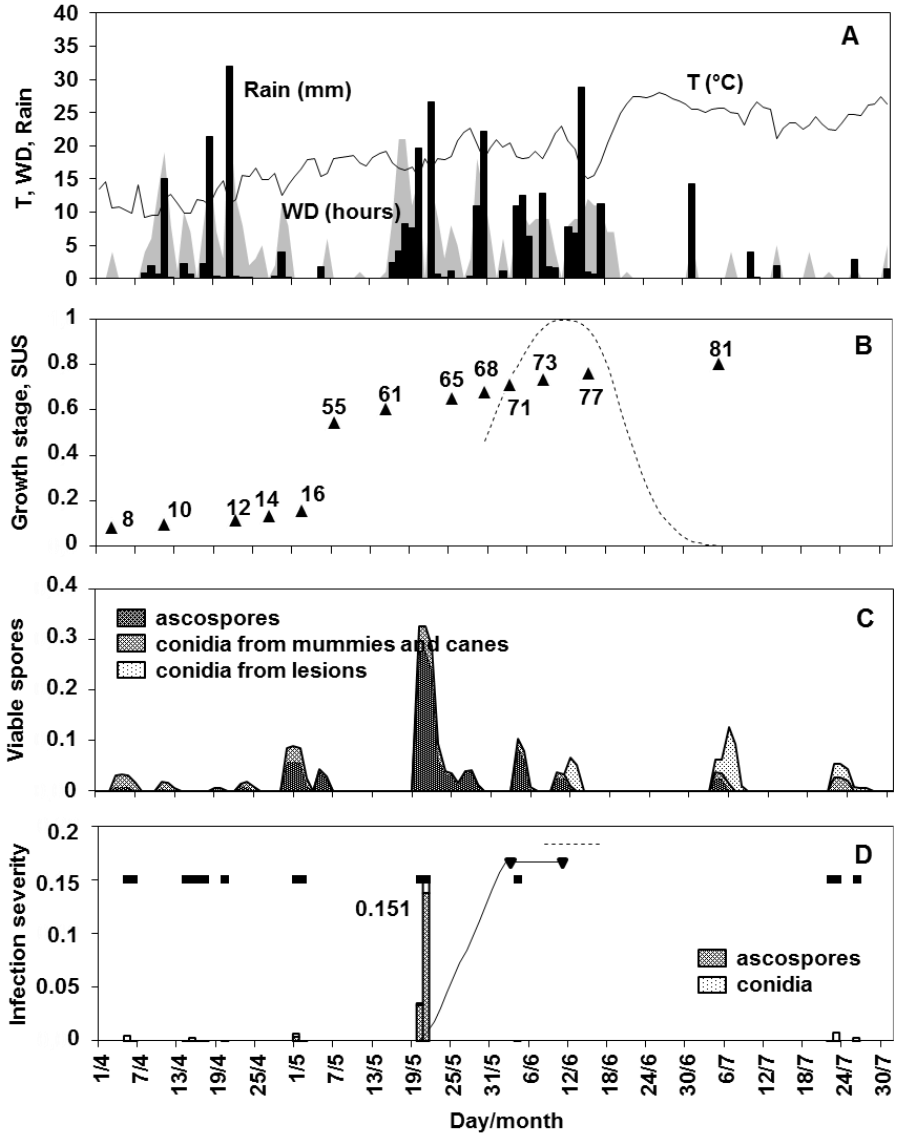

Figure 7. Model output for the Piacenza vineyard in 2012. (**A**) Air temperature (line), rainfall (bars), and leaf wetness duration (area). (**B**) Growth stages of the vines based on the BBCH scale (triangles) and relative susceptibility of clusters based on equation 15. (**C**) Viable ascospores, conidia from overwintered mummies or canes, and conidia from black-rot lesions. (**D**) Infection events (dots), relative severity of infections by ascospores or conidia (bars), progress of incubation (line), period of lesion onset (line between inverted triangles), and pycnidia production on lesions (dotted line); values are relative severity data for significant infection clusters.

DISCUSSION

Our literature search, which was carried out using systematic literature search principles, confirmed that many studies have been published concerning the epidemiology of *G. bidwellii*; 468 papers were retrieved, and 39 were used as information/data sources for drawing the relational diagram of the pathogen life cycle and for developing the model.

Organization of the current knowledge, which was based on systems analysis, revealed incomplete knowledge about some important aspects of the *G. bidwellii* life cycle. Identifying important interactions not known before and revealing weaknesses in the current knowledge are benefits of systems analysis (Jeffers, 1978).

Weather conditions leading to infection by *G. bidwellii* conidia have been considered by several authors (Caltrider, 1961; Spotts, 1977; Ferrin and Ramsdell, 1978; Northover, 1998; Northover and Travis, 1998) with consistent findings, while ascosporic infection has been infrequently studied (Jailloux, 1992; Northover, 2008) and with inconclusive results. Data on germination dynamics indicate that ascospores and conidia differ in their response to temperature and wetness duration (Caltrider, 1961; Ferrin and Ramsdell, 1977); therefore, the two kinds of spores probably also differ in their infection dynamics. Because ascospores are the main form of primary inoculum and are present in the vineyards for a long time, it seems necessary to further investigate the influence of wetness duration and temperature on infection by ascospores.

The dynamics of pycnidia production on black-rot lesions also requires further investigation. This is a key aspect in modeling the disease because black-rot severity increases almost linearly when the dose of conidia used for inoculation increases (Loskill *et al.*, 2009). Duration of the latent period (i.e., the time between infection and onset of conidia production) has not been considered in depth, and only occasional, qualitative observations are available in the form of "days elapsed after symptom appearance" (Spotts 1980). Duration of the infectious period (i.e., the time when a lesion continues to produce pycnidia) was considered only by Northover (1998). This is an important knowledge gap because of the key role of latent and infectious periods in epidemic development and in epidemic modeling (Vanderplank, 1963; Cunniffe *et al.*, 2012; Ferrandino, 2012) and because berry infection is mainly caused by secondary inoculum (Ramsdell and Milholland, 1988; Carisse *et al.*, 2009). In other pycnidia-producing fungi, these aspects have been carefully considered. In *Leptosphaeria maculans*, for example, the latent period was shortened by increasing temperature, relative humidity, and photoperiod and by injury to the host at the site of infection but was unaffected by age and variety of host and density of inoculum (Vanniasingham and Gilligan, 1989). In *Septoria tritici*, the latent period ranged from 14 to 21 days at the optimal temperature (15-20°C) to 40 days at 5°C (Eyal *et al.*, 1987; Shaw, 1990). In plants kept in continuously water-saturated air, the latent period was 6 days; in plants kept in alternating

wet and dry (85-90% relative humidity) air, pycnidia maturation was delayed by 5.6 days; in dry air, no sporulation occurred (Shearer and Zadoks, 1972).

In addition to the lack of knowledge about the length of latent and infectious periods, there is no information about the number of pycnidia produced per unit of lesion surface area, pycnidia ad conidia production dynamics over the infectious period, and the relationships between pycnidia production and weather conditions during infectiousness. Caldier (1961) and Viala and Pacottet (1904) studied the effect of temperature on pycnidia production on artificial media, while Northover (2008) studied pycnidia production on shoot lesions as affected by temperature and wetness duration at the time of infection but not during the time when pycnidia are produced. In other pycnidia-producing fungi, production of pycnidia is influenced not only by temperature but also by humidity. In *Didymella rabiei*, for example, pycnidia and conidia production on infected chickpea leaves increased slightly with high relative humidity but increased greatly over an 8-day period when the leaves were kept wet (Jhorar *et al.*, 1998). In *Phomopsis amygdali*, optimal temperatures for cirri formation and conidia production range from 19 to 20°C and from 22 to 23°C, respectively, and most sporulation occurs between 16 and 48 h after a period of high humidity (Lalancette *et al.*, 2003).

Conidia production in and extrusion from pycnidia also require further investigation. In particular, there is no information about conditions under which pycnidia extrude mature conidia and on the number of extrusion cycles before pycnidia are depleted (Northover, 1998). In *Leucostoma cincta*, for example, pycnidia extrude conidia in cirri when they have been wet for a few hours or under high humidity conditions, and conidia survive in cirri until they are removed by splashing rain; afterwards, pycnidia extrude new conidia, and this cycle repeats for several wetting periods (Barakat *et al.*, 1995). In *Septoria tritici*, 40 to 60% of the conidia were extruded at the first wetting period, the number of extruded conidia decreased markedly with successive wettings, and extrusion nearly ceased after four to five wettings (Gough, 1978; Eyal *et al.*, 1987).

The model developed in this paper provides detailed output concerning the life cycle of *G. bidwellii*. All the relevant stages of the life cycle were considered as well as the interactions between variables within the pathosystem, so that the model can be considered fundamental or mechanistic (Rossi *et al.*, 2010). Meta-analysis of published data made it possible to develop equations that linked external variables regarding weather and host plant to the pathogen; therefore, the model is dynamic. The lack of knowledge was bypassed by making explicit assumptions (Rossi *et al.*, 2010). Based on the results obtained by comparing model output with three typical black-rot epidemics, it can be stated that the model structure and its mathematical formulation give a reliable picture of *G. bidwellii* biology and epidemiology. Nevertheless, the model will be improved by the filling of the discussed knowledge gaps.

At present, the model can be used to increase our understanding of black-rot epidemics in vineyards. Because of its mechanistic structure and its dependence on weather conditions and vine growth, the model could be used in the future as a predictive tool for disease management, as is the case for similar models for grapevine downy and powdery mildews (Rossi *et al.,* 2008; Caffi *et al.,* 2011). This will require model validation by comparing model output with real-word observation in multiple years and vineyards. The use of the model as a predictive tool will also require the comparison of the control obtained with fungicide applications based on the model vs. those based on the calendar or grower schedules. Once validated, the model could be finally integrated into decision-support systems (Rossi *et al.,* 2012).

LITERATURE CITED

Aust, H., Kranz, J., 1988. Experiments and procedures in epidemiological field studies. In: J. Kranz and J. Rotem (Ed.), *Experimental techniques in plant disease epidemiology* (pp. 7-17). Berlin: Springer-Verlag.

Barakat, R.M., Johnson, D.A., Grove, G.G., 1995. Factors affecting conidial exudation and survival, and ascospore germination of *Leucostoma cincta*. Plant Disease 79, 1245-1248.

Becker, C.M., Pearson, R.C., 1996. Black-rot lesions on overwintered canes of *Euvitis* supply conidia of *Guignardia bidwellii* for primary inoculum in the spring. Plant Disease 80, 24-27.

Clabassi, I., 2000. Black-rot, Nuova ampelopatia in Friuli Venezia Giulia. In: A. Morando, M. Morando, and D. Morando (Ed.), *Vitenda 2000. L'agenda del vitivinicultore* (pp. 58-60). Calosso (Italy): Vit. En.

Caffi, T., Bugiani, R., Rossi, V., 2010. New forecasting models as effective tools for rational diseases control strategies in vineyards. Petria 20, 562-563.

Caffi, T., Legler, S.E., Rossi, V., Bugiani, R., 2012. Evaluation of a warning system for early-season control of grapevine powdery mildew. Plant Disease 96, 104-110.

Caffi, T., Rossi, V., Legler, S.E., Bugiani, R., 2011. A mechanistic model simulating ascosporic infections by *Erysiphe necator*, the powdery mildew fungus of grapevine. Plant Pathology 60, 522-531.

Caltrider, P.G., 1961. Growth and sporulation of *Guignardia bidwellii*. Phytopathology 51, 860-863.

Carisse, O., Bacon, R.M., Lasnier, J., Lefebvre, A., *et al.*, 2009. Grape disease management in Quebec. Agriculture and Agri-Food Canada 10372, 36-39.

Cunniffe, N.J., Stutt, R.O.J.H., van den Bosch, F., Gilligan, C.A., 2012. Time-dependent infectivity and flexible latent and infectious periods in compartmental models of plant disease. Phytopathology 102, 365-380.

Devaut, T.,1990. Contribution a la modelisation des contaminations de la vigne Par *Guignardia bidwellii* (Ellis) Viala e Ravaz agent responsable du Black-rot. Section de troisiéme cycle intércoles. Montpellier: Ecole nationale superieure agronomiqe.

Doufor, R., 2006. Grapes: Organic production. Resource document. ATTRA IP031. https://attra.ncat.org/attra-pub/summaries/summary.php?pub=5. Accessed 19 May 2014.

Ellis, M.A., Madden, L.V., Wilson, L.L., 1986. Electronic grape black rot predictor for scheduling fungicides with curative activity. Plant Disease 70, 938-940.

Emele, L.R., Wilcox, W.F., Gadoury, D.M., Seem, R.C., 1998. Critical period for control of black rot of grape. Phytopathology 88, S25.

Eyal, Z., Scharen, A.L,, Prescott, J.M., Ginkel, M.V., 1987. The *Septoria* diseases of wheat: concepts and methods of disease management. Mexico, DF: CIMMYT.

Ferrandino, F.J., 2012. Time scales of inoculum production and the dynamics of the epidemic. Phytopathology 8, 728-732.

Ferrin, D.M., Ramsdell, D.C., 1977. Ascospore dispersal and infection of grapes by *Guignardia bidwellii*, the causal agent of grape black-rot disease. Phytopathology 67, 1501-1505.

Ferrin, D.M., Ramsdell, D.C., 1978. Influence of conidia dispersal and environment on infection of grape by *Guignardia bidwellii*. Phytopathology 68, 892-895.

Funt, R.C., Ellis, M.A., Madden, L.V., 1990. Economic analysis of protectant and disease-forecast-based fungicide spray programs for control of apple scab and grape black-rot in Ohio. Plant Disease 74, 638-642.

Galet, P., 1977. Black-rot. In: Les Maladies et les Parasites de la vigne: Les Champignons et les Virus. Vol 1. (pp. 223-260). Montpellier, France: Paysan du Midi.

Gough, F.J., 1978. Effect of wheat host cultivars on pycnidiospore production by *Septoria tritici*. Phytopathology 68, 1343-1345.

Harms, M., Holz, B., Hoffmann, C., Lipps, H.P., *et al.*, 2005. Occurrence of *Guignardia bidwellii*, the causal agent of Black-rot on grapevine, in the vine growing areas of Rhineland-Palatinate, Germany. In: Proc. Int. Symposium on Introduction and Spread of Invasive Species. Berlin, Germany.

Hoffman, L.E., Wilcox, W.F., Gadoury, D.M., Seem, R.C., 2002. Influence of grape berry age on susceptibility to *Guignardia bidwellii* and its incubation period length. Phytopathology 92, 1068-1076.

Hoffman, L.E., Wilcox, W.F., Gadoury, D.M., Seem, R.C., Riegel, D.G., 2004. Integrated control of grape black-rot: Influence of host phenology, inoculum availability, sanitation, and spray timing. Phytopathology 94, 641-650.

Jailloux, F., 1992. In-vitro production of the teleomorph of *Guignardia bidwellii*, causal agent of black rot of grapevine. Canadian Journal of Botany 70, 254-257.

Jeffers, J.N.R., 1978. An introduction to Systems analysis: with Ecological Applications. London: Edward Arnold.

Jermini, M., Gessler, C., 1996. Epidemiology and control of grape black-rot in southern Switzerland. Plant Disease, 80, 322-325.

Jhorar, O.P., Butler, D.R., Mathauda, S.S., 1998. Effects of leaf wetness duration, relative humidity, light and dark on infection and sporulation by *Didymella rabiei* on chickpea. Plant Pathology 47, 586-594.

Kranz, J., Hau, B., 1980. Systems analysis in Epidemiology. Annual Review of Phytopathology 18, 67-83.

Lalancette, N., Foster, K.A., Robison, D.M., 2003. Quantitative models for describing temperature and moisture effects on sporulation of *Phomopsis amygdali* on peach. Phytopathology 93, 1165-1172.

Leffelaar, P.A., Ferrari, T.J., 1989. Some elements of dynamic simulations. In: R. Rabbinge, S.A. Ward, H.H. van Laar (Ed.). Simulation and systems management in crop protection (pp. 19-45). Wageningen: Pudoc.

Lorenz, D.H., Eichhorn, K.W., Bleiholder, H., Klose, R., *et al.*, 1995. Phenological growth stages of the grapevine, *Vitis vinifera* L. ssp. vinifera. Codes and descriptions according to the extended BBCH scale. Australian Journal of Grape and Wine Research 1, 100-103.

Loskill, B., Molitor, D., Koch, E., Harms, M., *et al.*, 2009. Management of Black-rot (*Guignardia bidwellii*) in organic viticulture. Resource document. BÖL-Bericht-ID 17072, Accessed 19 May 2014.

Lovell, D.J., Powers, S.J., Welham, S.J., Parker, S.R., 2004. A perspective on the measurement of time in plant disease epidemiology. Plant Pathology 53, 705-712.

Luestner, G., 1935. Auftreten der Schwarzfäule (Black-Rot) der Rebe in Deutschland. Nachr Dtsch Pflanzenschutzd 15,27.

Madden, L.V., Hughes, G., van den Bosch, F., 2007. The Study of Plant Disease Epidemics. APS Press, St Paul (MN, USA).

Magarey, R.D., Sutton, T.B., Thayer, C.L., 2005. A simple generic infection model for foliar fungal plant pathogens. Phytopathology 95, 92-100.

Maurin, G., Cartolaro, P., Clerjeau, M., 1992. Black-rot: vers une methode de previsions des risques. IOBC/WPRS Bulletin 15(2), 62.

Molitor, D., 2009. Biologie und Bekämpfung der Schwarzfäule (*Guignardia bidwellii*) an Weinreben. Geisenheimer Berichte Bd. 65. Geisenheim (Germany): Gesellschaft zur Förderung der Forschungsanstalt.

Molitor, D., Berkelmann-Loehnertz, B., 2011. Simulating the susceptibility of clusters to grape black-rot infections depending on their phenological development. Crop Protection 30, 1649-1654.

Molitor, D., Fruehauf, C., Baus, O., Berkelmann-Loehnertz, B., 2012. A cumulative degree-day-based model to calculate the duration of the incubation period of *Guignardia bidwellii*. Plant Disease 96, 1054-1059.

Mueller, K., 1934. Jahresbericht des BadischenWeinbauinstitutes in Freiburg i. B. für das Jahr, vol. 13.

Northover, P.R., 1998. The relationship of the number of wetting periods and accumulated degree-days to sporulation of *Guignardia bidwellii* (Ellis) Viala and Ravaz in vineyards. M.Sc. Thesis. Pennsylvania State University.

Northover, P.R., 2008. Factors influencing the infection of cultivated grape (*Vitis* spp. section *Euvitis*) shoot tissue by *Guignardia Bidwellii* (Ellis) Viala and Ravaz. Ph.D. Thesis. Pennsylvania State University.

Northover, P.R., Travis, J.W., 1998. Infection requirements of *Guignardia bidwellii* conidia on grapevine shoots. Phytopathology 88, S68.

Okoli, C., Schabram, K., 2010. A Guide to Conducting a Systematic Literature Review of Information Systems Research. Sprouts: Working Papers on Information Systems 10:26. Resource document. http://sprouts.aisnet.org/10-26/. Accessed 01 April 2014.

Ramsdell, D.C., Milholland, R.D., 1988. Black-Rot. In: R.C. Pearson, A.C. Goheen (Ed.). Compendium of Grape Diseases (pp 15-17). St. Paul: APS press.

Rinaldi, P.A., Mugnai, L., 2012. Marciume nero degli acini, potenziale pericolo in viticoltura. Informatore Agrario 68, 68-70.

Rossi, V., Caffi, T., Giosuè, S., Bugiani, R., 2008. A mechanistic model simulating primary infections of downy mildew in grapevine. Ecological Modelling 212, 480-491.

Rossi, V., Caffi, T., Salinari, F., 2012. Helping farmers face the increasing complexity of decision-making for crop protection. Phytopathologia Mediterranea 3, 457-479.

Rossi, V., Giosuè, S., Caffi, T., 2010. Modelling Plant diseases for decision making in crop protection. In: E.C. Oerke, R. Gerhards, G. Menz, R.A. Sikora (Ed.). Precision Crop Protection - The Challenge and Use of Heterogeneity (pp 241-258). Dordrecht: Springer Science.

Rotem, J., 1988. Techniques of controlled-condition experiments. In: J. Kranz, J. Rotem (Ed.). Experimental techniques in plant disease epidemiology (pp 19-31). Heidelberg: Springer-Verlag.

Roussel, C., 1971. Etude comparative de l'évolution du mildiou et du black-rot de la vigne. Phytoma 228, 19-24.

Scribner, F.L., 1886. Report on the Fungus Diseases of the Grapevine. U. S. Dep. Agric. Bot. Div. Sect. Plant Pathol. Bull. 2 GPO, Washington D. C.

Shaw, M.W., 1990. Effects of temperature, leaf wetness and cultivar on the latent period of *Mycosphaerella graminicola* on winter wheat. Plant Pathology 39, 255-268.

Shearer, B.J., Zadoks, J.C., 1972. The latent period of *Septoria nodorum* in wheat I. The effect of temperature and moisture treatments under controlled conditions. Netherlands Journal of Plant Pathology 78, 231-241.

Spotts, R.A., 1977. Effect of leaf wetness duration and temperature on the infectivity of *Guignardia bidwellii* on grape leaves. Phytopathology 76, 1378-1381.

Spotts, R.A., 1980. Infection of grape by *Guignardia bidwellii*-factors affecting lesion development, conidia dispersal and conidial populations on leaves. Phytopathology 70, 252-255.

Vanderplank, J.E., 1963. Plant Disease: Epidemics and Control. New York: Academic Press.

Vanniasingham, V.M., Gilligan, C.A., 1989. Effects of host, pathogen and environmental factors on latent period and production of pycnidia of *Leptosphaeria maculans*on oilseed rape leaves in controlled environments. Mycological Research 93, 167-174.

Viala, P., Pacottet, P., 1904. Recherches sue les maldies de la vigne: "Black-rot II, Sur le développment du Black-rot", réceptivitédes fruits, influence de la temperature, de l'humiditéet des milieux toxique. Paris: Bordeaux de la "Revue de viticulture".

Weber, M., 1987. Le Black-rot: éléments de biologie et moyens de lutte chimiqhe. Phytoma 376, 43-46.

Zadoks, J.C., 1971. Systems analysis and the dynamic of epidemics. Phytopathology 61, 600-10.

Zins, C., 1999. Success - structured search strategy: information retrieval in the age of global information systems. Resource document. http://archive.ifla.org/IV/ifla65/papers/081-143e.htm. Accessed 01 April 2014.

SUPPLEMENTARY MATERIAL 1

This supplementary material shows the meta-synthesis of the literature used to develop the relational diagram of the life cycle of *G. bidwellii* (Figure 1) and the different model compartments.

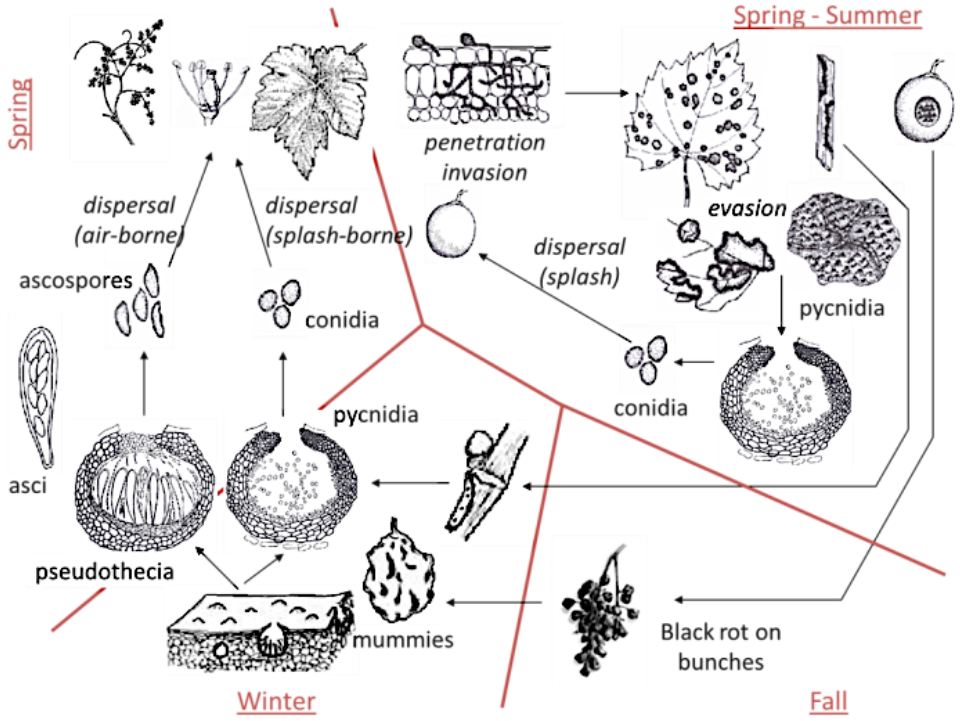

Figure 1. *Guignardia bidwellii* life cycle on grapevine.

Ascospores from mummies. Ascospores from 1-year-old rotted berries (mummies) that overwintered in the vineyard (on the ground or in the trellis) are the major form of primary inoculum, although conidia produced from overwintered mummies and cane lesions may also contribute to primary infections (Reddick, 1911; Roussel and Bouard, 1971; Ferrin and Ramsdell, 1977; Becker and Pearson, 1996). Ascogonial stromata are produced toward the end of the growing season in berry mummies (Pearson and Goheen, 1988), and they remain sterile until the end of winter, when they form ascii in locules, and the ascii produce ascospores (Arnaud, 1931; Roussel, 1971; Arpin, 1990). Studies carried out in different areas have consistently indicated that ascospores begin to mature shortly after bud break (Reddick, 1911; Ferrin and Ramsdell, 1977). In the area of Bordeaux (France), the first mature pseudothecia are observed 2±4.5 days after bud break (18-year average), and the first ascospores are released 8±4.8 days after bud break

(Roussel, 1971). Pseudothecia form and mature depending on the time when the lesions formed in the previous season (Arpin, 1990; Cartolaro *et al.*, 1992). In several studies, most ascospores were mature (and then released into the air) within 3 weeks to 2 months after bloom (Reddick, 1911; Ferrin and Ramsdell, 1977; Becker and Pearson, 1992; Jermini and Gessler, 1996). Airborne ascospores were found until September (preharvest) in Michigan (MI, USA) (Ferrin and Ramsdell, 1977) and until late August in Germany (Loskill *et al.*, 2009). Ascospores mature more slowly in mummies in the trellis than on the ground (Luestner, 1935; Becker and Pearson, 1992; Loskill *et al.*, 2009), and the rate of ascospore maturation differs between years. In NY (USA), 80 to >90% of the total ascospores were airborne between bud break and immediately before bloom in 1996, 1998, and 1999, while only 17% of the total ascospores were airborne in that period in 1997 (Hoffman *et al.*, 2004). These differences may be related to environmental conditions, because both production and maturation of pseudothecia depend on temperature, light, and humidity (Reddick, 1911; Arpin, 1990; Jailloux, 1992). Jailloux (1992) found that pseudothecia form between 5 and 15°C but differentiate ascospores only at 10 and 15°C, and that neither ascospore production nor maturation occurs at 20°C.

Conidia from mummies. Pycnidia are formed in affected berries during the previous season and persist during winter on the mummies (Clatrider, 1961). These winter pycnidia are granulous or undifferentiated conceptacles (Arpin, 1990), and they begin producing conidia after favorable conditions return (Clatrider, 1961): the pycnidium develops into a fertile central cavity that is then covered by conidiogenous cells, which produce conidia; afterwards, an ostiole is formed at the top of the cavity (Janex-Favre *et al.*, 1993). Conidia production occurs later than ascospore production (Arpin, 1990). Peaks of conidia occurred in late July in MI, i.e., 4 to 6 weeks after bloom (Ferrin and Ramsdell, 1978; Hoffman *et al.*, 2004). Production and maturation of conidia is also temperature-dependent and occurs between 12 to 30°C, with an optimum of 24°C (Northover, 2008).

Conidia from cane lesions. Production of conidia on cane lesions that have overwintered begins before bud break, indicating that inoculum from cane lesions would be available when susceptible tissue emerges. In NY, most conidia were released from lesions before or at bud break in 1990 to 1992; fewer conidia were detected as the season progressed but some conidia were still present near harvest in 1990 and 1991 but not in 1992, when no conidia were detected after mid-June (Becker and Pearson, 1996).

Spore release and deposition. Spring rains trigger release of ascospores from pseudothecia: increased pressure inside the ascus from water uptake forces the ascus to move up to the ostiole of the pseudothecium; the ascospores are then forcibly discharged

through the ostiole and into the air, where they can be blown for moderate distances by wind (Reddick, 1911). Rain and wind are key components of ascospore dispersal. Ascospore release occurred with as little as 0.3 mm of rain (Roussel and Board, 1971; Ferrin and Ramsdell, 1977). Ascospores are liberated as soon as rain begins and mummies are wetted. In the first hour of rain, over 90% of ascospores were airborne, and the release ended in 4 to 6 h (Ferrin and Ramsdell, 1977; Jermikni and Gessler, 1996). Release of conidia is also caused by rain. Pycnidia absorb water, and conidia are extruded in a white to hyaline colored cirrus that is dispersed for short distances by splashing rain drops. Pycnidia released conidia following 2.5 mm of rain (Ferrin and Ramsdell, 1978). The number of conidia dispersed by rain increases with the duration of rain. Maximum numbers of conidia in runoff water from lesions carrying pycnidia were collected between 60 and 120 min after a rain began; few conidia were collected during the first 45 min or after 3 h of exposure to rain (Spotts, 1980). In France, a threshold of 0.5 mm of rain was considered useful for estimating a release event (Maurin *et al.*, 1992).

Spore survival. Once spores are on the host surface, they either germinate in the presence of water or survive in dryness. Germination of ascospores incubated on dry leaves decreased as the period of incubation increased before rewetting of the leaves allowed germination; germination was 97% with no dry period but was 18% and 0% after 24 and 48 h of dryness, respectively, before rewetting (Ferrin and Ramsdell, 1977). Infection by conidia occurred after rewetting of leaves that had been kept dry for up to 2 days after inoculation, but a 1-day post-inoculation dry period caused a 1/3 reduction in infection severity; no infection occurred after three or more days of dryness (Spotts, 1977; Molitor, 2009).

Infection. Infection by ascospores and conidia involves the development of appressoria and subcuticular hyphae (Ullrich *et al.*, 2009). An extracellular matrix surrounds the spore, germling, and appressorium; the matrix is thought to be involved in adhesion to the substratum and host recognition (Kuo and Hoch, 1995). Within a few hours after attachment, spores germinate and form mature appressoria (Shaw *et al.*, 1998). A penetration peg breaches the cuticle, giving rise to hyphae that colonize the leaf by growing primarily between the cuticle and the anticlinal cell walls; only in later stages do they occasionally overgrow the periclinal walls of the epidermal cells (Kuo and Hoch, 1996; Ullrich *et al.*, 2009). Spotts (1977) determined the minimum wetness duration for leaf infection by conidia to be 6 h at 26.5°C, 24 h at 10.0°C, and 12 h at 32.0°C; Molitor (2009) documented leaf infection after 16 h of wetness at 10°C. Northover (2008) confirmed the above results for shoot infection. After the minimum requirements for infection have been met, disease severity increases over time until 72 h post-infection or when 1800 degree-days (base 0°C) have accumulated after inoculation of berries

(Molitor, 2009). Less information is available for infection caused by ascospores (Ferrin and Ramsdell, 1977). Relative to conidia, ascospores seem to germinate faster and at lower temperatures (Caltrider, 1961; Ferrin and Ramsdell, 1977). At 16°C, 16% of ascospores and about 1% of conidia germinated after 24 h; at 27°C, about 10% and 16% of ascospores germinated after 12 and 24 h, respectively, while germination of conidia was 4% and 9%, respectively. No ascospores germinated at 32°C, while germination of conidia was >40% after 36 h at 32°C (Caltrider, 1961; Ferrin and Ramsdell, 1977).

Host susceptibility. Leaf infection is possible as early as bud burst (Carisse *et al.*, 2009). Leaves are highly susceptible to the disease as they unfold and become resistant about the time when they finish expanding (Scribner and Viala, 1888; Prunet, 1898; Reddick, 1911; Manns, 1928). Young leaves (2^{nd} and 3^{rd} leaf from the shoot apex) show typical disease symptoms, whereas very young (1^{st} leaf) and older leaves ($\geq 5^{th}$ leaf) are not infected or only lightly infected. Spores germinate and form appressoria on all leaves irrespective of leaf position and age (Ullrich *et al.*, 2009); in mature leaves, the fungus penetrates the cuticle, but further development is limited to a few subcuticular hyphae that fail to branch and fail to form the typical subcuticular hyphal nets seen in young tissue (Kuo and Hoch, 1996; Ullrich *et al.*, 2009). Initial infection of inflorescences is possible from pre-bloom on the flower stalks (Molitor and Berkerlmann-Loehnertz, 2011). Fruit infection occurs from "cap fall" until veraison. In *V. vinifera*, berries remain highly susceptible from midbloom until 3 to 5 weeks later, and maintain a reduced level of susceptibility until they become highly resistant 6 or 7 weeks after bloom (Hoffman *et al.*, 2002). Under warm conditions, age-related resistance develops more quickly (Hoffman and Wilcox, 2002). Because temperatures after bloom vary from year to year, Molitor and Berkelmann-Loehnertz (2011) described changes in susceptibility as a function of the growth stage of the berries rather than by the temporal span after blooming; they estimated the berry growth stage and the relative susceptibility with a degree day-based model.

Incubation and latency periods. The time required for symptoms to appear depends on both the temperature and the age of the tissue when it was infected; relative humidity does not influence the incubation time or pycnidia formation on grape leaves (Spotts, 1980). Young leaves and fruit generally begin showing symptoms about 2 weeks after they become infected, and symptoms from a single infection period continue to appear over a period of 1 to 2 weeks following initial symptom expression (Kuo and Hoch, 1996; Hoffman *et al.*, 2002). Most berries that become infected near the end of their period of susceptibility do not show symptoms until at least 3 weeks later, and the majority do not begin to rot until 4 to 5 weeks after the infection event (Hoffman *et al.*, 2002). Pycnidia appear 3 to 5 days after lesion onset (Roussel and Bouard, 1971). The

duration of both incubation and latency (i.e., the time required for pycnidia to appear) periods in leaves is influenced by temperature (Spotts, 1980). The shortest duration of incubation and latency is 8 and 12 days, respectively, at 24°C; the duration of both periods increases as temperature either increases or decreases. Hoffman *et al.*, (2002) and Molitor *et al.,* (2012) expressed the duration of incubation as degree-hours and degree-days, respectively, with similar results. The first symptoms on leaves appear after reaching a threshold of 175 cumulative degree-days (calculated as the sum of average daily temperatures between 6 and 24°C starting on the day after the infection); on clusters, the duration of the incubation period is additionally affected by the growth stage at the time of infection (Molitor *et al.*, 2012). Symptoms continue to appear on berries for about 4,400 degree-hours (base 0°C) (Hoffman *et al.*, 2002), which corresponds to about 130 degree-days (base 6°C).

Production of pycnidia in lesions. After the first pycnidia have appeared, they continue to appear for 10-14 days (Luttrell, 1946). Production of pycnidia depends on temperature; Caltrider (1961), Viala and Pacottet (1904), and Northover (2008) consistently found that pycnidia are produced when the temperature is >10°C and <35°C, with an optimum at 24°C. Northover (1998) found that the duration of the infectious period was about 200°C (degree-days accumulated using a base threshold of 7°C and an upper limit of 26°C), with 90% of the pycnidia being produced in 140-150 degree-day. Pycnidia on leaf and berry lesions are the source of inoculum from secondary infections. Release of conidia from these pycnidia was studied by Ferrin and Ramsdell (1978), who found that lesions release pycnidia repeatedly during a black-rot epidemic.

LITERATURE CITED

Arnaud, G., 1931. Traité de la pathologie végétale 1. P. Lechevalier and Fils, Paris.

Arpin, N., 1990. Etude des formes hivernales de conservation de *Guignardia bidwellii* (Ellis) Viala et Ravaz, agent responsable du black-rot de la vigne. Diplome d'etudes approfondies d'oenologie –ampelologie. Station de pathologie vegetale, Bordeaux.

Becker, C.M., Pearson, R.C., 1992. Patterns of spore release from black rot (*Guignardia bidwellii*) infected grape mummies that overwintered on the ground or in the canopy. Phytopathology 82, 1084.

Becker, C.M., Pearson, R.C., 1996. Black rot lesions on overwintered canes of *Euvitis* supply conidia of *Guignardia bidwellii* for primary inoculum in the spring. Plant Disease 80, 24-27.

Caltrider, P.G., 1961. Growth and sporulation of *Guignardia bidwellii*. Phytopathology 51, 860-863.

Carisse, O., Bacon, R.M., Lasnier, J., Lefebvre, Levasseur, A., Rolland, D., Jobin, T., 2009. Grape disease management in Quebec. Agriculture and Agri-Food Canada 10372, 36-39.

Cartolaro, P., Arpin, N., Clerjeau, M., 1992. Influence de la date de contamination au vignoble sur l'evolution de la maturation des peritheces de *Guignardia bidwellii*. IOBC/WPRS Bull. 15(2), 63.

Ferrin, D.M., Ramsdell, D.C., 1977. Ascospore dispersal and infection of grapes by *Guignardia bidwellii*, the causal agent of grape black rot disease. Phytopathology 67, 1501-1505.

Ferrin, D.M., Ramsdell, D.C., 1978. Influence of conidia dispersal and environment on infection of grape by *Guignardia bidwellii*. Phytopathology 68, 892-895.

Funt, R.C., Ellis, M.A., Madden, L.V., 1990. Economic analysis of protectant and disease-forecast-based fungicide spray programs for control of apple scab and grape black rot in Ohio. Plant Disease 74, 638-642.

Hoffman, L.E., and Wilcox, W.F. 2002. Utilizing epidemiological investigations to optimize the management of grape black-rot. *Phytopathology* 92, 676-680.

Hoffman, L.E., Wilcox, W.F., Gadoury, D.M., Seem, R.C., 2002. Influence of grape berry age on susceptibility to *Guignardia bidwellii* and its incubation period length. Phytopathology 92, 1068-1076.

Hoffman, L.E., Wilcox, W.F., Gadoury, D.M., Seem, R.C., Riegel, D.G., 2004. Integrated control of grape black-rot: Influence of host phenology, inoculum availability, sanitation, and spray timing. Phytopathology 94, 641-650.

Jailloux, F., 1992. In-vitro production of the teleomorph of *Guignardia bidwellii*, causal agent of black-rot of grapevine. Canadian Journal of Botany 70, 254-257.

Janex-Favre, M.C., Parguey-Leduc, A., Jailloux, F., 1993. The ontogeny of pycnidia of *Guignardia bidwellii* in culture. Mycological Research 97, 1333-1339.

Jermini, M., Gessler, C. 1996. Epidemiology and control of grape black rot in southern Switzerland. Plant Disease 80, 322-325.

Kuo, K., Hoch, H.C., 1995. Visualization of the extracellular matrix surrounding pycnidiospores, germlings, and appressoria of *Phyllosticta ampelicida*. Mycologia 87, 759-771.

Kuo, K., Hoch, H.C., 1996. Germination of *Phyllosticta ampelicida* pycnidiospores: Prerequisite of adhesion to the substratum and the relationship of substratum wettability. Fungal Genetics and Biology 20, 18-29.

Kuo, K., Hoch, H.C., 1996. The parasitic relationship between *Phyllosticta ampelicida* and Vitis vinifera. Mycologia 88, 626-634.

Loskill, B., Molitor, D., Koch, E., Harms, M., Berkelmann-Löhnertz, B., Hoffmann, C., Kortekamp, A., Porten, M., Louis, F., Maixner, M., 2009. Management of Black-rot (*Guignardia bidwellii*) in organic viticulture. Online pubblication/BÖL-Bericht-ID 17072.

Luestner, G., 1935. Auftreten der Schwarzfäule (Black-Rot) der Rebe in Deutschland. Nachr. Dtsch. Pflanzenschutzd 15, 27.

Luttrell, E.S., 1946. Black-rot of muscadine grapes. Phytopathology 36, 905-924.

Manns, T.F., 1928. Grape disease control in Delaware. Univ. Del. Agric. Exp. Stn. Bull. 154.

Maurin, G., Cartolaro, P., Clerjeau, M., 1992. Black-rot: vers une methode de previsions des risques. IOBC/WPRS Bull. 15(2), 62.

Molitor, D., 2009. Biologie und Bekämpfung der Schwarzfäule (*Guignardia bidwellii*) an Weinreben. Geisenheimer Berichte Bd. 65. Gesellschaft zur Förderung der Forschungsanstalt Geisenheim, Germany.

Molitor, D., Berkelmann-Loehnertz, B., 2011. Simulating the susceptibility of clusters to grape black rot infections depending on their phenological development. Crop Protection 30, 1649-1654.

Molitor, D., Fruehauf, C., Baus, O., Berkelmann-Loehnertz, B., 2012. A cumulative degree-day-based model to calculate the duration of the incubation period of *Guignardia bidwellii*. Plant Disease 96, 1054-1059.

Northover, P.R. 1998. The relationship of the number of wetting periods and accumulated degree-days to sporulation of *Guignardia bidwellii* (Ellis) Viala and Ravaz in vineyards. M.Sc. Thesis. Pennsylvania State University.

Northover, P. R. 2008. Factors influencing the infection of cultivated grape (*Vitis* spp. section *Euvitis*) shoot tissue by *Guignardia bidwellii* (Ellis) Viala and Ravaz. Ph.D. Thesis. Pennsylvania State University.

Pearson, R.C., Goheen, A.C., 1988. Diseases caused by biotic factors fruit and foliar diseases caused by fungi. In: Compendium of grape diseases (pp. 9-59). St.Paul: APS Press.

Prunet, A., 1898. Observation et experiences sur le black-rot II. Conditions internes du development du black-rot. Rev. Vit. 9, 601-603.

Reddick, D., 1911. The black rot disease of grapes. Cornell Univ. Agric. Exp. Stn. Bull. 293, 289-364.

Roussel, C., 1971. Etude comparative de l'évolution du mildiou et du black-rot de la vigne. Phytoma 228, 19-24.

Roussel, C., Bouard, J., 1971. Maladies cryptomaniques. In: Traite d'Ampelologie; Sciences e Techniques de la Vigne (pp. 239-251). Paris : Dunod.

Scribner, F.L., Viala, P., 1888. Black-rot (*Laestadia bidwellii*). U. S. Dep. Agric. Bot. Div. Sect. Div. Pathol. Bull. 7, 1-29.

Shaw, B.D., Kuo, K., Hoch, H.C., 1998. Germination and appressorium development of *Phyllosticta ampelicida* pycnidiospores. Mycologia 90, 258-268.

Spotts, R.A., 1977. Effect of leaf wetness duration and temperature on the infectivity of *Guignardia bidwellii* on grape leaves. Phytopathology 76, 1378-1381.

Spotts, R.A., 1980. Infection of grape by *Guignardia bidwellii*-factors affecting lesion development, conidia dispersal and conidial populations on leaves. Phytopathology 70, 252-255.

Ullrich, I.C., Kleespies, R.G., Enders, M., Koch, E., 2009. Biology of the black-rot pathogen, *Guignardia bidwellii*, its development in susceptible leaves of grapevine *Vitis vinifera*. Journal für Kulturflanzen 61, 82-90.

Viala, P., Pacottet, P., 1904. Recherches sue les maldies de la vigne: "Black-rot II, Sur le développment du Black-rot", réceptivité des fruits, influence de la temperature, de l'humidité et des milieux toxique. Bordeaux de la "Revue de viticulture", Paris.

Weber, M., 1987. Le Black-rot: éléments de biologie et moyens de lutte chimiqhe. Phytoma 376, 43-46.

SUPPLEMENTARY MATERIAL 2

In this supplementary material, three examples on how the literature data were used to develop the model equations are provided.

Example 1. Equation 2 of the model was developed by combining data from Ferrin and Ramsdell (1977) and from Jermini and Gessler (1996). Ferrin and Ramsdell (1977) trapped airborne ascospores with a Burkard 7-day volumetric spore trap located in two Michigan vineyards during the 1974 and 1975 grape-growing seasons. Jermini and Gessler (1996) carried out a similar study in Ticino, Switzerland, in 1990. Both papers show ascospore trapping data over time, expressed as calendar days, and provide information about growth stage of the vines during the study. The cumulative numbers of ascospores trapped over the season were determined and expressed as relative values by dividing the cumulative number on each date by the total number for the season. The cumulative relative trapping values for the 3 years (dependent variable Y) were then pooled, plotted against days after bud break (dependent variable X), and fitted to a Gompertz equation in the form $Y = \exp(-a \times \exp(-b \times X / 100))$, with $a = 7.65 \pm 1.48$, $b = 0.071 \pm 0.006$, and $R^2 = 0.87$ (Figure 1A). The equation did not fit the data accurately, especially in the first 40 days after bud break, because the pattern of the ascospore trapping data differed in the different locations.

Time after bud break was then expressed as cumulative degree-days, by accumulating daily temperatures in the interval 9 to 19°C. The requirement of this temperature interval for pseudothecia to mature ascospores was drawn from Jailloux (1992), who determined the production of mature pseudothecia (i.e., with well-differentiated ascospores) at 5 to 25°C on oatmeal agar. The data of Jailloux (1992) were expressed as the relative production of mature pseudothecia (dependent variable Y) by dividing the number of pseudothecia formed at each temperature by the highest number formed in the experiment. These data were then regressed against temperature by using a bête equation in the form: $Y = (a \times X^b \times (1-X))^c$, where the independent variable X is an equivalent of temperature calculated as (T-Tmin) / (Tmax-Tmin). The best fit was obtained by setting Tmin and Tmax at 9 and 19°C, respectively, with $R^2 = 0.92$ (Figure 1B). According to these limits, no ascospores mature in pseudothecia when temperatures are less than 9°C or greater than 19°C.

The goodness-of-fit of the Gompertz equation increased when the cumulative relative trapping values of the 3 years were regressed against accumulated degree-days after bud break rather than days after bud break (Figure 1C); R^2 increased from 0.87 to 0.97. This equation was then used as equation 2 in the model.

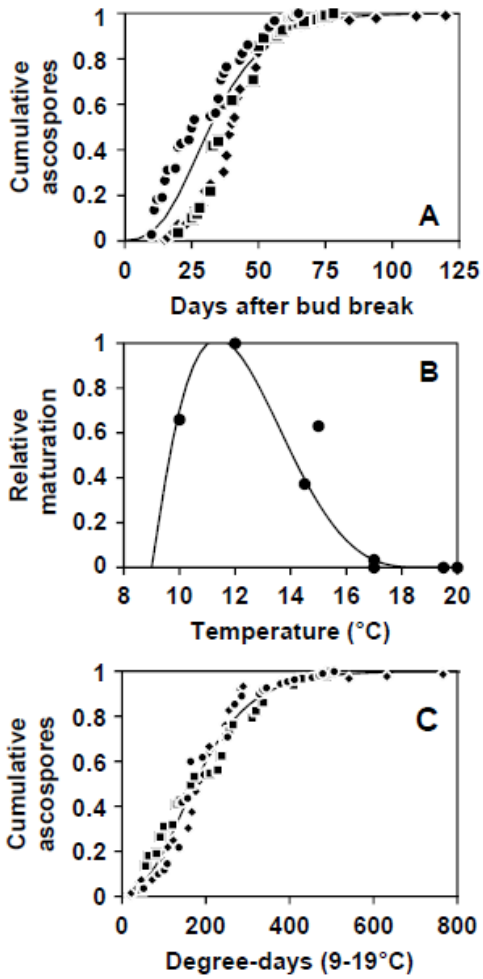

Figure 1. Cumulative proportion of mature ascospores of *Guignardia bidwellii* over time expressed in days (**A**) and accumulated degree-days (between 9 and 19°C) (**B**) after bud break and effect of temperature on ascospore maturation (**C**). In (**A**) and (**B**), dots show the data of Hoffman *et al.* (2004) for 1974 (◆) and 1975 (■) (MI) and of Jermini and Gessler (1996) for 1990 (●) (Switzerland); lines shows the fit of data with $R^2 = 0.87$ for (**A**) and 0.97 for (**B**). (**C**) Dots show the data of Jailloux (1992), and the line shows the fit of data with $R^2 = 0.92$.

Example 2. Equation 14 of the model was developed from an analysis of data from Molitor (2009). Black-rot severity was evaluated on leaves that were artificially inoculated with conidia and incubated at constant temperatures between 10 and 30°C for 4 to 24 h. Disease severity was highest (40.6%) after 24 h at 20°C. Artificial inoculation studies were also carried out on clusters in the field. After inoculation, clusters were enclosed in plastic bags to maintain surface wetness for 6 to 72 h; air temperature during these experiments fluctuated between 17.3 and 25.1°C. Disease severity increased with wetness duration until 72 h, when average disease severity of repeated experiments was 76.7%; after 24 h of wetness, disease severity was 25.3%.

To develop a common equation for infection by conidia, the data for percentage of severity on clusters recorded in each of three experiments was first expressed on a relative scale by dividing disease severity at each observation (6, 9, 12, 24, 36, and 48 h post-inoculation) by the disease severity at 72 h post-inoculation. These relative data (dependent variable Y) were pooled over experiments and regressed against the sum of hourly temperatures during each wetness period after inoculation (independent variable X). The best fit was obtained with a Gompertz equation, in the form of example 1, with a = 6.96±1.83, b = 0.075±0.009, and $R^2 = 0.96$. Based on this equation, when X = 480 (i.e., the sum of hourly temperatures when disease severity was the highest in leaf experiments, 24 h at 20°C), Y = 0.32. Data on leaf infection were then expressed as relative disease severity by dividing each observation at different temperatures and wetness duration by the following product: 40.6 × 0.32, where 40.6 is the highest disease severity of the experiment, and 0.32 is the correction factor to scale the disease severity after 24 h to that after 72 h (from the cluster experiment).

The entire data set (leaves and clusters) of relative severity scaled at 72 h (Y) was then regressed against the following equation: $Y = (a \times X1^b \times (1-X1))^c \times \exp(-d \times \exp(-e \times X2))$, where the first term accounts for the effect of temperature following a bête equation, and the second term accounts for post-inoculation wetness duration based on a Gompertz equation. In this equation, X1 is an equivalent of temperature calculated as (T-Tmin) / (Tmax-Tmin), and X2 is wetness duration (in h); Tmin and Tmax were set at 7 and 33°C as in equation 12. Estimates of equation parameters were those in equation 14. The dynamics of relative infection severity on either leaves or clusters as a function of wetness duration and temperature are shown in Figure 2A; goodness-of-fit is shown in Figure 2B. For the linear regression between predicted and observed data, the R^2 was 0.94 (significant at $P < 0.001$), the intercept (= 0.005) was not different from 0 (at $P < 0.001$), and the slope (= 0.96) was not different from 1 (at $P < 0.001$); residues did not show systematic deviations from the prediction line.

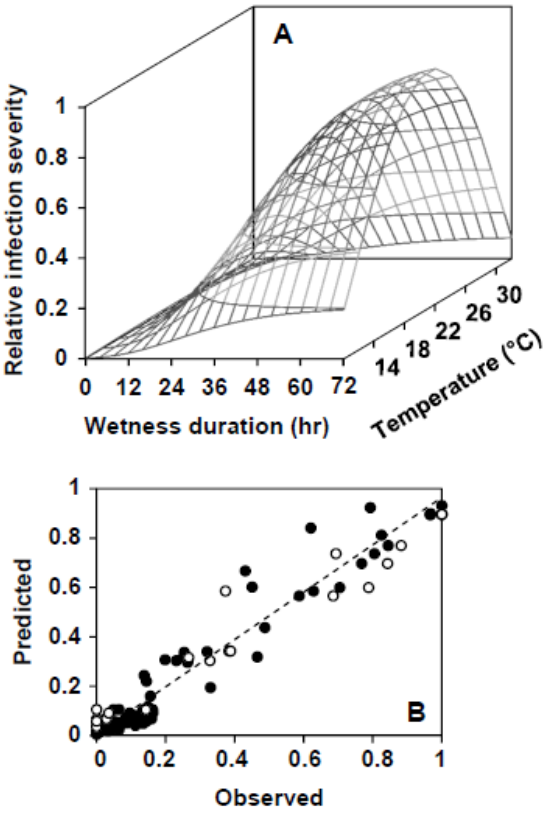

Figure 2. Relationship between temperature, wetness duration, and relative infection severity of *Guignardia bidwellii* based on equation 14 of the model (**A**), and the plot of predicted vs. real data of Molitor (2009) for leaves (●) and bunches (○) (**B**).

Example 3. The model uses a multiplication factor of 1.5 to calculate duration of latency from the duration of incubation. This multiplication factor was calculated from data of Spotts (1980) as follows. Effect of temperature (from 15.0 to 26.5°C) on incubation time and pycnidia formation (in days) on grape leaves has been determined both in growth chambers (with constant temperatures) and in vineyards (with fluctuating temperature) (Spotts, 1980). To make the two data sets homogeneous, the data from growth chamber experiments were multiplied by a correction factor of 1.29 for incubation and 1.35 for latency. To determine the multiplication factor for incubation, incubation length in the vineyard was considered to be 12 days at 19°C and 8.5 days at 22°C; assuming a linear reduction of incubation time between the above temperatures, incubation length in vineyards was 9.7 days at 21°C. In growth chambers, incubation length was 7.5 days at 21°C. Therefore, incubation under fluctuating temperature was 1.29 time longer than at constant temperature (i.e., 9.7/7.5). A similar procedure was used for pycnidia formation.

The rescaled data from growth chambers were then pooled with the vineyard data (independent variable Y) and fitted with the equation of Magarey *et al.* (2005) in the form: $Y = \min / ((Tmax–T) / (Tmax–Top) \times (T-Tmin) / (Topt-Tmin)^{(Topt–Tmin)/(Tmax–Topt)})$ (Figure 3A). Based on Spott's data (1980), min was set equal to 8 days for incubation and to 12 days for latency, while cardinal temperatures were estimated by evaluating goodness-of-fit of a set of equations calculated by changing the three cardinal temperatures in turn by 0.5°C. The best fit for incubation was obtained with Tmin = 11°C, Topt = 24°C, and Tmax = 27.5°C. The best fit for latency was obtained with Tmin = 10°C, Topt = 24°C, and Tmax = 27°C. In both cases, $R^2 = 0.97$ and residues were small and regularly distributed (Figure 3B). The average ratio between latency and incubation length between Tmin and Tmax was 1.5±0.01, which is the value used in the model.

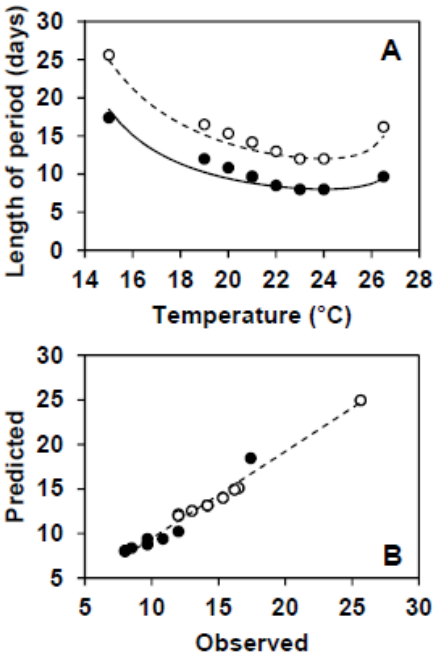

Figure 3. Effect of temperature on length of incubation (line) and latency (dashed line) periods, expressed in days after infection by *Guignardia bidwellii*, and the plot of predicted vs. real data for incubation and latency (**B**). In (**A**), dots show the data of Spotts (1980), and lines show the length of each period as predicted by the equation of Magarey *et al.* (2005). In (**B**), filled circles refer to incubation (●) and open circles (○) refer to latency.

LITERATURE CITED

Ferrin, D.M., Ramsdell, D.C., 1977. Ascospore dispersal and infection of grapes by *Guignardia bidwellii*, the causal agent of grape black-rot disease. Phytopathology 67, 1501-1505.

Jermini, M., Gessler, C., 1996. Epidemiology and control of grape black-rot in southern Switzerland. Plant Disease 80, 322-325.

Jailloux, F., 1992. In-vitro production of the teleomorph of *Guignardia bidwellii*, causal agent of black-rot of grapevine. Canadian Journal of Botany 70, 254-257.

Hoffman, L.E., Wilcox, W.F., Gadoury, D.M., Seem, R.C., *et al.*, 2004. Integrated control of grape black-rot: Influence of host phenology, inoculum availability, sanitation, and spray timing. Phytopathology 94, 641-650.

Magarey, R.D., Sutton, T.B., Thayer, C.L., 2005. A simple generic infection model for foliar fungal plant pathogens. Phytopathology 95, 92-100.

Molitor, D., 2009. Biologie und Bekämpfung der Schwarzfäule (*Guignardia bidwellii*) an Weinreben. Geisenheimer Berichte Bd. 65. Gesellschaft zur Förderung der Forschungsanstalt Geisenheim, Germany

Spotts, R.A., 1980. Infection of grape by *Guignardia bidwellii*-factors affecting lesion development, conidia dispersal and conidial populations on leaves. Phytopathology 70, 252-255.

Chapter 3

Chapter 3

Accurate prediction of black-rot epidemics in vineyards using a weather-driven disease model

ABSTRACT

A model predicting black-rot epidemics was evaluated by comparing model output with real disease development in a vineyard of north Italy, in 2013 to 2015. The model predicts the occurrence of infection, infection severity, and periods when symptoms are expected to appear on leaves and bunches based on weather data. Model accuracy was evaluated by comparing predicted and observed disease data. The disease was assessed on leaves (as lesion number per leaf) and bunches (as disease severity) 2 or 3 times per week between the first leaf unfolded and veraison. Leaf lesions in 2015 were more than 10 times higher than those in 2013 and 2014; the severity on clusters varied from 7% in 2013 to 47% in 2015. Disease assessments were compared with model output; exactly it was verified whether, on each disease assessment date, the model predicted or not the appearance of new disease symptoms. The model showed good accuracy in predicting disease onset; area under the ROC curve was 0.870 for leaves and 0.770 for clusters, and both were significantly >0.5. The probability to provide an unjustified alarm was ≤0.180, while the probability of missing real infections was 0.175 for leaves and 0.263 for bunches. Since in the 78% of these false negative predictions the difference between expected and real disease onset was ±2 days, most of these errors were caused by inaccuracies in calculating the incubation length rather than in predicting infection occurrence. Only one infection period was really missed by the model, which caused the appearance of few new leaf lesions (14 lesions) between end of July 27 and early-August 2013. When used to predict the epidemic development of black-rot, the model provided a slight overestimation of the disease severity, mainly on leaves, when the observed disease severity was >0.6. These discrepancies were likely caused by different patterns of inoculum availability in the considered vineyard compared to those used for model development. The model can be used for scheduling fungicide sprays against black-rot.

Key words: *Guignardia bidwellii,* plant disease model, validation, leaf lesion, cluster severity.

INTRODUCTION

Grapevine black-rot, caused by the ascomycete *Guignardia bidwellii* (Ellis) Viala and Ravaz (anamorph: *Phyllosticta ampelicida* (Englem.) van der Aa), is a serious threat, especially in grape-growing areas characterized by fresh and moist weather in spring and early summer (Ramsdell and Milholland, 1988; Harms *et al.*, 2005).

Originated in the United States (Andersen, 1956), in Europe black-rot was firstly detected in France in 1885 (Scribner, 1886; Jermini and Gessler, 1996; Northover, 2008; Harms *et al.*, 2005), and progressively spread to other European grape-growing areas (Besselat and Bouchet, 1984; Mauri and Kobel, 1988). In Italy, *G. bidwellii* has been detected for the first time in Tuscany at the end of 19th century (Martinelli, 1891). In the 1990s, the pathogen was repeatedly detected: in the "Cinque terre" area, western Liguria (Corte, 1975); in Friuli Venezia Giulia (north-east Italy) (Rui, 1989; Clabassi *et al.*, 2000); and in Veneto (Costacurta *et al.*, 2004). A recrudescence of black-rot epidemics was observed in Friuli (Bigot G., personal communication) and Tuscany (Rinaldi and Mugnai, 2012) in recent years, where the disease has been considered endemic.

G. bidwellii can affect all the green host tissue: leaves, petioles, tendrils and shoots, where symptoms appear as necrotic light brown lesions containing small, black pycnidia (Kuo and Hoch, 1996; Ullrich *et al.*, 2009; Ferrin and Ramsdell, 1978). Berries are susceptible from mid-bloom and beyond (Hoffman *et al.*, 2002). Early symptoms appear as circular whitish spots surrounded by a reddish brown ring, which quickly enlarge until the entire berry became rotten, culminating in shriveled, hard blue-black mummies covered by pycnidia and perithecia (Ramsdell and Milholland, 1988; Hoffman *et al.*, 2002; Rinaldi and Mugnai, 2012; Bottura, 2011; Reddick, 1911; Sosnowski *et al.*, 2012).

Black-rot is a potentially destructive disease, with yield losses up to 80% and serious lowering of the wine quality (Scribner, 1886; Ellis *et al.*, 1986; Ferrin and Ramsdell, 1977, 1978; Ramsdell and Milholland, 1988; Funt *et al.*, 1990). Under favorable conditions, repeated infection cycles can develop between bud break of vines and berry ripening, caused by ascospores and conidia from the overwintered inoculum sources (berry mummies and cane lesions) and by conidia produced on leaf and shoot lesions and on rotted berries (Ramsdell and Milholland, 1988).

Black-rot is traditionally controlled through repeated application of fungicides on a calendar basis from the early shoot growth stage through veraison (Wilcox, 2003). The crucial sprays are: (i) as new shoots are 2-3 cm long and repeated at 7-14 days intervals; (ii) just before bloom; and (iii) just after bloom, when the fruit has set. After fruit set, applications continue at about 10-day intervals as long as the weather is rainy and muggy, or they can be discontinued when the weather turns dry (RPD, 2001). To optimize fungicide timing, simple disease forecasting models have been developed (Ellis *et al.*, 1986; Devaut, 1990; Maurin *et al.*, 1991; Spotts, 1977).

In Chapter 2 of this Thesis, a new mechanistic, dynamic, weather-driven model was developed for detailed prediction of black-rot epidemics; model outputs were compared with three typical black-rot epidemics and they gave a reliable picture of the disease development (Rossi *et al.*, 2014). However, no detailed validation is still available for this model. The present work was then conducted to validate the accuracy of the model of Rossi *et al.* (2014) in predicting black-rot epidemics.

MATERIALS AND METHODS

Vineyard site and characteristics

A three-year (2013 to 2015) experiment was carried out in a vineyard of cv. Barbera at the University campus of Piacenza (North Italy, 45° 2' N latitude and 9° 43' E longitude). Plants were 7-year old in 2013 and trained with a Guyot system. No fungicide treatments were applied all season long.

A standard weather station (MeteoSense 2.0, Netsens s.r.l., Firenze, Italy) was located into the vineyard provided hourly records of air temperature (T, °C), relative humidity (RH, %), rainfall (R, mm), and leaf wetness (WD, min).

At the end of February of each year, 20 g of grape berry mummies affected by black-rot were arranged in metallic net boxes, and boxes were fixed on the trellis at 1.80 m from the ground; there were 9 boxes, 1.5 meters apart along the vine row. To obtain berry mummies, grape clusters have been sampled at the end of the previous season from 3 to 5 commercial vineyards severely affected by black-rot, in northern Italy, and exposed outdoor during winter. Mummified berries were then collected from these clusters in February and included in a unique bulk sample, from which sub-samples (20 g of berry mummies) were randomly collected and placed in the metallic nets. Berry mummies remained on the trellis all season long for providing *G. bidwellii* inoculum.

Disease assessment

Disease assessments were done on leaves and clusters from the first leaf unfolded (stage 11 of the BBCH scale of Lorenz *et al.*, 1995) until softening of berries (BBCH 85), which is the period when plants are susceptible (Hoffman *et al.*, 2002).

Leaf assessments were performed every 2 to 3 days by counting the black-rot lesions, and the average number of lesions per leaf was calculated. Since the final number of lesions was different in the three years, black-rot severity on leaves (BRL) in each year was rescaled to the maximum number of lesions observed in that year; so BRL was expressed in a 0 to 1 scale.

Clusters assessments were performed every 3 to 4 days, by assigning each cluster to one of the following 5 severity ratings, in a 0 to 1 scale (EPPO, 2000): 0 (healthy clusters), 0.025 (≤5% of the cluster surface affected by black-rot), 0.15 (5 to ≤25%),

0.375 (25 to ≤50%), and 0.75 (>50%). Black-rot severity on clusters (BRC) was then calculated by averaging the ratings of all the clusters.

Model operation

The weather data were used to operate the model described in chapter 2 of this Thesis (Rossi *et al.*, 2014). Briefly, the maturation course of ascospores and conidia on overwintered berry mummies was calculated. A spore release event was predicted when R ≥0.5 mm in 1h, and the correspondent inoculum dose (SPODOSE) calculated by combining spore release, deposition and survival. Following a spore release, an infection period was predicted based on temperature and wetness duration, with the correspondent infection severity (SEV'). Finally, the infection severity on leaves (SEVL) was calculated as SEVL = SPODOSE x SEV'. Starting from when 80% of flower caps have fallen (BBCH 68), infection severity was also calculated for clusters (SEVC). Black-rot lesion appearance was expected after an incubation window of 175 to 305 degree-days (calculated using 6 and 24°C as cardinal temperatures); SEVL and SEVC were distributed over the incubation period by using the first derivative of the equation ONS (Rossi *et al.*, 2014). Appearance of pycnidia on lesions was expected in 262 to 292 degree-days, and the abundance of pycnidia (PYC) calculated as a function of temperature, as sources of secondary inoculum (Rossi *et al.*, 2014).

Data analysis

A Bayesian analysis was used to evaluate the correspondence between infection periods predicted by the model and appearance of black-rot symptoms in the vineyard. Dates of disease assessments (or cases) were categorized as either 0 (there is no disease increase compared to the previous assessment) or 1 (there is an increase in leaf lesion number or cluster severity). Similarly, cases were categorized as either 1 or 0 based on whether new disease symptoms are expected to appear or not, respectively, as new lesions or increased cluster severity, based on a predicted infection. Afterwards, cases were classified as: (i) true positive, when predicted infection = 1 and disease increase = 1; (ii) true negative, when predicted infection = 0 and disease increase = 0; (iii) false positive, when predicted infection = 1 and disease increase = 0; and (iv) false negative, when predicted infection = 0 and disease increase = 1. A contingency Table (2 × 2) was prepared with the cells containing the true positive proportion (TPP or sensitivity), the true negative proportion (TNP or specificity), the false positive proportion (FPP), and the false negative proportion (FNP) (Madden, 2006).

The posterior probability to predict the disease occurrence based on model output was calculated, as described by Madden *et al.* (2006). The following posterior probabilities were considered: (i) the probability of the disease to increase when predicted by the model, P(P+|O+); (ii) the probability of no disease increase when not predicted, P(P-|O-);

(iii) the probability of no disease increase when predicted, P(P+|O-); and (iv) the probability of disease increase when not predicted, P(P-|O+). The prior probabilities of disease increase were calculated as the proportion of cases (assessment dates) with P(O+) or without P(O-) disease increase in the vineyard over the total cases. The overall accuracy of the predictor was finally calculated as the ratio between correct and total predictions. The analysis was performed separately for leaves and clusters.

A receiver operating characteristic (ROC) curve was used to investigate whether it is possible to define thresholds (or cut-off values) for the infection severity predicted by the model (either SEVL or SEVC) to result in real infection. Since at any disease assessment date (case), the expected disease increase can be originate by one or more predicted infections, SEVL (or SEVC) used as cut-off values in the ROC analysis consisted of the sum of the infection severity values of all the infections that are expected to produce new symptoms at that date. Two curves were created (one for leaves and one for clusters) by plotting the true positive proportion (TPP or sensitivity) against the false positive proportion (FPP or 1-specificity) at various cut-off values. The closer the ROC curve is to the upper left corner of the plot, the greater the accuracy of the test (Zweig and Campbell, 1993; Hanley, 2005). The area under the ROC curve (AUROC) and its standard error were used to evaluate the analysis; AUROC values between 0.5 and 1 indicate that the variable (SEVL or SEVC in this case) is a good predictor of the response variable (disease increase in this case). The *P* value was calculated as the probability that the AUROC is significantly different from 0.5 (i.e., the ROC curve coincides with the line of no discrimination, having 0,0 and 1,1 as coordinates). The statistical software SPSS (V21.0; SPSS Inc.) was used for the ROC analysis.

A Bayesian analysis was conducted as described before for four cut-off values specifically: SEVL (or SEVC) >0.001, >0.002, >0.005 and >0.01.

To validate the ability of the model to predict epidemic development through the season, predicted infection severities for leaves and clusters (SEVL and SEVC, respectively) were accumulated between BBCH 11 and BBCH 85, and BBCH 68 and BBCH 85, respectively. Accumulated infection severities were then rescaled to the final value of the year, and expressed as ISL and ISC, respectively, in a 0 to 1 scale. These values were then regressed against the values of BRL and BRC, respectively, observed in the vineyard. The null hypotheses that the intercept of the regression line is = 0 and slope is = 1 were tested using a t-test; when this test is not significant, both null hypotheses were accepted and the model was considered a statistically accurate predictor of the real data (Teng, 1981). The distribution of residuals of predicted versus observed values was examined to evaluate the goodness-of-fit, assessed by the adjusted R^2, the root mean square error (RMSE), the coefficient of residual mass (CRM) and the concordance correlation coefficient (CCC) (Lin, 1989; Nash and Sutcliffe, 1970). RMSE represents the average distance of real data from the fitted line, and CRM is a measure of the

tendency of the equation to overestimate or underestimate the observed values (a negative CRM indicates a tendency of the model toward overestimation)(Nash and Sutcliffe, 1970). The concordance correlation coefficient (CCC) was calculated as a measure of model accuracy (Madden *et al.*, 2007); CCC is the product of two terms: the Pearson product-moment correlation coefficient between observed and predicted values and the coefficient Cb (bias estimation factor), which is an indication of the difference between the best fitting line and the perfect agreement line (CCC = 1 indicates perfect agreement) (Madden *et al.*, 2007).

RESULTS

In 2013, the period of vine susceptibility to black-rot started on April 23 (first leaf unfolded, BBCH 11) and ended on August 30 (softening of berries, BBCH 85); cluster susceptibility started on June 8. During this period, there were 240.2 mm of rainfall, over two main periods: from late-April to late-May and in second half of August. Between these two rainy periods, there were only four rainy days: two on June, 9 and 27 with 2.6 and 13.6 mm rain, respectively; and two on July, 14 and 29, with 1 and 1.8 mm of rain, respectively (Figure 1A). The model predicted a total of 19 infection periods (Figure 1B). Most of these infection periods (13 periods) were predicted during the first rainy period (Figure 1B) and then they applied to leaves only. The accumulated infection severity of these infections accounted for approximately 80% of the seasonal ISL (Figure 1C). Disease symptoms caused by these predicted infections were expected to appear between May 8 and mid-June (Figure 1B). Others symptoms were expected to appear in the last decade of June (because of the predicted infection on June 10, which accounted for about 10% of ISL, Figure 1C), in the second decade of July (infection on June 28), and finally and the end of August (few infection after mid-August) (Figure 1B). The latter two infection periods accounted for an irrelevant part of SEVL (Figure 1C) and they also applied to clusters. Actually, new black-rot lesions appeared on leaves when predicted by the model (Figure 1B). Approximately 85% of the total lesions on leaves appeared within mid-June, and 96% of them within early July, in substantial agreement with the model predictions (Figure 1C). Approximately 2% of leaf lesions appeared between late-July and early August, which were not predicted by the model (Figure 1B and 1C). According to the model predictions, few black-rot symptoms were observed on clusters staring from early July, with a final disease severity index of 0.07 (Figure 1C).

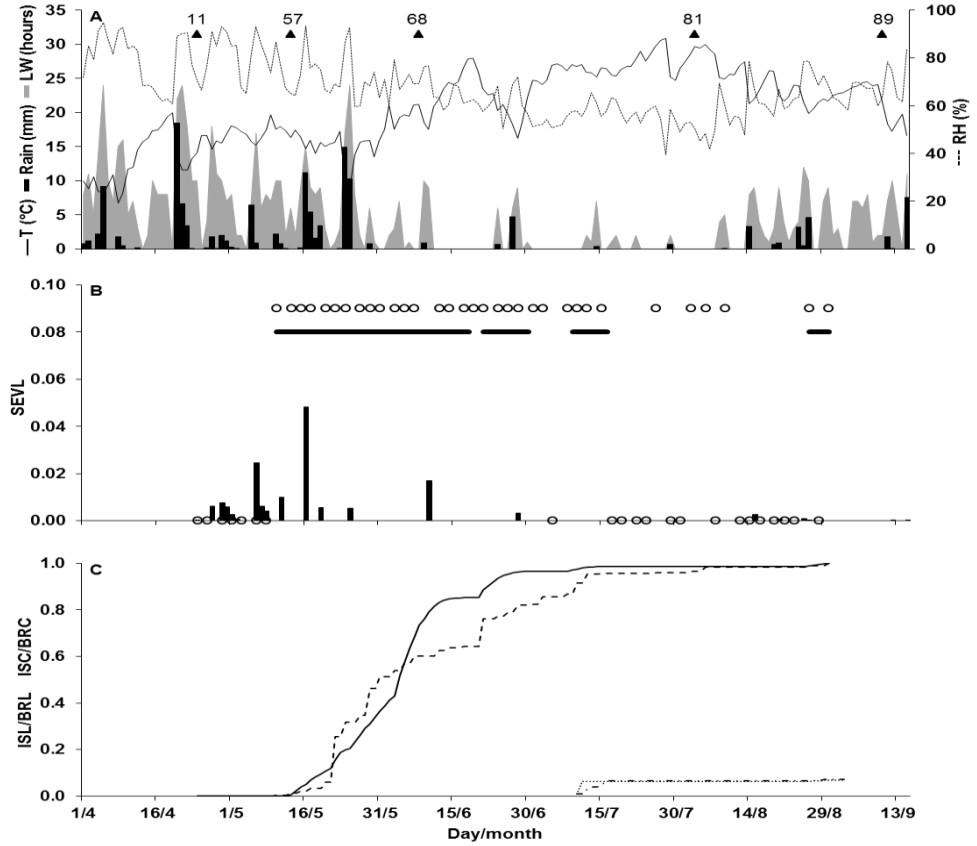

Figure 1. Model output for the University campus of Piacenza vineyard in 2013. **A,** weather variables: air temperature (T, °C, solid line), rainfall (Rain, mm, black bars), leaf wetness duration (LW, hours, grey area) and relative humidity (RH, %, dashed line). Black triangles (▲) show the vine grow stages according to Lorenz *et al.* (1995): 11 (first leaf unfolded and spread away from shoot), 57 (inflorescences fully developed; flowers separating), 68 (80% of flowerhoods fallen), 75 (berries pea-sized, bunches hang), 81 (beginning of ripening: berries begin to develop variety-specific color) and 89 (berries ripe for harvest). **B,** bars represent the infection severity on leaves (SEVL) predicted by the model. Thick black lines over the bars represent the expected appearance of black-rot lesion after the incubation period. The empty circles represent the results of the field leaf assessments: new lesions were observed when the circles are in the upper part of the graph, and new lesions were not observed when the circles are on the bottom of the graph. **C,** solid and dash dot lines represent the accumulated infection severity predicted by the model and rescaled to the final value of the year (solid line for leaves and dash dot line for clusters). Dashed line represents the accumulated value of black-rot lesions on leaves (BRL) rescaled to the maximum number of lesions observed in that year. Dotted line represents black-rot severity on clusters (BRC) calculated by averaging the ratings of all the clusters. Maximum value of BRC is 0.071.

In 2014, the period of vine susceptibility to *G. bidwellii* infection started on April 3 (first leaf unfolded, BBCH 11) and ended on August 1 (softening of berries, BBCH 85); clusters were susceptible starting on May 30 (80% of flower hoods fallen, BBCH 68). A total of 121 mm of rain were accumulated over the season, almost regularly distributed (Figure 2A). A total of 28 infection events were predicted by the model (Figure 2B). These predicted infections were also regularly distributed over the season, even though there were two relevant periods for model predictions: (i) the repeated infections predicted between April 5 (first seasonal infection predicted) and May 4, with predicted onset of lesion on leaves between late-April and late-May; and (ii) the infection on May 23, with symptoms onset on leaves between June 5 to 12 (Figure 2B). These two relevant periods accounted for 87% of the accumulated infection severity on leaves predicted (Figure 2C). The disease really appeared on leaves in the two relevant periods predicted by the model (Figure 2B), and the accumulated disease severity at the end of these periods was approximately 65% of the final one (Figure 2C). First bunch infection was correctly predicted by the model on May 31, as well as the others infections predicted in the second half of June, which contributed to the increase in the infection severity expected on both leaves and clusters (Figure 2B and 2C). Final disease severity index on clusters was 0.22.

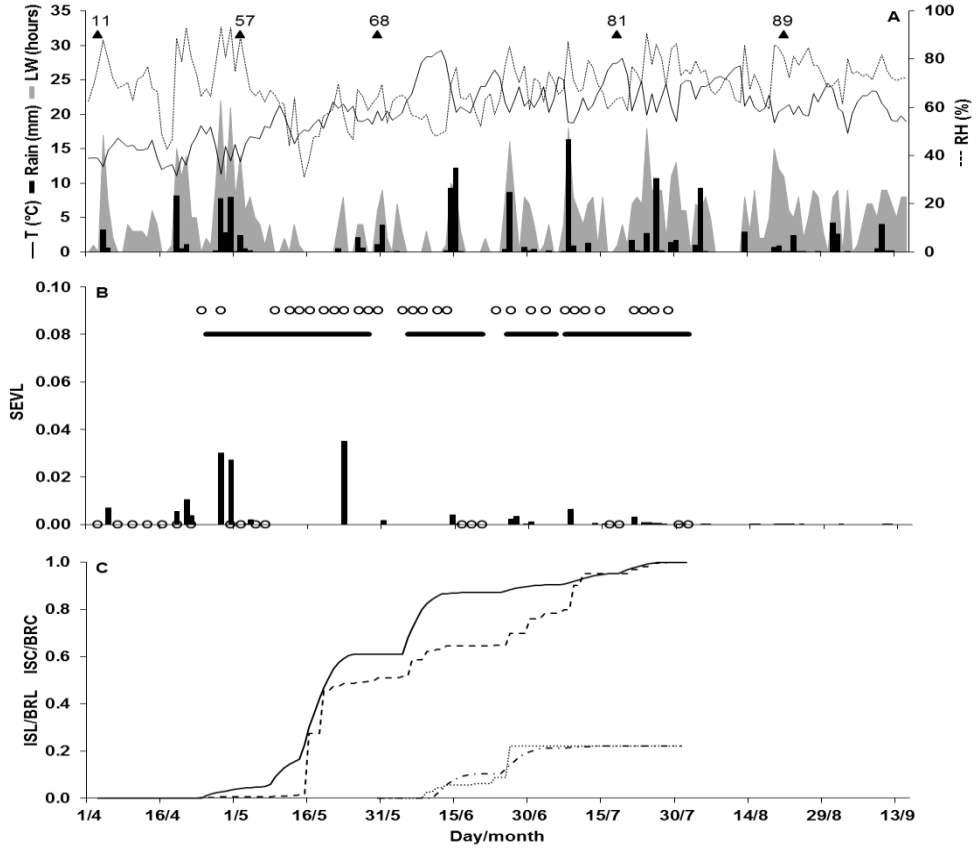

Figure 2. Model output for the University campus of Piacenza vineyard in 2014. **A,** weather variables: air temperature (T, °C, solid line), rainfall (Rain, mm, black bars), leaf wetness duration (LW, hours, grey area) and relative humidity (RH, %, dashed line). Black triangles (▲) show the vine grow stages according to Lorenz *et al.* (1995): 11 (first leaf unfolded and spread away from shoot), 57 (inflorescences fully developed; flowers separating), 68 (80% of flowerhoods fallen), 75 (berries pea-sized, bunches hang), 81 (beginning of ripening: berries begin to develop variety-specific color) and 89 (berries ripe for harvest). **B,** bars represent the infection severity on leaves (SEVL) predicted by the model. Thick black lines over the bars represent the expected appearance of black-rot lesion after the incubation period. The empty circles represent the results of the field leaf assessments: new lesions were observed when the circles are in the upper part of the graph, and new lesions were not observed when the circles are on the bottom of the graph. **C,** solid and dash dot lines represent the accumulated infection severity predicted by the model and rescaled to the final value of the year (solid line for leaves and dash dot line for clusters). Dashed line represents the accumulated value of black-rot lesions on leaves (BRL) rescaled to the maximum number of lesions observed in that year. Dotted line represents black-rot severity on clusters (BRC) calculated by averaging the ratings of all the clusters. Maximum value of BRC is 0.221.

In 2015, first unfolded leaves (BBCH 11) were observed on April 12, 80% of flower hoods fallen (BBCH 68) on May 25, and softening of berries (BBCH 85) on August 12. A total of 192.8 mm of rain occurred over the growing season, mainly until end of May, around mid-June, and in August (Figure 3A). The model predicted a total of 16 infection events. Ten of these infections were predicted between April 18 and May 27, and 3 of them had high infection severity, with expected disease onset on leaves between early May and mid-June; 3 further infections were predicted between June 15 and 20, with expected symptoms on both leaves and clusters between late-May and early July (Figure 3B). Actually, periods of disease symptoms appearance in the vineyard and infection severity on both leaves and clusters did agree with model predictions (Figure 3B and 3C). Final disease was very severe: BRL was 10 times higher than in 2013 and 2014 (which were similar) and BRC was 0.47, with all the bunches affected by black-rot, indicating a substantial loss of yield.

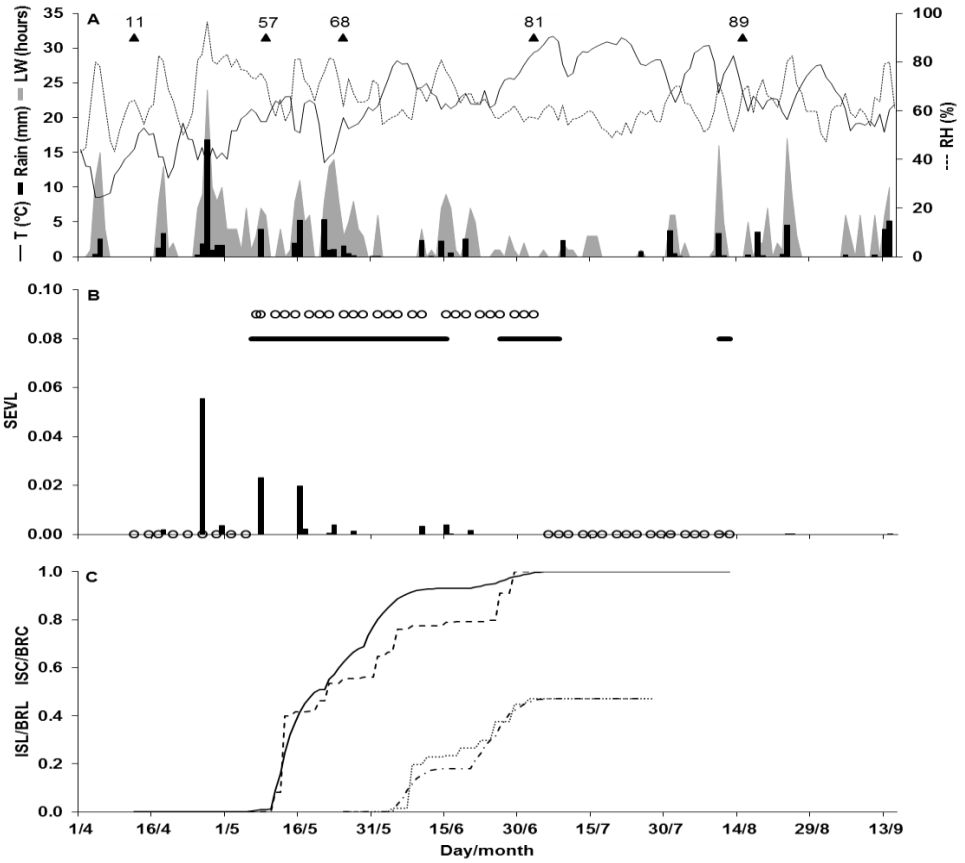

Figure 3. Model output for the University campus of Piacenza vineyard in 2015. **A,** weather variables: air temperature (T, °C, solid line), rainfall (Rain, mm, black bars), leaf wetness duration (LW, hours, grey area) and relative humidity (RH, %, dashed line). Black triangles (▲) show the vine grow stages according to Lorenz *et al.* (1995): 11 (first leaf unfolded and spread away from shoot), 57 (inflorescences fully developed; flowers separating), 68 (80% of flowerhoods fallen), 75 (berries pea-sized, bunches hang), 81 (beginning of ripening: berries begin to develop variety-specific color) and 89 (berries ripe for harvest). **B,** bars represent the infection severity on leaves (SEVL) predicted by the model. Thick black lines over the bars represent the expected appearance of black-rot lesion after the incubation period. The empty circles represent the results of the field leaf assessments: new lesions were observed when the circles are in the upper part of the graph, and new lesions were not observed when the circles are on the bottom of the graph. **C,** solid and dash dot lines represent the accumulated infection severity predicted by the model and rescaled to the final value of the year (solid line for leaves and dash dot line for clusters). Dashed line represents the accumulated value of black-rot lesions on leaves (BRL) rescaled to the maximum number of lesions observed in that year. Dotted line represents black-rot severity on clusters (BRC) calculated by averaging the ratings of all the clusters. Maximum value of BRC is 0.471.

Bayesian and ROC analysis showed a high accuracy of the model in predicting the appearance of black-rot symptoms on both leaves and clusters. AUROC (Figure 4) was 0.870±0.029 for leaves and 0.770±0.089 for clusters, and both were significantly >0.5 ($P < 0.001$ for leaves and $P = 0.005$ for clusters). Using SEVL or SEVC >0 as a threshold for predicting an infection provided an overall accuracy of 0.804 for leaves and 0.769 for bunches (Table 1). The posterior probability of providing unjustified alarms was $P(P+|O-) \leq 0.180$ for both leaves and clusters, and the probability of missing real infections was $P(P-|O+) = 0.175$ for leaves and = 0.263. These unpredicted disease onsets occurred on 18 cases (16 cases for leaves and 2 cases for clusters) and they accounted for 1.3% of total leaf lesions and 8.3% of bunch severity. In the 78% of these false negate predictions (14 cases), the difference between expected and real disease onset was within ±2 days; exactly, it was ±1 day in 11 cases and ±2 days in 3 cases (Figure 1B, 2B, and 3B). In 4 cases (22% of total FNP), the difference was between 5 and 9 days; that occurred for the 4 disease assessment dates between July 27 and August 9, 2013, when 14 new lesions were observed on leaves which have not been predicted (Figure 1B and 1C). Using SEVL or SEVC >0.001 as a threshold, overall accuracy of the model predictions increased for both leaves and clusters, as well as the probability to correctly predict disease increase. The probability of providing unjustified alarms also decreased while the probability of missing infections did not diminish (Table 1). No improvements in the model performances were observed by further increasing the infection severity threshold (Table 1).

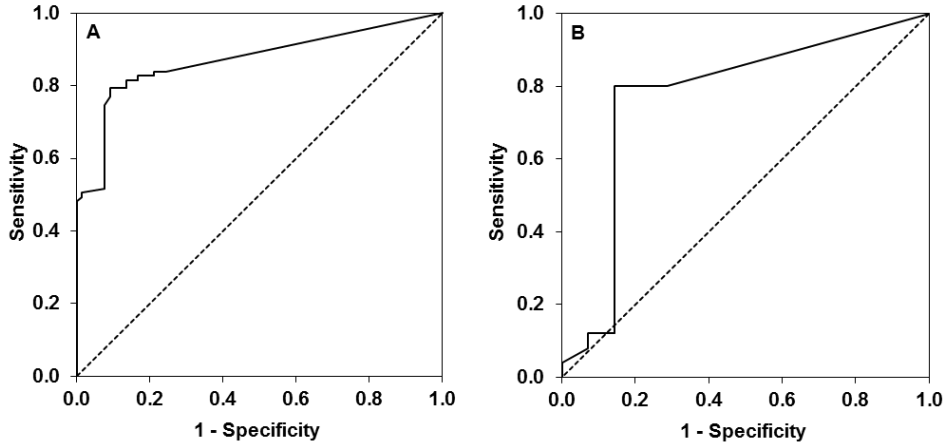

Figure 4. Receiver operating characteristic (ROC) curve for predicting black-rot occurrence in the field (i.e., disease increase) based on the model output new leaf lesions (**A**) or increased cluster severity (**B**) during three monitoring years (2013, 2014 and 2015) in the vineyard of the University campus of Piacenza. The dotted line (0.0; 1.1) represents no discrimination.

Table 1. Evaluation of the infection severity calculated by the model as predictor of the appearance of *Guignardia bidwellii* symptoms on leaves and clusters. Data derive from the model prediction and monitoring in a vineyard in Piacenza (North Italy), between first leaf unfolded and veraison, in 2013 to 2015.)

Predicted infection severity[a]	Proportions[b]				Overall accuracy[c]	Posterior probabilities[d]			
	TPP	FNP	FPP	TNP		(P+|O+)	(P-|O-)	(P+|O-)	(P-|O+)
Leaves									
>0	0.839	0.161	0.242	0.758	0.804	0.820	0.825	0.180	0.175
>0.001	0.828	0.172	0.182	0.818	0.824	0.857	0.815	0.143	0.185
>0.002	0.793	0.207	0.091	0.909	0.843	0.920	0.786	0.080	0.214
>0.005	0.644	0.356	0.076	0.924	0.765	0.918	0.680	0.082	0.320
>0.01	0.471	0.529	0.000	1.000	0.699	1.000	0.589	0.000	0.411
Clusters									
>0	0.800	0.200	0.286	0.714	0.769	0.833	0.737	0.167	0.263
>0.001	0.800	0.200	0.143	0.857	0.821	0.909	0.737	0.091	0.263
>0.002	0.600	0.400	0.143	0.857	0.692	0.882	0.583	0.118	0.417
>0.005	0.320	0.680	0.143	0.857	0.513	0.800	0.452	0.200	0.548
>0.01	0.080	0.920	0.071	0.929	0.385	0.667	0.378	0.333	0.622

[a] Cut-off values for the infection severity predicted by the model.
[b] *TPP* (true positive proportion, or sensitivity): the were symptoms when predicted by the model; *FNP* (false negative proportion): there were symptoms not predicted by the model; *FPP* (false positive proportion): there were no symptoms but the model predicted disease onset; and *TNP* (true negative proportion, or specificity): there were no symptoms and the model did not predict disease onset.
[c] Overall accuracy calculated as the proportion of correct predictions.
[d] Posterior probabilities for: (i) there is a disease increase when predicted by the model, P(P+|O+); (ii) there is no disease increase when not predicted, P(P-|O-); (iii) there is no disease increase when predicted, P(P+|O-); and (iv) there is no disease increase when not predicted, P(P-|O+). Prior probabilities for disease incease (O+) and no increase (O-) were Prob(O+) = 0.569 and Prob(O-) = 0.431 for leaves; Prob(O+) = 0.641 and Prob(O-) = 0.359 for clusters.

The linear regression of predicted versus observed data for leaves (Figure 5A) had slope not significantly different from 1 (P = 0.186) but the intercept was significantly different from zero (P = 0.006); for clusters (Figure 5B), intercept and slope were not significantly different from zero (P = 0.434) and one (P = 0.115), respectively. Goodness-of-fit of predicted versus observed data had $R^2 = 0.962$ and CCC = 0.974 for leaves, $R^2 = 0.975$ and CCC = 0.982 for clusters. RMSE was low for both leaves and clusters (0.091

and 0.066, respectively). CRM indicated slight overestimation of real data for leaves (-0.077) and underestimation for clusters (+0.0601) (Figure 5). For leaves, overestimation mainly occurred when observed ISL was >0.6 (Figure 5), which usually occurred between end of May and early-June (Figure 1C, 2C, and 3C).

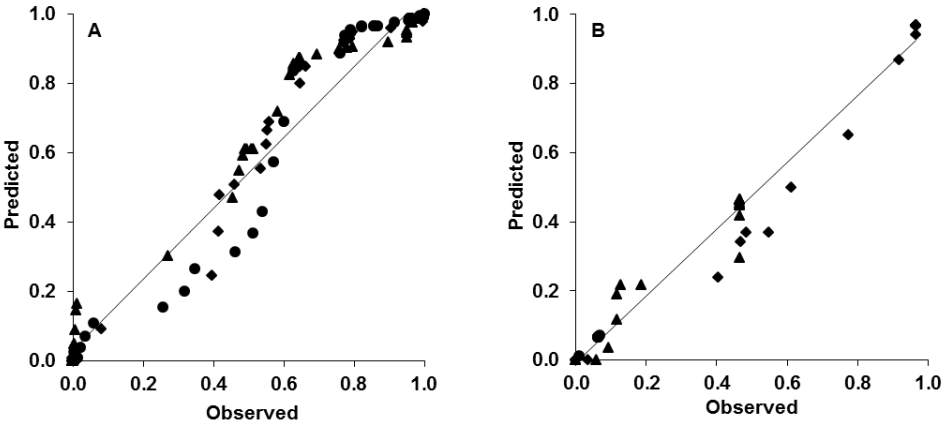

Figure 5. Plots of predicted versus observed values of black-rot infection severity for leaves (**A**) and clusters (**B**) for three monitoring years, 2013 (●), 2014 (▲) and 2015 (♦), at the vineyard of the University campus of Piacenza. Predicted were accumulated values of infection severity for leaves and clusters (ISL and ISC, respectively) through the growing season and rescaled to the final value of the year. Observed in **A** were the accumulated number of lesions on leaves (BRL) rescaled to the maximum number of lesions observed in that year. Observed in **B** were accumulated infection severity (BRC) on clusters rescaled to the final value of the year.

DISCUSSION

In this work, a recently published model predicting black-rot epidemics was evaluated by comparing model output with real data about the disease development on leaves and bunches, for a 3-year period (2013 to 2015) in a vineyard of North Italy. The black-rot epidemics observed in these three years showed different severity: leaf lesions in 2015 were more than 10 times higher than those observed in 2013 and 2014; the severity on clusters varied from 7% in 2013 to 47% in 2015, when all the bunches became affected. Therefore, the dataset used for model validation provided useful information for evaluating both model accuracy (i.e., the closeness of a predicted value to its "true" value) and robustness (i.e., the capacity of the model to perform equally well across different epidemical conditions) (Rossi *et al.*, 2012).

The model was evaluated by comparing predicted and observed disease data. The disease was assessed on leaves (as lesion number per leaf) and bunches (as disease severity) 2 or 3 times per week; these assessments were compared with model output. Exactly, it was verified whether, on each disease assessment date, the model predicted or not the appearance of new disease symptoms. The model then provided true positive prediction when symptoms were expected to appear and they really appeared as new lesions on leaves or increased disease severity on bunches. Similarly, the model provided false negative or positive predictions (which are both errors) based on this comparison. It may be considered that the model predicts disease appearance on any day depending on (i) infection occurrence and (ii) length of incubation. Therefore, model errors may have two main sources: (i) errors in predicting infection occurrence and (ii) errors in predicting incubation length.

Overall, the model showed good accuracy in predicting disease onset. The probability to predict a disease increase that actually did not occur, which is an unjustified alarm, was $P(P+|O-) \leq 0.180$ for both leaves and clusters, while the probability of missing to predict a disease increase that really occurred, which is an omitted warning, was $P(P-|O+) = 0.175$ for leaves and 0.263 for bunches. This meant missing to predict a few of the total disease developed in the vineyard. Since in most of these false negative predictions the difference between expected and real disease onset was ±2 days, it may be considered that most of these errors were caused by inaccuracies in calculating the incubation length rather than in errors in predicting infection occurrence. Under the assumption that a difference of ±2 days between predicted and actual disease onset was caused by errors in the incubation length, the only infection not predicted by the model was that causing the appearance of few new leaf lesions (14 lesions) between end of July 27 and early-August 2013. Model accuracy increased by using a threshold of >0.001 for predicting an infection period; particularly, the probability of unjustified alarms was lower than using >0.

In the model operated in the present work, an incubation period ended when 175 degree-days (using 6 and 24°C as cardinal temperatures) were accumulated after infection (Molitor *et al.*, 2012) and symptoms continued to appear until 305 degree-days were accumulated (Hoffman *et al.*, 2002). Molitor *et al.* (2012) found that first disease symptoms became visible on leaves after 165.6 to 198.2 degree-days have accumulated after infection. Similar incubation length was observed for cluster when cluster have been inoculated between the growth stage BBCH 68 (80% of flowerhoods fallen) and BBCH 77 (berries beginning to touch); the incubation length was longer for later inoculation dates in Riesling vines (Molitor *et al.*, 2012) due to ontogenic or age-related resistance (Hoffman *et al.*, 2002). This variability in incubation length strongly supports the previous conclusion that most of the false negative predictions of infection observed in the present work were related to variability incubation length rather than to errors in predicting infection occurrence. Even though the prediction of the incubation period can be improved, this fact may not reduce the ability of the model to correctly predict infection periods or reduce the value of the model for timing fungicides applications.

When used to predict the epidemic development of black-rot, the model provided a slight overestimation of the disease severity, mainly on leaves. This overestimation mainly occurred in the second part of the disease epidemic, when the observed disease severity was >0.6. This result was likely caused by an overestimation of the predicted infection severity in the first part of the epidemic, i.e., in April and May. The model calculates infection severity by combining, for any infection period, the available inoculum dose and the infection efficiency of this inoculum. The inoculum dose is composed by both primary and secondary inoculum. Availability of primary inoculum is determined by equations developed by using field data collected in vineyards of Michigan (Ferrin and Ramsdell, 1978), New York (Hoffman *et al.*, 2004; Becker and Pearson, 1996), and Switzerland (Jermini and Gessler, 1996). Availability of secondary inoculum is mainly based on assumptions on the production of pycnidia and conidia on lesions, because no precise data are available in the literature for *G. bidwellii*. Infection efficiency is calculated by an equation developed based on the data obtained by Molitor (2009) under environment controlled experiments: artificially inoculated leaves were kept at constant temperatures between 10 and 30°C, with 4 to 24 h of wetness duration, and bunches were kept at fluctuating temperatures between 17.3 and 25.1°C, with 6 to 72 h wetness duration. It may be then supposed that discrepancies between predicted and actual infection severities observed in the present work may be caused by different patterns of inoculum availability in the considered vineyard compared to those used for model development rather than by differences in the response of infection efficiency to temperature and wetness duration. Further studies on the dynamics of both primary and secondary inoculum should be therefore useful for improving the model accuracy in predicting infection severity.

Different methods have been developed for better scheduling fungicide applications against black-rot (Devaut, 1990; Ellis *et al.*, 1986; Maurin *et al.*, 1991; Spotts, 1977). The majority of these methods were based on the work of Spotts (1977), who developed a Table with the combination of hours of wetness and temperatures necessary for *G. bidwellii* infection to occur. The use of the Spotts Table for two sesons in a vineyard in Ohio (US) led to predict a high number of infection periods (54 and 34 infection periods in the two seasons) and fungicide treatments (8 and 12). Ellis *et al.* (1986), Maurin *et al.* (1991), and Smith (2009), all used the work of Spotts (1977) to predict infection periods and schedule fungicides treatments accordingly, obtaining good control of the disease and a reduction in the fungicide usage compared to calendar applications. Gadoury *et al.* (1993) also developed a set of simple rules to define the criteria for black-rot infection based on a combination of wetness duration and temperature.

The model developed by Rossi *et al.* (2014) represents an improvement of the Spotts-based forecasters because considers not only infection periods, but also production, dispersal and survival of the inoculum; in addition, the model provides a quantification of the infection risk, while the Spotts-based methods only predict whether an infection can occur or not. In the present work, the model has proven to be highly accurate and robust in predicting infection periods and dynamics of black-rot epidemics. The model can be then used for scheduling fungicide sprays in the vineyards. As illustrative information, applying the model output to schedule the application of fungicides in the vineyard of this work would result in 5 treatments in 2013 and 2014, and 4 in 2015; 9, 10 and 8 treatments should have been performed, respectively, by using a calendar-based timing. The model of Rossi *et al.* (2014) could be integrated into the decision-support system named vite.net (Rossi *et al.*, 2012) that already includes models for downy and powdery mildews. That should make it possible to schedule fungicide applications and to select the most appropriate fungicides to be used taking into account the risk of the three main diseases at the same time.

LITERATURE CITED

Andersen, 1956. Diseases of grapes: black-rot. In: Disease of Fruit Crops. pp. 355–364.

Becker, C.M., Pearson, R., 1996. Black-rot lesions on overwintered canes of Euvitis supply conidia of *Guignardia bidwellii* for primary inoculum in spring. Plant Disease 80, 24–27.

Besselat, B., Bouchet, J., 1984. Black-rot: situation inquiétante dans certains vignobles. Phytoma - défense des Culture 33–35.

Bottura, M., 2011. Black-rot o marciume nero della vite. In: Manuale Di Viticoltura. Fondazione Edmund Mach, San Michele all'Adige (TN), pp. 43–45.

Clabassi, I., 2000. Black-rot, nouva ampelopatia in Friuli Venezia Giulia,. In A. Morando, M. Morando, and D. Morando (Eds.) Vitenda 2000. L'agenda Del Viticultore. Calosso: Vit. En., pp. 58–60.

Corte, A., 1975. Il marciume nero degli acini o "Black-rot" della vite in provincia di La Spezia. Informatore Fitopatologico 8, 15–20.

Costacurta, A., Lavezzi, A., Tomasi, D., Giorgessi, G., Antoniazzi, P., 2004. Guida per il viticoltore. Azienda regionale Veneto agricoltura, Legnaro (Pd).

Devaut, T., 1990. Contribution a la modelisation des contaminations de la vigne par *Guignardia bidwellii* (Ellis) Viala e Ravaz agent responsable du Black-rot. Section de troisiéme cycle intércoles. Montpellier: Ecole nationale superieure agronomiqe.

Ellis, M.A., Madden, L.V., Wilson, L.L., 1986. Electronic grape black-rot predictor for scheduling fungicides with curative activity. Plant Disease 70, 938–940.

EPPO, 2000. *Plasmopara viticola*. Guidelines for the efficacy evaluation of plant protection products. Eur. Mediterranean Plant Protection Organisation Paris 3, 1/31.

Ferrin, D.M., Ramsdell, D.C., 1978. Influence of conidia dispersal and environment on infection of grape by *Guignardia bidwellii*. Phytopathology 68, 892–895. doi:10.1094/Phyto-68-892

Ferrin, D.M., Ramsdell, D.C., 1977. Ascospore dispersal and infection of grapes by *Guignardia bidwellii*, the causal agent of grape black-rot disease. Phytopathology 67, 1501–1505.

Funt, R., Ellis, M., Madden, L., 1990. Economic analysis of protectant and disease-forescast-based fungicide spray programs for control of apple scab and grape black-rot in Ohio. Plant Disease 74, 638–642.

Gadoury, D., 1993. Integrating management decisions for several pests in fruit production. Plant Disease 77, 299–302.

Hanley, J.A., 2005. Receiver operating charatteristic (ROC) curves. In: Armitage, P., Colton, T. (Eds.), Encyclopedia of Biostatistics. Jhon wiley and Sons, New York, NY, USA, p. 6100.

Harms, M., Holz, G., Hoffmann, C., Lipps, H., Silvanus, W., 2005. Occurrence of

Guignardia bidwellii, the causal fungus of black-rot on grapevine, in the vine growing areas of Rhineland-Palatinate, Germany. BCPC Symposium 81, 127–132.

Hoffman, L.E., Wilcox, W.F., Gadoury, D.M., Seem, R.C., 2002. Influence of grape berry age on susceptibility to *Guignardia bidwellii* and its Incubation period length. Phytopathology 92, 1068–76. doi:10.1094/PHYTO.2002.92.10.1068

Hoffman, L.E., Wilcox, W.F., Gadoury, D.M., Seem, R.C., Riegel, D.G., 2004. Integrated control of grape black-rot: influence of host phenology, inoculum availability, sanitation, and spray timing. Phytopathology 94, 641–50. doi:10.1094/PHYTO.2004.94.6.641

Jermini, M., Gessler, C., 1996. Epidemiology and control of grape black-rot in Southern Switzerland. Plant Disease 80, 322–325.

Kuo, K.C., Hoch, H.C., 1996. The parasitic relationship between *Phyllosticta ampelicida* and *Vitis vinifera*. Mycologia 88, 626–634.

Lin, L., 1989. A concordance correlation coefficient to evaluate reproducibility. Biometrics 45, 255–268.

Lorenz, D.H., Eichhorn, K.W., Bleiholder, H., Klose, R., Meier, U., Weber, E., 1995. Phenological growth stages of the grapevine. *Vitis vinifera* L. ssp. vinifera. Codes and descriptions according to the extended BBCH scale. Australian Journal of Grape Wine Research 1, 100–103.

Madden, L.V., Hughes, G., van den Bosch, F., 2007. The study of plant disease epidemics. APS-Press, St. Paul, MN, USA.

Madden, L. V., 2006. Botanical epidemiology: some key advances and its continuing role in disease management. European Journal of Plant Pathology. 115, 3–23. doi:10.1007/s10658-005-1229-5

Martinelli, U., 1891. Il black-rot sulle viti presso Firenze. Nuovo Giornale Botanico Italiano 23, 604–610.

Mauri, G., Kobel, U., 1988. Black-rot – a new severe grape disease in Ticino. Schweizer Zeitschrift für Obstund Weinbau (SZOW) Wädenswil 124, 473–475.

Maurin, G., Cartolaro, P., Clerjeau, M., Benac, G., 1991. Black-rot: vers une méthode de prévisions des risques. Phytoma - La Défence des Végétaux 433, 39–42.

Molitor, D., 2009. Untersuchungen zur biologie und bekämpfung der schwarzfäule (*Guignardia bidwellii*) an weinreben.

Molitor, D., Fruehauf, C., Baus, O., Berkelmann-Loehnertz, B., 2012. A Cumulative Degree-day-based model to calculate the duration of the incubation period of *Guignardia bidwellii*. Plant Disease 96, 1054–1059.

Nash, J., Sutcliffe, J., 1970. River flow forecasting through conceptual models part I. J. Hidrol. 10, 282–290.

Northover, P., 2008. Factors influencing the infection of cultivated grape (*Vitis* spp. section Euvitis) shoot tissue by *Guignardia bidwellii* (Ellis) Viala and Ravaz. The

Pennsylvania State University.

Ramsdell, D.C., Milholland, R., 1988. Black-rot. In: Pearson, R., Goheen, A. (Eds.), Compendium of Grape Diseases. APS Press, St. Paul, pp. 15–17.

Reddick, D., 1911. The black-rot disease of grapes. Cornell University Agricultural Experiment Station Bulletin 239, 289–364.

Rinaldi, P.A., Mugnai, L., 2012. Marciume nero degli acini, potenziale pericolo in viticoltura. Informatore Agrario 15, 68–71.

Rossi, V., Caffi, T., Salinari, F., Srl, H., 2012. Helping farmers face the increasing complexity of decision-making for crop protection. Phytopathologia Mediterranea 51, 457–479.

Rossi, V., Onesti, G., Legler, S.E., Caffi, T., 2014. Use of systems analysis to develop plant disease models based on literature data : grape black-rot as a case-study. European Journal of Plant Pathology 141, 427–444. doi:10.1007/s10658-014-0553-z

RPD, 2001. Report on plant disease N° 703 – Black-rot of grapes. Department of crop Sciences University of Illinois at Urbana-Champaign.

Rui, D., 1989. "Ultimissime" sul black-rot della vite. Informatore Agrario 39, 67–69.

Scribner, F., 1886. Report on the fungus diseases of the grapevine. US Dep. Agric. Bot. Div. Sect. Plant Pathol. Bull. 2 GPO. Washington DC.

Smith, D.L., 2009. Grape Pathology Research Update: black-rot advisory. Le Vigneron 4, 7–8.

Sosnowski, M.R., Emmett, R.W., Wilcox, W.F., Wicks, T.J., 2012. Eradication of black-rot (*Guignardia bidwellii*) from grapevines by drastic pruning. Plant Pathol. 61, 1093–1102. doi:10.1111/j.1365-3059.2012.02595.x

Spotts, R.A., 1977. Effect of leaf wetness duration and temperature on the infectivity of *Guignardia bidwellii* on grape leaves. Phytopathology 67, 1378–1381. doi:10.1094/Phyto-67-1378

Teng, P.S., 1981. Validation of computer models of plant disease epidemics: a review of philosophy and methodology. Journal of Plant Disease Protection 88, 49–63.

Ullrich, C.I., Kleespies, R.G., Enders, M., Koch, E., 2009. Biology of the black-rot pathogen, *Guignardia bidwellii* , its development in susceptible leaves of grapevine *Vitis vinifera*. Journal Für Kulturflanzen 61, 82–90.

Zweig, M.H., Campbell, G., 1993. Receiver-operating characteristic (ROC) plots, a fundamental evaluation tool in clinical medicine. Clinical Chemistry 39, 561–577.

Wilcox, W.F., 2003. Black-rot *Guignardia bidwellii* (Ellis) Viala and Ravaz. Disease Identification Sheet No. 102GFSG-D4. Cornell Cooperative Extension.

Chapter 4

Chapter 4

Dispersal patterns of *Guignardia bidwellii* ascospores and conidia from grape berry mummies overwintered in the vineyard

ABSTRACT

Black-rot of grapevine, caused by the ascomycete *Guignardia bidwellii*, is a polycyclic disease with repeated primary and secondary infection cycles. In this work, the dynamic of primary inoculum (both ascospores and conidia) from overwintered grape mummies of *G. bidwellii* was investigated in an experimental vineyard during three years. Ascospores and conidia were frequently found in runoff water samples, with a similar trend between the years. The seasonal cumulative number of both *G. bidwellii* ascospores and conidia as a function of degree-days (DD) was well described by a Gompertz equation, confirming that it is a temperature dependent process. The best thresholds for DD calculation were base 10°C for conidia and between 9 and 25°C for ascospores. The numbers of both spore types dispersed in the runoff water significantly increased as the amount of rain, its duration, and rain intensity increased. ROC and Bayesian analysis showed >1 and >3 mm of rain as the best cut-off points for predicting the dispersal of conidia and ascospores. The number of black-rot lesions on leaves sharply decreased as the distance from the inoculum source increased, this indicate a typical gradient for splash-borne pathogens.

Keywords: *Guignardia bidwellii*, black-rot, primary inoculum, splash-borne, disease gradient.

INTRODUCTION

The ascomycete *Guignardia bidwellii* (Ellis) Viala and Ravaz (anamorph: *Phyllosticta ampelicida* (Englem.) van der Aa) is a serious pathogen on grapevines. Causal agent of black-rot, the fungus can cause yield loses up to 80% and affect wine quality, largely in grape-growing areas with warm and moist conditions in spring and early summer (Ellis *et al.*, 1986; Ferrin and Ramsdell, 1977, 1978; Funt *et al.*, 1990; Harms *et al.*, 2005; Ramsdell and Milholland, 1988; Scribner, 1886).

Black-rot is a polycyclic disease, with repeated primary and secondary infection cycles during the grape-growing season, which progressively affect expanding leaves, petioles, young shoots, and tendrils. Lesion on these plant tissues appear as circular to

elliptic, necrotic lesions, with a light brown centre and a dark border. Bunches are also affected from mid-bloom and onward (Hoffman *et al.*, 2002; Molitor and Berkelmann-Loehnertz, 2011). Symptoms appear as flower cluster blight in early season, and as a typical berry rot during berry ripening (Kummuang *et al.*, 1996); the affected berries progressively become rotten, then they shrivel and form black mummies (Bottura, 2011; Hoffman *et al.*, 2002; Kong, 2012; Reddick, 1911; Rinaldi and Mugnai, 2012; Sosnowosky *et al.*, 2014).

Primary infections are caused by ascospores and conidia produced in perithecia and pycnidia, respectively, which are both formed in the overwintered berry mummies in the vineyard (Becker and Pearson, 1992, 1996; Ferrin and Ramsdell, 1977; Hoffman *et al.*, 2004; Ramsdell and Milholland, 1988). Conidia from canes and tendrils also contribute to primary infections (Gadoury, 1995; Hoffman *et al.*, 2004). Secondary infections are caused by conidia produced by pycnidia developing in the black-rot lesions on leaves and other green tissues; pycnidia also form in the rotted and shriveled berries.

Ascospores are considered the main form of primary inoculum (Ramsdell and Milholland, 1988). However, no studies have been performed to show the relative abundance of ascospores and conidia in the same vineyard, with the exception of the 2-year study of Hoffman *et al.* (2004) in New York, US. In that study, much more conidia than ascospores were found in mummies repeatedly sampled in the vineyard and soaked with water.

Ascospores began to mature shortly after bud break and have been found in the perithecia as late as October in New York (Reddick, 1911). However, trapping studies have indicated that ascospore release ends in early July (approximately 3 to 4 weeks post-bloom) in Switzerland (Jermini and Gessler, 1996), and in September (pre-harvest) in Michigan (Ferrin and Ramsdell, 1977). In discharge tests, mummies from New York vineyards released approximately 90 to 100% of the available ascospores by bloom to one month post-bloom (Becker and Pearson, 1992; Gadoury *et al.*, 1997). Ascospore release occurred even later from mummies collected from the trellis rather than from the ground (Becker and Pearson, 1992). In Michigan, conidia were first trapped in the rainwater running off from overwintered rotted berries in late April (shoots approximately 5 cm in length); conidia were then released at relatively low numbers till mid-June (petal fall), and progressively increased till late July (berry diameter of about 1 cm) (Ferrin and Ramsdell, 1978). Conidia from canes were dispersed from bud-break until harvest (Becker and Pearson, 1996).

Rossi *et al.* (2014) used the above literature information to develop and parameterize equations relating days after bud break of vines or accumulated degree-days to cumulative numbers of air-borne ascospores trapped over the season. These equations gave R^2 = 0.87 and 0.97 for days and degree-days, respectively, indicating that ascospore availability during the season is temperature dependent. Similarly, Rossi *et al.* (2014)

used the literature data to describe the cumulative proportion of mature conidia released from mummies by means of an equation based on the degree-days accumulated after bud break.

Rainfall is essential for the dispersal of both ascospores and conidia. Ascospores are produced in perithecia; mature perithecia need to absorb water to forcibly discharge ascospores into the air (Reddick, 1911). As little as 0.03 cm rain was capable of triggering ascospores discharge, but the number of the ascospores increased with the duration of rainfall, because the longer the rainfall was, the more likely the mummies were to be wetted (Ferrin and Ramsdell, 1977). Conidia, being exuded from pycnidia in mucilaginous cirri, are dispersed by rainwater run-off from mummies and by splashing rain (Ferrin and Ramsdell, 1978). Conidia are expected to be released by lesser amounts of rain than ascospores (Ferrin and Ramsdell, 1978), but no precise information is available on minimum amount of rain for the release of conidia.

The present work was carried out to further investigate the dynamics of the primary inoculum of *G. bidwellii* in vineyards. The specific objectives were to: (i) study the dispersal dynamics of both ascospores and conidia produced in grape mummies overwintered in the vineyard over a 3-year period; (ii) relate this dispersal to the environmental conditions; and (iii) define the disease dispersal gradient in relation to a line source of primary inoculum.

MATERIALS AND METHODS

Experimental vineyard

A three-year field study was carried out (2013 to 2015) in a 7-year old (in 2013) vineyard of cv. Barbera at the University campus of Piacenza (North Italy, 45°2’N, l 9°43’E). Plants were trained on a Guyot trellis system and they were not sprayed with fungicides. The experimental vineyard consisted of 8 rows of vines, with 13 plants in each row, 1.1 m spaced. The between-row distance was irregular, being 3.2, 1.5, 1.9, 1.9, 1.9, 5.1, and 1.3 m. The growth stage of vines was assessed weekly between March and mid-September by using the BBCH scale of Lorenz *et al.* (1995).

A standard weather station (MeteoSense 2.0, Netsens s.r.l., Firenze, Italy) located into the vineyard provided hourly records of air temperature (T, °C), relative humidity (RH, %), rainfall (R, mm), and leaf wetness duration (WD, hours).

Spore trappings

Spore samplers were designed for trapping ascospores and conidia from rotted berry mummies (Figure 1). A spore sampler consists of a 100-ml plastic bottle (Figure 1, f) having a funnel (9.5 cm in diameter) inserted in the cap (Figure 1, e). The funnel cup hold a cylindrical box (9 cm in diameter and 5 cm in height) made with metal net (0.5 × 0.5

cm grid), most of the box emerging from the funnel border (Figure 1, a); the box was designed in such a way to hold mummified berries as inoculum source. The funnel is lodged in a wood support (15 × 15 cm wide) (Figure 1, d) carrying two opposite clips (Figure 1, g) for vertically positioned microscope slides (Figure 1, h) at a distance of 2 cm from the metallic box. The microscope slides (75 × 25 mm) were equipped with transparent double-side adhesive tape (Tesa AG, Hamburg, Germany) (50 × 12 mm). The sampler was then designed to trap both spores washed of by rainfall (flowing into the bottle of Figure 1, f) and dispersed by air currents or by splashed droplets (impacting on the adhesive tape of the microscope slides of Figure 1, h) (Campbell and Madden, 1990).

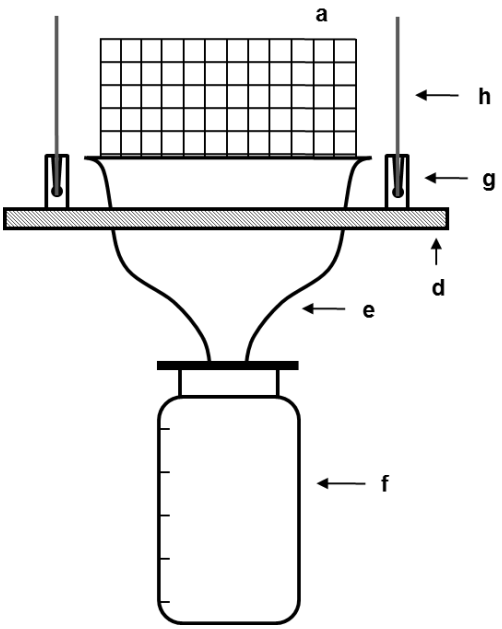

Figure 1. Schematic representation of the spore sampler used for trapping *Guignardia bidwellii* conidia and ascospores from grape berry mummies placed in the metal net (a). The spore sampler is composed by a wood support (d) with a plastic funnel (e). The funnel neck enters in a removable plastic bottle (f) used for collecting the spores in the runoff water. Special plastic clips (g) were glued on the wood support (d); microscope slides (h) were inserted in clips and equipped with transparent double-side adhesive tape to collect spores dispersed by air currents or by splashed droplets.

Nine spore samplers were randomly installed over the trellis at 1.80 m above the ground, 1.5 m apart, in the 4th row of the experimental vineyard. Twenty grams of berry mummies were arranged in the metal box (Figure 1, a) of each sampler at the end of February each year. Berry mummies were obtained as follows. Grape bunches severely affected by black-rot were collected in late August from 3 to 5 vineyards (not sprayed against black-rot) in northern Italy, and overwintered outdoor at the University campus, where they dried out and mummified. At the end of February, bunches were collected and mummified berries observed under a dissecting microscope for checking the presence of the typical *G. bidwellii* stromata which hold perithecia and pycnidia. All the mummified

berries with stromata were included in a unique bulk sample, from which sub-samples of 20 g were randomly collected and placed in the spore samplers.

Bottles of the spore traps (Figure 1, f) were replaced after every rain event (i.e., ≥0.2 mm rain), and microscopes slides were replaced with new ones every 2 or 3 days, at 9:00 am, from March to mid September each year. After each rain event, the volume of water in the bottles was measured and the numbers of *G. bidwellii* conidia and ascospores were enumerated by a haemocytometer, and expressed as number per ml of water. The microscope slides were stained with a fuchsine glycerine jelly under a 22 × 50 mm coverslip (80 g of gelatin, 440 ml of glycerine, 1.5 ml of fuchsine, 15 ml of phenol and 465 ml of distilled water) (Lanzoni srl, Bologna, Italy). The *G. bidwellii* conidia and ascospores present on two lengthwise stripes (1.08 mm wide) were enumerated using a microscope (×200 magnification) and expressed as number per cm^2 of slide. Spores were identified as either ascospores or conidia based on morphology and size (Ramsdell and Milholland, 1988).

Disease assessment

The black-rot lesions present in all leaves of the experimental vineyard were enumerated at the end of May 2015, and expressed as the number of the lesions per m of vine row.

Data analysis

A preliminary analysis of the spore countings revealed that most of the spores were found in the water running off from berry mummies during rain events. Very low numbers of spores were trapped by the microscope slides, in few periods with rain, and these spores were always spatially aggregated in clusters, demonstrating that they were dispersed by rain splashes. Therefore, the data analysis was carried out by using the trappings from rainwater only.

Temporal dynamics of spore trappings. To study the dynamic of spore trappings over time, the numbers of ascospores and conidia found in the runoff water were accumulated, and expressed as the proportion of the total ascospores (PSA, proportion of the seasonal ascospores) and conidia (PSC, proportion of the seasonal conidia) found in the whole season. PSA and PSC were regressed against time, expressed as either days (DOY, days of the year) or degree-days (DD) accumulated after bud break. Degree-days were calculated as in Rossi *et al.* (2014) for ascospores and conidia, precisely as $DD_{9\text{-}19}$ for PSA and DD_{10} for PSC. $DD_{10}(j)$ were cumulative degree-days accumulated from bud break of vines, as follows. For $DD_{9\text{-}19}$: when $T(j) \leq 9$, $T(j) = 0$; when $9 < T(j) \leq 25$, $T(j) = T(j)-9$; when $T(j) > 25$; $T(j) = 16$ (i.e., 25-9). For DD_{10}: when $T(j) \leq 10$, $T(j) = 0$; when $T(j) > 10$, $T(j) = T(j)-10$. Additional DD were also calculated, by using different cardinal temperatures, e.g., DD_{10}, $DD_{9\text{-}25}$, and $DD_{9\text{-}29}$, for PSA.

In a preliminary analysis, different equations were fitted to the observed PSA and PSC data by using DOY and the different DD values as independent variables, and compared by using the AIC criterion (Burnham and Anderson, 2002). The best fit was obtained by using DD as the independent variable and a Gompertz equation, in the form (Campbell and Madden, 1990):

$$Y = \exp[-a \times \exp(-b \times t)] \quad (1)$$

where: Y is either PSA and PSC; *a* is the equation parameter accounting for the length of the lag phase of the S-shaped curve; *b* is the rate parameter; and *t* is the time expressed as either DD_{10} (for PSC) or $DD_{9\text{-}25}$ (for PSA) accumulated after bud break of vines. The equation parameters were estimated using the nonlinear regression procedure of SPSS (ver. 21; SPSS Inc.), which minimizes the residual sums of squares using the Marquardt algorithm. Goodness-of-fit was assessed by using the adjusted R^2, the magnitude of the standard error of the parameters, the root mean square error (RMSE), the coefficient of residual mass (CRM), the concordance correlation coefficient (CCC) (Lin, 1989; Nash and Sutcliffe, 1970). Briefly, RMSE represents the average distance of real data from the fitted line, and CRM is a measure of the tendency of the equation to overestimate or underestimate the observed values (a negative CRM indicates a tendency of the model toward overestimation) (Nash and Sutcliffe, 1970). CCC is the product of two terms: the Pearson correlation coefficient and the coefficient Cb, which is an indication of the difference between the best fitting line and the perfect agreement line (CCC = 1 means perfect agreement) (Madden *et al.*, 2007).

Effect of rain on spore trapping. A correlation analysis was performed to evaluate the relationships between the amount of rain (mm) fell during a rain event, the duration of the rain event (h), the average intensity of rain (mm/h), and the natural logarithm of the number of *G. bidwellii* conidia and ascospores found in the runoff water. Pearson and Spearman correlation coefficients were calculated; the Spearman rank correlation coefficient is less sensitive to strong outliers because it limits the outlier to the value of its rank.

The degree of association between the occurrence of a rain event and the detection of spores in the runoff water was also investigated. A rain event was defined based on five rain thresholds (or "cut-off" values), specifically: >0.2, >0.6, >1, >2, >3, >5, >8 and >10 mm rain. For each cut-off value, cases were then categorized as either 0 or 1. For instance, for the cut-off value >2 mm rain, the rain event was = 0 when rain ≤2 mm, and = 1 when rain >2 mm. Similarly, cases were categorized for spore detection as = 0 when no spores were detected, and = 1 when ≥1 conidium or ascopore was detected in the rainwater. Afterwards, cases were classified as: (i) true positive, when rain = 1 and spore

detection = 1; (ii) true negative, when rain = 0 and spore detection = 0; (iii) false positive, when rain = 1 and spore detection = 0; and (iv) false negative, when rain = 0 and spore detection = 1. For each cut-off value, contingency Tables (2 × 2) were prepared with the cells containing the true positive proportion (TPP or sensitivity); the true negative proportion (TNP or specificity), the false positive proportion (FPP), and the false negative proportion (FNP) (Madden, 2006).

A receiver operating characteristic curve (ROC) analysis was used to evaluate the possibility of predicting presence of *G. bidwellii* spores in rainwater based on the different cut-off values for rain. ROC analysis measures the accuracy of different cut-off values as predictors. Sensitivity calculated as previously described was plotted against 1-specificity. The closer the ROC curve is to the upper left corner of the plot, the greater the accuracy of the test (Hanley, 2005; Zweig and Campbell, 1993). The area under the ROC curve (AUROC) and its standard error were used to evaluate the analysis; AUROC values between 0.5 and 1 indicate that the variable (an amount of rain event in this case) is a good predictor of the response variable (presence of spores in rainwater in this case). The *P* value was calculated as the probability that the AUROC is significantly different from 0.5 (i.e., the ROC curve coincides with the line of no discrimination, having 0,0 and 1,1 as coordinates).

The posterior probability to predict the presence of conidia or ascospores in runoff water for each of the rainfall cut-off values was calculated, as described by Madden *et al.* (2006). The following conditional probabilities were considered: (i) the probability that *G. bidwellii* spores are present in runoff water when predicted based on rainfall amount, P(P+|O+); (ii) the probability that no spores are present when not predicted, P(P-|O-); (iii) the probability that no spores are present when predicted, P(P+|O-); and (iv) the probability that spores are present when not predicted, P(P-|O+). These probabilities were compared to the prior probabilities of spores being present in runoff water, calculated for each rainfall cut-off value as the proportion of cases with P(O+) or without P(O-) spores in runoff water. The overall accuracy of the predictor was finally calculated as the ratio between correct and total predictions. The analysis was performed separately for conidia and ascospores. The statistical software SPSS (ver. 21.0; SPSS Inc.) was used for ROC analysis.

Disease gradient. The relationship between numbers of black-rot lesions and distance (m) from the *G. bidwellii* inoculum source (mummies in the fourth row) was modelled using the power law and other exponential models (Madden *et al.*, 2007). These models were fit to the observed data and compared by using the AIC criterion (Burnham and Anderson, 2002). The best fit was obtained by using an exponential equation (negative exponential) in the form:

$$Y = a \times \exp(-b \times s) \quad (2)$$

in which Y represents the number of lesions per m of vine row, and *a*, *b* and *s* are the equation parameters. Parameter *a* represent the (theoretical) level of *Y* at the inoculum source (*s* = 0) and *s* represent the distance (m) from the inoculum source (Madden *et al.*, 2007). The equation parameters were estimated using the nonlinear regression procedure of SPSS (ver. 21.0; SPSS Inc.), and goodness-of-fit was assessed as described before.

RESULTS

Dynamics of spore dispersal

In total 1,608 microscope slide samples (264 in 2013, 848 in 2014, and 496 in 2015) and 70 runoff water samples (25 in 2013, 24 in 2014, and 21 in 2015) were analysed. No *G. bidwellii* ascospores were found on microscope slides. Conidia were found on microscope slides every year, on approximately 2% of the total samples (Figure 2, horizontal black lines). These conidia were observed only on slides exposed during rain periods, in few numbers and clustered in circular aggregates, probably corresponding to droplets splashing from mummies during rainfall.

G. bidwellii conidia and ascospores were both frequently found in runoff water samples (Figure 2). A total, 3.6×10^4, 2.8×10^4, and 3.9×10^5 spores ml^{-1} were collected in the runoff water in 2013, 2014 and 2015, respectively. In 2013 (Figure 2A), numbers of conidia found in runoff water were approximately 5 times higher than ascospores, with a total of 3.0×10^4 conidia and 6.0×10^3 ascospores ml^{-1} water, respectively, over a total of 26 rain events (501.7 mm of rain in aggregate). The first seasonal conidia (322 conidia ml^{-1} water) were found in the runoff water collected on April 30, after 15 mm rain while the first ascospores (257 ascospores ml^{-1} water) were found in the rainwater collected on May 13, after 8.6 mm rain. The last seasonal conidia and ascospores (257 and 900 spores ml^{-1} water, respectively) were both found in the runoff water collected on August 26, after 27.6 mm rain (Figure 2A). In 2014 (Figure 2B), more ascospores were found than conidia, with a total of 2.1×10^4 and 7.1×10^3 ml^{-1} water, respectively, in 26 rain events and 463.7 mm of rain. Both spore types were found earlier than in the previous year, with the rain event on March 28 8.8 mm rain; 514 conidia and 64 ascospores ml^{-1} water), and the spore trapping season was longer, being the last spores found in the runoff water collected on September 10 (1.2 mm rain; 64 conidia and 386 ascospores ml^{-1} water) (Figure 2B). In 2015 (Figure 2C), a total of 3.8×10^5 conidia and 6.5×10^3 ascospores were found over 26 rain events and 329.3 mm rain. First conidia were found one month earlier than ascospores. First conidia were found on the runoff water collected on March 26 (26 mm of rain; 129 conidia ml^{-1} water) and first ascospores on April 30 (66.2 mm of rain;

154 ascospore ml^{-1} water). Trapping of both spore types finished with the runoff water sampled on September 14 (26.8 mm of rain; 5015 conidia and 707 ascospores ml^{-1} water) (Figure 2C).

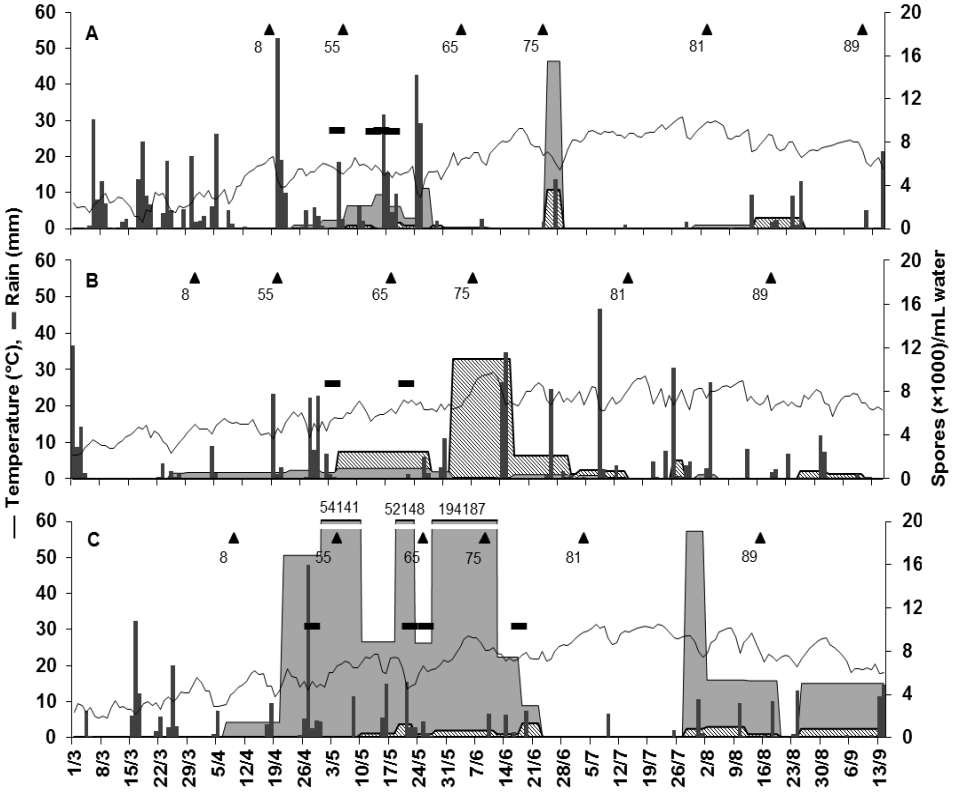

Figure 2. Numbers of *Guignardia bidwellii* conidia (grey area) and ascospores (hatched area) found in the rainwater running off from grape berry mummies overwintered in an experimental vineyard in Piacenza (North Italy), in 2013 (**A**), 2014 (**B**), and 2015 (**C**). Spores were caught through the spore trap of Figure 1 and expressed as numbers found per ml of runoff water in plastic bottles after each rain event (Figure 1, f). Weather data are shown as temperature (solid line) and rainfall (dark grey bars). Horizontal black lines (▬) represent the periods when conidia were found on microscope glass slides (Figure 1, h); no ascospores were found on microscope slides. Triangles (▲) show the vine grow stages according to Lorenz *et al.* (1995): 8 (bud burst: green shoot tips clearly visible), 55 (inflorescences swelling, flowers closely pressed together), 65 (full flowering: 50% of flowerhoods fallen), 75 (berries pea-sized, bunches hang), 81 (beginning of ripening: berries begin to develop variety-specific color) and 89 (berries ripe for harvest).

Some similarities were observed in the spore release dynamics in the three years. In all the years, first conidia were found at approximately bud break of vines (stage 08), which occurred in late March in 2014 and 2015, and at the end of April in 2013 (Figure 2). A relevant proportion of the seasonal conidia were found in the runoff water collected before mid-bloom (stage 65), being PSC = 45, 54 and 35% in 2013, 2014, and 2015, respectively (Figure 2). In addition, a peak of spore release (either ascospores or conidia, depending on the year) occurred at approximately the pea-sized berries (stage 75). Finally, most of the spores were already found before veraison (stage 81), specifically, >90% of PSC and >85% of PSA, with the only exception of 2015, where approximately 39% of the total ascospores were found after veraison.

The fitting of PSA and PSC data to a Gompertz equation provided better results by using DD than DOY; specifically, the standard errors of the parameter estimates were lower for DD than for DOY (not shown), so that the 95% confidence bands of the curves were wider for DOY (cfr. Figure 3A and 3B with 3C and 3D). For PSA and $DD_{9\text{-}25}$ (Figure 3B), the parameter estimates were: a = 12.75±3.03, b = 0.005±0.0001, with R^2 = 0.945, and a CCC = 0.963; the root mean square error (RMSE) and the coefficient of residual mass (CRM) were low (0.119 and -0.003, respectively). For PSC and DD_{10}, the parameter estimates were: a = 4.00±0.65, b = 0.005±0.001, with R^2 = 0.92 and CCC = 0.944; values of RMSE and CRM were low (0.143 and -0.022, respectively).

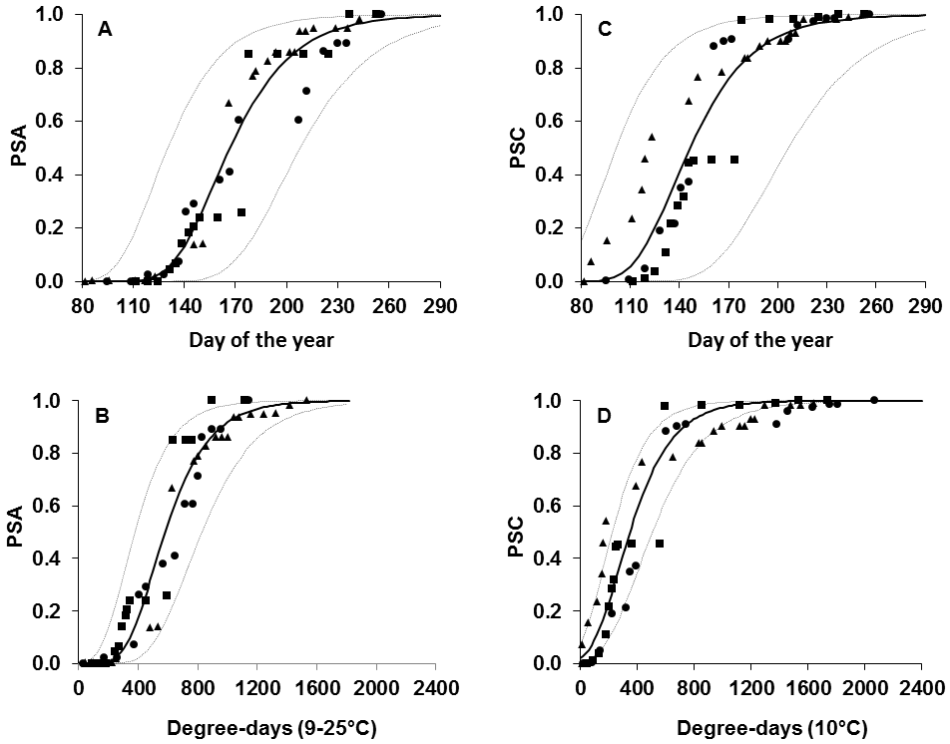

Figure 3. Proportion of the seasonal ascospores (PSA) and conidia (PSC) of *Guignardia bidwellii* found over time in the rainwater running off from grape berry mummies overwintered in an experimental vineyard in Piacenza (North Italy), in 2013 (♦), 2014 (■), and 2015 (▲). Time is expressed as day of the year (**A** and **C**) or degree-days accumulated between 9 and 25°C for ascospores (**B**) and with base 10°C for conidia (**D**). Solid line represents the Gompertz equation fitting the data and dotted lines its 95% confidence bands.

Rain and spore release

No *G. bidwellii* conidia and ascospores were found in runoff water during rain events with ≤0.2 and ≤1 mm of rain, respectively (Figure 4). The numbers of both conidia and ascospores increased with the amount of rain in a rain event (Figure 4). Positive and significant correlations were found between the number of *G. bidwellii* ascospores and conidia in the runoff water and the amount of rain, the duration of the rain event, and the average rain intensity (Table 1).

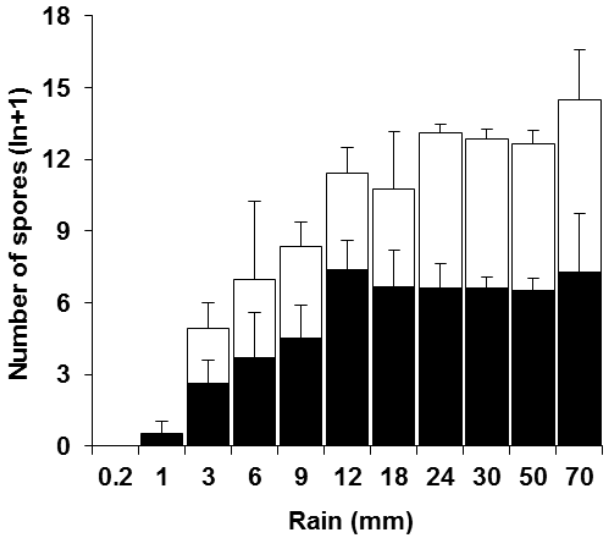

Figure 4. Numbers of *Guignardia bidwellii* conidia (black bars) and ascospores (white bars) found in the rainwater running off from grape berry mummies overwintered in an experimental vineyard in Piacenza (North Italy) after rain events with increasing amount of rain. Spores were caught in 2013 to 2015 through the spore trap of Figure 1 and expressed as the natural logarithm of spore numbers found per mL of runoff water in plastic bottles after each rain event (Figure 1, f). Bars show the average and whiskers the standard error of the spore numbers found in the rain events belonging to each rain interval; rain intervals are: ≤0.2 mm, >0.2 to ≤1 mm; >1 to ≤3 mm; etc.

Table 1. Correlation coefficients between the amount of rain, duration and intensity of a rain event and the number of *Guignardia bidwellii* ascospores and conidia in the runoff water from berry mummies.

Rain variables	Conidia[a]		Ascospores	
	r[b]	ρ[c]	r	ρ
Total rainfall (mm)	0.465[d]	0.608	0.570	0.629
Duration (h)	0.387	0.424	0.453	0.480
Rain intensity (mm/h)	0.454	0.572	0.489	0.553

[a] The numbers of *G. bidwellii* conidia and ascospores were counted in the runoff water from berry mummies overwintered in a vineyard in Piacenza (Italy) in 2013 to 2015, and expressed as natural logarithm of the number per ml of water; n = 67 for conidia and n = 56 for ascospores;
[b] correlation coefficient of Pearson;
[c] correlation coefficient of Spearman;
[d] all the correlation coefficients were significant with P <0.001.

In the ROC analysis, the use of rain amount for predicting the occurrence of spore trapping in runoff water from black-rot mummies gave AUROC = 0.897±0.040 and 0.893±0.039 for ascospores and conidia, respectively. Both AUROC were significantly >0.5 (*P* <0.001) (Figure 5). Increasing the cut-off value of rainfall used for predicting

spore trappings led to a decrease in TPP and FPP for both spore types, and to an increase of FNP and TNP (Table 2). The best combination of sensitivity *vs* specificity, and the highest overall accuracy, were obtained with a rainfall cut-off of >1 mm for conidia and >3 mm for ascospores (Table 2). Bayesian analysis indicated that using >1 mm of rain for conidia and >3 mm for ascospores as cut-off points provided high probability to correctly predict the release of spores in the runoff water (P+|O+) (0.784 and 0.796 for ascospores and conidia, respectively), and low probability of failing to predict a spore release (P-|O+) (0.111 and 0.042 for ascospores and conidia, respectively); only 0.02% and 2.2% of the total conidia and ascospores were released in those false negative prediction of spore release.

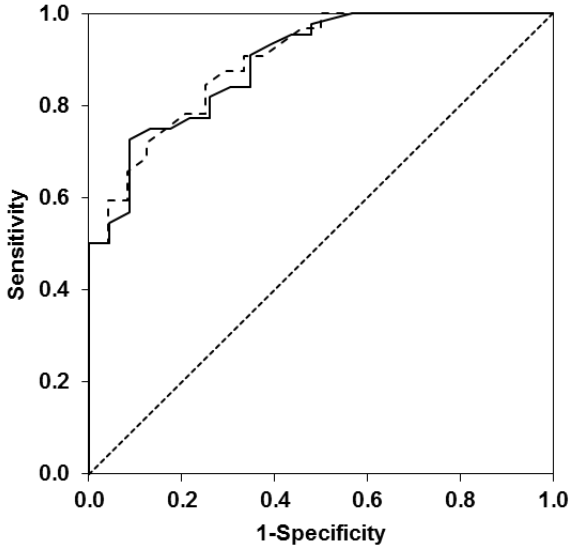

Figure 5. Receiver operating characteristic (ROC) curve for the accumulated rainfall (mm) in relation to the probability of collecting conidia (solid line) or ascospores (dashed line) of *Guignardia bidwellii* during three monitoring years (2013, 2014 and 2015). The dotted line (0,0; 1,1) represents no discrimination.

By using higher rainfall cut-off points, the probability of correctly predicting a spore release event (P+|O+) increased, but the probability of not predicting a spore release event that actually occurred (P-|O+) increased too (Table 2).

Table 2. Evaluation of rainfall to predict collection of *Guignardia bidwellii* conidia and ascospores in the rainwater running off from grape berry mummies in a vineyard in Piacenza, Italy, in 2013 to 2015.

Rain[a]	Proportions[b]				Overall accuracy[c]	Posterior probabilities[d]			
	TPP	FNP	FPP	TNP		(P+|O+)	(P-|O-)	(P+|O-)	(P-|O+)
Conidia									
>0.2	1.000	0.000	0.783	0.217	0.731	0.710	1.000	0.290	0.000
>0.6	1.000	0.000	0.696	0.304	0.761	0.733	1.000	0.267	0.000
>1	0.977	0.023	0.478	0.522	0.821	0.796	0.958	0.204	0.042
>2	0.932	0.068	0.391	0.609	0.821	0.820	0.885	0.180	0.115
>3	0.886	0.144	0.348	0.652	0.806	0.830	0.821	0.170	0.179
>5	0.841	0.159	0.348	0.652	0.776	0.822	0.767	0.178	0.233
>8	0.773	0.227	0.217	0.783	0.776	0.872	0.697	0.128	0.303
>10	0.659	0.341	0.087	0.913	0.746	0.935	0.605	0.065	0.395
Ascospores									
>0.2	1.000	0.000	0.792	0.208	0.661	0.627	1.000	0.373	0.000
>0.6	1.000	0.000	0.708	0.292	0.696	0.653	1.000	0.347	0.000
>1	1.000	0.000	0.500	0.500	0.786	0.727	1.000	0.273	0.000
>2	0.938	0.063	0.417	0.583	0.786	0.750	0.923	0.250	0.077
>3	0.906	0.094	0.333	0.667	0.804	0.784	0.889	0.216	0.111
>5	0.875	0.125	0.333	0.667	0.786	0.778	0.857	0.222	0.143
>8	0.781	0.219	0.208	0.792	0.786	0.833	0.774	0.167	0.226
>10	0.656	0.344	0.083	0.917	0.768	0.913	0.686	0.087	0.314

[a] Total rainfall (mm) that were used as cut-off values, i.e., to define a rain event;

[b] *TPP* (true positive proportion, or sensitivity), periods when rain = 1 and spore detection = 1 divided by the total number of periods with detection; *TNP* (true negative proportion, or specificity), periods when rain = 0 and spore detection = 0 divided by the total number of periods with no detection; *FPP* (false positive proportion), periods when rain = 1 and spore detection = 0 divided by the total number of periods with no detection; *FNP* (false negative proportion), periods when rain = 0 and spore detection = 1 divided by the total number of periods with detection;

[c] Overall accuracy calculated as the proportion of correct predictions;

[d] Posterior probability that *G. bidwellii* spores are present in runoff water when predicted based on rainfall amount, P(P+|O+); posterior probability that no spores are present when not predicted, P(P-|O-); posterior probability that no spores are present when predicted, P(P+|O-); and posterior probability that spores are present when not predicted, P(P-|O+). Prior probabilities of spores being present in runoff water, calculated for each rainfall cut-off value as the proportion of cases with P(O+) or without P(O-) spores in runoff water were Prob(O+) = 0.657 and Prob(O-) = 0.343 for conidia; Prob(O+) = 0.571 and Prob(O-) = 0.429 for ascospores.

Disease gradient

The number of black-rot lesions on leaves sharply decreased as the distance from the inoculum source increased, following a negative exponential equation, with estimated parameters: a = 246.8±17.2 and b = 0.65±0.08, and R^2 = 0.964 (Figure 6). At 2 and 5 m of distance from the inoculum source, the number of lesions were reduced by 73% and >96%, respectively.

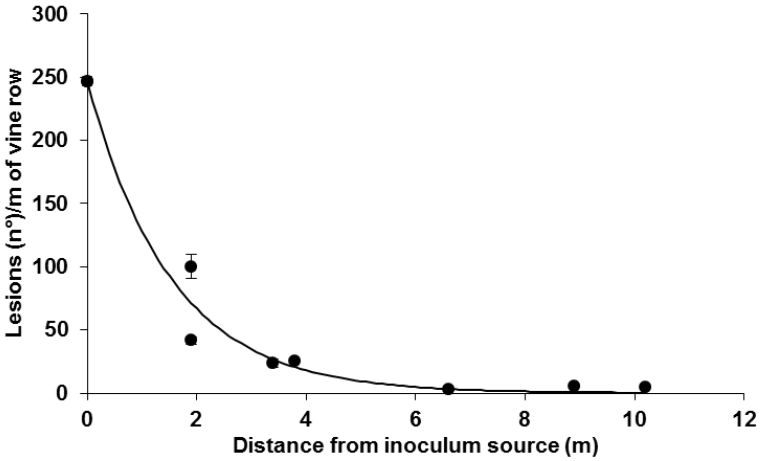

Figure 6. Numbers of the *Guignardia bidwellii* lesions found on the leaves present in 1 meter of vine row at increasing distances from an inoculum source represented by grape berry mummies overwintered in an experimental vineyard in Piacenza (North Italy). Mummies (20 g) were placed in nine spore samplers (Figure 1) installed each 1.5 m over one vine row (inoculum source; distance = 0). Dots represent the number of black-rot lesions on leaves per meter of row. Solid line represents a negative exponential equation fitting the data.

DISCUSSION

Substantial differences were found between years in the number of *G. bidwellii* conidia and ascospores found in this work, which maybe related with the characteristics of the berry mummies used as inoculum source. Although the amount of mummies used each year was the same (20 g per spore sampler), differences may have occurred in the severity of *G. bidwellii* colonization and the presence of stromata bearing pycnidia and perithecia in the mummies, depending on bunch disease severity and weather conditions in the vineyards from where the mummies have been collected. As mentioned in the materials and method section, mummies used as inoculum source were a bulk of mummies collected, every year, in different vineyards and areas affected by black-rot, but

no precise information about black-rot severity on bunches in those vineyards was available. The output of the black-rot model (Rossi *et al.*, 2014) and chapter 3 of this Thesis) indicated that in 2012 and 2013 the weather conditions were less conducive for the disease than in 2014. Therefore, mummies used in 2015 (which have been infected in 2014) may bear more fruiting bodies than those used in 2013 and 2014. Really, total spores found in runoff water from mummies were 6 to 10 times greater in 2015 than in 2013 and 2014, respectively.

Irrespective of the between years differences in the spore numbers, the trend of the seasonal cumulative number of conidia and ascospores was similar in the three years. First conidia were dispersed at approximately bud break, and ascospores two weeks later; the majority of both conidia and ascospores were already dispersed before pre-bunch closure. For both spore types, dispersal peaks occurred at pea-sized berries, but spores were found until the first two weeks of September, when berries were ripe. The time the first seasonal ascospores and conidia were dispersed was in agreement with the results obtained in previous works (Ferrin and Ramsdell, 1977, 1978; Jermini and Gessler, 1996). Ferrin and Ramsdell (1978), in Michigan (USA), collected the highest number of *G. bidwellii* conidia when berry were 1 cm in diameter, and continued to collect conidia until September. As in the present work, Hoffman *et al.* (2004) and Becker and Pearson (1992) found ascospores release all season long, with peaks at bloom, in laboratory discharge tests with black-rot mummies.

When the seasonal cumulative numbers of *G. bidwellii* ascospores and conidia were regressed against degree-days (DD), the differences between years were lower than when using the day of the year, confirming that this is a temperature dependent process (Rossi *et al.*, 2014). The best thresholds for DD calculation were base 10°C for conidia and between 9 and 25°C for ascospores, and the best equation was the Gompertz.

In a previous work, Rossi *et al.* (2014) (see Chapter 2 of this Thesis) also used a Gompertz equation for fitting literature data on ascospore dispersal (Ferrin and Ramsdell, 1977; Jermini and Gessler, 1996) by using DD between 9 and 19°C. The cumulative ascospore numbers in the runoff water from mummies did not fit well with the equation of Rossi *et al.* (2014) (not shown). This result was not unexpected, because the above mentioned literature data used by Rossi *et al.* (2014) have been collected by using volumetric spore samplers (Ferrin and Ramsdell, 1977; Jermini and Gessler, 1996). In addition, the temperature interval used by Rossi *et al.* (2014) for accumulating degree-days has been defined based on the results of Jailloux (1992), who observed production of perithecia at constant temperatures between 5 and 15°C, but not at 20 and 25°C. In the present work, the interval 9 to 25°C for accumulating degree-days was defined as the best interval among a series of different intervals (not shown), based on the goodness-of-fit and the AIC criterion (Burnham and Anderson, 2002). In the work of Jailloux (1992), an alternation of periods at 10 and 25°C resulted in the production of perithecia, and this

result indirectly validates the interval 9 to 25°C used in the present work. Similarly to ascospores, the cumulative conidia numbers in the runoff water from mummies did not fit well with the logistic equation of Rossi *et al.* (2014), based on DD base 10°C (not shown). The equation of Rossi *et al.* (2014) has been developed by using the data of Ferrin and Ramsdell (1978) and Hoffman *et al.* (2004), which were collected with different methods (in runoff water from mummies and by dipping mummies in water, respectively) and in different periods (from 23 April to 30 July, and from early-May to late-August, respectively). Therefore, the equations developed in the present work may be considered an improvement of the equations developed by Rossi *et al.* (2014). Further studies are needed to verify the accuracy of the new equations under different epidemiological conditions.

In the present work, *G. bidwellii* ascospores and conidia were both released during rain events, mainly in the water running off from berry mummies. Rain-related dispersal of *G. bidwellii* has been previously indicated for conidia (Ferrin and Ramsdell, 1978) but not for ascospores. The numbers of both spore types dispersed in the runoff water significantly increased as the amount of rain, its duration, and rain intensity increased. ROC and Bayesian analysis showed that the amount of rainfall was a good predictor of the dispersal of *G. bidwellii* spores in the runoff water from berry mummies. Specifically, using >1 and >3 mm rain as cut-off points for predicting the dispersal of conidia and ascospores, respectively, provided high posterior probability of predicting the dispersal when it actually occurred, and low probability of predict dispersal that actually did not occur. Consistently with this result, Ferrin and Ramsdell (1978) indicated that 1 mm rain was enough to induce conidial release. Maurin *et al.* (1991) indicated a threshold of ≥0.5 mm rain for spore dispersal (not specified whether it refers to ascospores or conidia, or both).

In addition to those dispersed in runoff water, *G. bidwellii* conidia were dispersed by splashing droplets, as demonstrated by: (i) the recovery of conidial clusters, approximately rounded in shape, in the microscope slides placed vertically in the proximity of the mummies; and (ii) the dispersal gradient of the black-rot lesions, which was typical of the splash-borne pathogens (Campbell and Madden, 1990; Fitt *et al.*, 1989).

No ascospores were found on the microscope slides. *G. bidwellii* ascospores have been considered to be air-borne, with ascospores being forcibly discharged into the air from perithecia as soon as mummies were wet by rain (Ferrin and Ramsdell, 1977; Reddick, 1911; Roussel and Bouard, 1971). In the first hour of rain, over 90% of ascospores were air-borne; in the following 4 to 5 h the captures decreased rapidly, and continued to be detected at insignificant levels as long as rain continued, and also up to 8 h after cessation of rain (Ferrin and Ramsdell, 1977; Jermini and Gessler, 1996). Ascospores were caught in the vineyard air through volumetric spore samplers (Ferrin

and Ramsdell, 1978; Hoffman *et al.*, 2004; Jermini and Gessler, 1996), but no clear information was reported on the numbers of the ascospores caught; only Ferrin and Ramsdell (1978) reported an ascospore peak of 80 ascospores per day. The latter information may indicate that low numbers of *G. bidwellii* ascospores were airborne in comparison to the numbers found in other perithecial producing fungi. For instance, Urbez-Torres (2011) found >1,000 ascospores of *Diplodia seriata* per day in vine grapes, and Pusey (1989) and Sutton (1981) caught >200 ascospores of *Botryosphaeria dothidea* per hour in peach and apple orchards, respectively. In *Guignardia citricarpa*, >1,500 ascospores m^{-3} air were caught in a week in citrus orchards (Reis *et al.*, 2006), and peaks of approximately 2,000 ascospores m^{-3} air were also found (Fourie *et al.*, 2013). Even though volumetric spore samplers are more efficient than microscope slides in trapping air-borne spores (Campbell and Madden, 1990; Dhingra and Sinclair, 1985), the lack of *G. bidwellii* ascospores on more than 1,500 microscope slides located in close proximity of the ascospores source may indicate that this dispersal mean was irrelevant in the conditions of the present work. To be noticed, spores of other fungi, including *Fusarium* spp. or *Alternaria* spp., were commonly found in the microscope slides of the present work.

The results from the present work provided new information on the effect of temperature and rainfall on the dispersal of both *G. bidwellii* ascospores and conidia from berry mummies overwintered in vineyards. This new knowledge can be easily incorporated into the model developed in Rossi *et al.* (2014), due to the mechanistic structure of this model. Specifically, modifications may include: (i) new equations for the effect of degree-days on the proportion of ascospores and conidia being dispersed in the runoff water during rain episodes; and (ii) new cut-off values of rain for conidial and ascospore dispersal. The new rain thresholds will probably reduce the number of dispersal events, and so the number of infection periods, predicted by the model in comparison to the current threshold of ≥0.5 mm (from Maurin *et al.*, 1991). A validation work will be necessary to verify whether these modifications will increase the model accuracy in predicting true infection periods and reducing unjustified alarms.

LITTERATURE CITED

Becker, C.M., Pearson, R., 1996. Black-rot lesions on overwintered canes of Euvitis supply conidia of *Guignardia bidwellii* for primary inoculum in spring. Plant Disease 80, 24–27.

Becker, C.M., Pearson, R.C., 1992. Patterns of spore release from black-rot (*Guignardia bidwelli*) infected grape mummies that overwintered on the ground or in the canopy. Phytopathology 82, 1084.

Bottura, M., 2011. Black-rot o marciume nero della vite. In: Manuale di viticoltura. Fondazione Edmund Mach, San Michele all'Adige (TN), pp. 43–45.

Burnham, K.P., Anderson, D., 2002. Model selection and multimodel interference. Springer, New York.

Campbell, C.L., Madden, L.V., 1990. Introduction to plant disease epidemiology. Wiley, New York, NY, USA.

Dhingra, O.D., Sinclair, J.B., 1985. Basic plant pathology methods. CRC Press, INC., Boca raton, Florida.

Ellis, M.A., Madden, L.V., Wilson, L.L., 1986. Electronic grape black-rot predictor for scheduling fungicides with curative activity. Plant Disease 70, 938–940.

Ferrin, D.M., Ramsdell, D.C., 1978. Influence of conidia dispersal and environment on infection of grape by *Guignardia bidwellii*. Phytopathology 68, 892-895. doi:10.1094/Phyto-68-892

Ferrin, D.M., Ramsdell, D.C., 1977. Ascospore dispersal and infection of grapes by *Guignardia bidwellii*, the causal agent of grape black-rot disease. Phytopathology 67, 1501–1505.

Fitt, B.D.L., McCartney, H.A., Walklate, P.J., 1989. The role of rain in dispersal of pathogen inoculum. . 27, 241–70. Annual Review of Phytopathology 27, 241–270.

Fourie, P., Schutte, T., Serfontein, S., Swart, F., 2013. Modeling the effect of temperature and wetness on *Guignardia* pseudothecium maturation and ascospore release in citrus orchards. Phytopathology 103, 281–92. doi:10.1094/PHYTO-07-11-0194

Funt, R., Ellis, M., Madden, L., 1990. Economic analysis of protectant and disease-forescast-based fungicide spray programs for control of apple scab and grape black-rot in Ohio. Plant Disease 74, 638–642.

Gadoury, D.M., 1995. Controlling fungal diseases of grapevine under organic management practices. Organic Grape and Wine Productioin Symposium, 35–44.

Gadoury, D.M., Pearson, R., Seem, R.C., Park, E., 1997. Integrating the control programs for fungal diseases of grapevine in the Northeastern United States. Viticulture Enology Science 52, 140–147.

Hanley, J.A., 2005. Receiver operating charatteristic (ROC) curves. In: Encyclopedia of biostatistics, Armitage, P., Colton, T. (Eds.). Jhon wiley and Sons, New York, NY, USA, p. 6100.

Harms, M., Holz, G., Hoffmann, C., Lipps, H., Silvanus, W., 2005. Occurrence of *Guignardia bidwellii*, the causal fungus of black-rot on grapevine, in the vine growing areas of Rhineland-Palatinate, Germany. BCPC Symposium 127–132.

Hoffman, L.E., Wilcox, W.F., Gadoury, D.M., Seem, R.C., 2002. Influence of grape berry age on susceptibility to *Guignardia bidwellii* and its incubation period length. Phytopathology 92, 1068–76. doi:10.1094/PHYTO.2002.92.10.1068

Hoffman, L.E., Wilcox, W.F., Gadoury, D.M., Seem, R.C., Riegel, D.G., 2004. Integrated control of grape black-rot: influence of host phenology, inoculum availability, sanitation, and spray timing. Phytopathology 94, 641–50. doi:10.1094/PHYTO.2004.94.6.641

Jailloux, F., 1992. In vitro production of the teleomorph of *Guignardia bidwellii*, causal agent of black-rot of grapevine. Canadian Journal of Botany 70, 254–257.

Jermini, M., Gessler, C., 1996. Epidemiology and control of grape black-rot in Southern Switzerland. Plant Disease 322–325.

Kong, G., 2012. Diagnostic Methods for black-rot of grapes - *Guignardia bidwellii*, PaDIL - Plant Biosecurity Toolbox.

Kummuang, N., Diehl, S., Smith, B., Graves, C., 1996. Muscadine grape berry rot diseases in Mississippi: disease epidemiology and crop reduction. Plant Disease 80, 244–247.

Lin, L., 1989. A concordance correlation coefficient to evaluate reproducibility. Biometrics 45, 255–268.

Lorenz, D.H., Eichhorn, K.W., Bleiholder, H., Klose, R., Meier, U., Weber, E., 1995. Phenological growth stages of the grapevine. *Vitis vinifera* L. ssp. vinifera. Codes and descriptions according to the extended BBCH scale. Australian Journal of Grape Wine Research 1, 100–103.

Madden, L.V, Hughes, G., van den Bosch, F., 2007. The study of plant disease epidemics. APS-Press, St. Paul, MN, USA.

Madden, L.V., 2006. Botanical epidemiology: some key advances and its continuing role in disease management. European Journal of Plant Pathology. 115, 3–23. doi:10.1007/s10658-005-1229-5

Maurin, G., Cartolaro, P., Clerjeau, M., Benac, G., 1991. Black-rot: vers une méthode de prévisions des risques. Phytoma - La Défence. des Végétaux. 433, 39–42.

Molitor, D., Berkelmann-Loehnertz, B., 2011. Simulating the susceptibility of clusters to grape black-rot infections depending on their phenological development. Crop Protection 30, 1649–1654. doi:10.1016/j.cropro.2011.07.020

Nash, J., Sutcliffe, J., 1970. River flow forecasting through conceptual models part I. J. Hidrol. 10, 282–290.

Pusey, P.L., 1989. Availability and dispersal of ascospores and conidia of *Botryosphaeria* in peach orchards. Plant Disease 79, 635–639.

Ramsdell, D.C., Milholland, R., 1988. Black-rot. In: Compendium of Grape Diseases. Pearson, R., Goheen, A. (Eds.), APS Press, St. Paul, pp. 15–17.

Reddick, D., 1911. The black-rot disease of grapes. Cornell University Agricultural Experiment Station Bulletin 293, 289-364.

Reis, R.F., Timmer, L.W., Goes, A. De, 2006. Effect of temperature, leaf wetness, and rainfall on the production of *Guignardia citricarpa* ascospores and on black spot severity on sweet orange. Fitopatologia Brasileira 31, 29–34.

Rinaldi, P.A., Mugnai, L., 2012. Marciume nero degli acini, potenziale pericolo in viticoltura. Informatore Agrario 15, 68–71.

Rossi, V., Onesti, G., Legler, S.E., 2014. Use of systems analysis to develop plant disease models based on literature data : grape black-rot as a case-study. European Journal of Plant Pathology 141, 427–444. doi:10.1007/s10658-014-0553-z

Roussel, C., Bouard, 1971. Maladies cryptomatiquae. In: Traite d'Ampelologie; Science e tecnologiques de la vigne. Dunod, Paris.

Scribner, F., 1886. Report on the fungus diseases of the grapevine. US Dep. Agric. Bot. Div. Sect. Plant Pathol. Bull. 2 GPO. Washington DC.

Sosnowosky, M., Kong, G., Wilcox, W., 2014. Diagnostic Protocol for *Guignardia bidwellii* (Black-rot on grapevine). Subcommittee on plant health diagnostic standards, National Diagnostic Protocol n°13, Australia.

Sutton, T.B., 1981. Production and dispersal of ascospores and conidia by *Physalospora obtusa* and *Botryosphaeria dothidea* in apple orchards. Phytopathology 71, 584–589.

Úrbez-Torres, J.R., 2011. The status of Botryosphaeriaceae species infecting grapevines. Phytopathologia Mediterranea. 50, 5–45. doi:10.14601/Phytopathol_Mediterr-9316

Zweig, M.H., Campbell, G., 1993. Receiver-operating characteristic (ROC) plots, a fundamental evaluation tool in clinical medicine. Clinical Chemisty 39, 561–577.

Chapter 5

Chapter 5

Temperature and humidity affect production of pycnidia and conidia by *Guignardia bidwellii*, the causal agent of grape black-rot.

ABSTRACT

Black-rot, caused *Guignardia bidwellii*, is a policyclic disease affecting grape leaves and berries through repeated primary and secondary infection cycles. Secondary infections are caused by the conidia produced by pycnidia on lesions. The effect of temperature and humidity on: (i) formation of *G. bidwellii* pycnidia and of cirri in grape leaf lesions; (ii) production and germination of conidia; and (iii) length of the latency period were studied under both environment-controlled conditions and in the vineyard for a 3-year period. Pycnidia were produced between 5 and 35°C, and at 90 to 100% relative humidity, but numbers of pycnidia were higher, and their production faster, between 20 and 30°C. More conidia were produced in the pycnidia developed at 15 and 20°C than at 25 to 35°C. First pycnidia were produced in approximately 2 days after lesion appearance at temperature ≥20°C, and in 8 days at 5°C; pycnidia continued to be produced on the same lesion for 5 to 16 days after lesion appearance, depending on temperature. The fact that pycnidia are produced for several days on a leaf lesion, and that time is temperature dependent, was also confirmed under field conditions with fluctuating temperatures. Extrusion of cirri only occurred between 15 and 35°C, mainly at 100% RH. However, no clear relationship was found between the production of pycnidia on leaf lesions in field and rainfall and humidity conditions between lesion appearance and pycnidial development. Overall, the findings from present work showed that high humidity is necessary for pycnidia to be produced (as demonstrated by no pycnidia produced at constant low humidities), but some hours at high humidity may be enough to provide sufficient moisture.

Key words: *Guignardia bidwellii*, leaf lesions, pycnidia, cirri, germination, latency, conidia.

INTRODUCTION

Black-rot of grape, caused by the ascomycete *Guignardia bidwellii* (Ellis) Viala and Ravaz (anamorph: *Phyllosticta ampelicida* (Englem.) van der Aa), is a serious disease causing yield losses up to 80% and lowering of wine quality, especially in grape-growing areas with cold and humid conditions in spring and early summer (Ellis *et al.*, 1986; Ferrin and Ramsdell, 1978, 1977; Funt *et al.*, 1990; Ramsdell and Milholland, 1988; Scribner, 1886; Magarey *et al.*, 1993).

Guignardia bidwellii overwinters in mummified berries on the soil surface and on vines, and in cane lesions as pycnidia (Ramsdell and Milholland, 1988). During the next grape-growing season, the fungus produces both ascospores and conidia on these inoculum sources (Hoffman *et al.*, 2004). Both spore types are repeatedly dispersed and cause primary infections to leaves and all the green tissues (Chapter 4; Ferrin and Ramsdell, 1977). After at least 12 to 14 days of incubation, typical black-rot lesions appear on leaves as circular, light brown necrosis, that later become bordered by a narrow band of dark brown tissue (Kuo and Hoch, 1996; Ramsdell and Milholland, 1988). After at least 3 to 5 additional days, pycnidia form on these lesions as small black protuberances (Ramsdell and Milholland, 1988; Spotts, 1980). On shoots, tendrils and petioles lesions are elongate, with pycnidia in the lesion center (Northover, 2008). In the presence of free water, mature pycnidia extrude conidia in a mucilaginous exudate, the cirrhus (Janex-Favre *et al.*, 1993). These conidia are dispersed by rain and cause secondary infections that contribute to the disease development during the grape-growing season (Chapter 4; Ferrin and Ramsdell, 1978). *G. bidwellii* also causes berry rot (Ramsdell and Milholland, 1988; Reddick, 1911). Rotted berries progressively turn in hard blue-black mummies at the end of the season (Bottura, 2011; Kong, 2012; Reddick, 1911; Rinaldi and Mugnai, 2012; Sosnowski *et al.*, 2012).

Although the importance of the secondary inoculum in the development of black-rot epidemics, there is few and fragmentary information on the effect of environmental conditions on the duration of the latency period (i.e., the time elapsed between lesion appearance and formation of pycnidia), on production dynamics of pycnidia and conidia, and on the formation of cirri (Rossi *et al.*, 2014).

In other pycnidial fungi, like *Didymella rabiei* (Jhorar *et al.*, 1998), *Phomopsis amygdali* (Lalancette *et al.*, 2003), and *Phomopsis viticola* (Anco *et al.*, 2013), the production of pycnidia and conidia is affected by temperature and humidity. In *Leptosphaeria maculans* (Vanniasingham and Gilligan, 1989) and *Septoria tritici* (Shaw, 1990; Shearer and Zadoks, 1972), the length of the latency period is also influenced by temperature and humidity conditions. Caltrider (1961) and Viala and Pacottet (1904) studied the production of *G. bidwellii* pycnidia at different temperatures on artificial media, but not on grape tissue; no observations were conducted in these studies on the

production and extrusion of the conidia. Northover (2008) studied the production of pycnidia on shoot lesions as affected by temperature and wetness duration at the time of infection, so this information did not refer to the different conditions during the latency and infectious period.

The objective of this paper was to study the effect of temperature and humidity on: (i) formation of *G. bidwellii* pycnidia and of cirri in grape leaf lesions; (ii) production and germination of conidia; and (iii) length of the latency period. Studies were conducted on leaves under both environment-controlled conditions and in the field for a 3-year period.

MATERIALS AND METHODS

In vitro experiments

Fungal material. The strain G1.16 of *G. bidwellii* was used, provided by Prof. L. Mungnai, Università degli Studi di Firenze (Italy), isolated from a severely affected vineyard of cv. Colorino located in Quarrata (Tuscany, Italy). The strain was maintained at 5°C in glass tubes (5 ml) containing water-agar (WA; 20 gL^{-1} HIMEDIA, Mumbai, India). For the production of conidia to be used for artificial inoculations, a small plug of the colonized water-agar was transferred from glass tubes to Petri plates containing malt extract agar (MEA; 50 gL^{-1} HIMEDIA, Mumbai, India), and plates were incubated for three weeks at 25°C, 12-h photoperiod. Conidial suspensions were obtained by flooding the plates with 10 ml of sterile distilled water and gently scrapping the agar surface with a sterile spatula. The resulting suspension was filtered through a double gauze layer and adjusted to 10^4conidia ml^{-1} with a haemocytometer.

Plant material and artificial inoculations. One year old *Vitis vinifera* plants cv. Barbera, which is susceptible to *G. bidwellii* (Coldiretti, 2013; Rubboli *et al.*, 2014), were grown in a greenhouse at the University campus of Piacenza (Italy). The plants were rooted in plastic pots (10 cm in diameter) containing a mixture of sand, peat moss and soil (20:50:30), and grown between 18 and 26°C, 12-h photoperiod of withe light (provided by Philips Master Tl-D 90 Deluxe 18 W/950 lamps) until they had shots with 4 to 6 unfolded leaves. Shoots were positioned vertically and the adaxial surface of the second, third and fourth unfolded leaves from the shoot apex were inoculated with 10 µL drops of the conidial suspension prepared as described before (3 to 5 drops per leaf). After inoculation, the plants were covered with transparent plastic bags to ensure a saturated atmosphere, and incubated at 25°C, 12-h photoperiod, to favour infection. Plastic bags were removed after 48 h and the plants were kept in the same temperature and photoperiod conditions as before, with 50 to 60% relative humidity (RH), until the onset

of the typical black-rot lesions. Lesions appeared after about 12 days and at that time they did not bear pycnidia yet.

Leaf pieces were cut from the leaves, one leaf piece incorporating a single lesion. Leaf pieces were disinfected with sodium hypochlorite (2%) for 2 minutes, rinsed with sterile water, and finally dried under a laminar flow cabinet. To keep the leaf tissue lying, a leaf disc was laid on a slip of sterile plastic net and then covered with another slip fixed to the previous one with sterile clips, the upper slip bearing a hole slightly larger than the disease lesion.

Effect of relative humidity and temperature. To study the effect of relative humidity and temperature on the development of pycnidia and on extrusion of cirri, leaf pieces prepared as described before were placed in Petri dishes (one leaf piece per Petri dish) containing potato dextrose agar (PDA; 39 gL^{-1}; HIMEDIA, Mumbai, India) amended with streptomycin sulfate (0.1 gL^{-1}; Sigma Aldrich, St Louis, USA), and kept in incubators at: (i) 25°C, 12-h photoperiod, with 65, 80, 90, 95 or 100% RH (experiment 1), or (ii) 5, 10, 15, 20, 25, 30, 35 or 40°C, 12-h photoperiod, with 100% RH (experiment 2). The different RH levels were obtained by adding different aliquots of glycerol to PDA (Dallyn and Fox, 1980) and the actual RH value was measured using an AquaLab LITE meter (version 1.3, Decagon Devices Inc., Pullman, WA). There were 5 dishes (replicates) per RH or temperature treatment. Every one or two days, the lesions were photographed with a digital camera until the 16th day after lesion appearance (DALA). Lesion size (in cm^2) was determined and total numbers of pycnidia and of pycnidia bearing cirri were counted by using Assess 2.0 (Image analysis software for plant diseases quantification, by Lanhdar Lamari, APS PRESS, Saint Paul, Minnesota), and expressed as numbers per cm^2 of lesion. The experiments were performed twice.

To determine the production of conidia at the different temperatures, three replicate groups of 50 cirri were randomly collected with a needle from 10 random lesions for each temperature regime at the end of experiment 2 (i.e., at 16 DALA). Cirri were placed in an Eppendorf tube with 0.5 mL of distilled sterile water and vortexed for one minute (2,400 rpm) to favor liberation of conidia. The number of conidia in the suspension was determined with a haemocytometer on three replicate drops, and expressed as the number of conidia per cirrhus. The experiment was performed twice.

To determine the effect of temperature at which conidia were produced on conidial germination, conidial suspensions obtained as previously described were adjusted to 5 x 10^4 conidia ml^{-1}. Ten drops (10 µL) of each conidial suspension were placed on plugs of WA (5 mm diameter) which have been placed on microscope slides (75 × 25 mm); there were three microscope slides, each of them with three agar plugs, per temperature treatment. Microscope slides were then incubated in darkness at 25°C and 100% RH. Germination was determined after 0, 3, 6, 12, 24 and 48 h of incubation by examining

100 conidia on each agar plug by using a microscope (×200 magnification), and expressed as percent of germinated conidia. The experiment was performed twice.

Data analysis

A preliminary analysis of variance showed no significant differences between repeated experiments; therefore, the data were pooled.

The numbers of pycnidia per cm^2 lesion found in experiments 1 and 2 were rescaled by dividing each value by the maximum observed in the experiment (i.e., under optimal conditions of temperature and RH, respectively). The rescaled values were used as response variables in different non-linear regression models. These models were compared based on the Akaike's Information Criterion (AIC) and the models providing the smallest AIC values were selected (Burnham and Anderson, 2002).

Effect of time after lesion appearance and relative humidity on production pycnidia (experiment 1) was best fitted by a modified Gompertz equation. In the general form of the Gompertz equation ($Y = \lambda \times \exp[-\alpha \times \exp(-\beta \times t)]$ (Madden *et al.*, 2007), the three equation parameters describe the response variable Y at any time t, with λ being an estimate of the asymptotic (maximal) value, α the weighted mean relative growth rate, and β the time at which maximum growth rate occurs (i.e., the point of inflection). In the modified equation (1), $\lambda = 1$ because data were rescaled to the maximal value, and α and β are linear functions of RH, as follows:

$$Y = \exp[(-a \times RH + b) \times \exp(-(c \times RH + d) \times DALA)] \quad (1)$$

where: Y is the rescaled number of pycnidia per cm^2 of lesion; DALA is the number of days after lesion appearance; *a*, *b*, *c* and *d* are the equation parameters; and RH is the relative humidity (in %).

The effect of time after lesion appearance and temperature on production of pycnidia (experiment 2) was best fitted by a Weibull equation (Duthie, 1997) in the following form:

$$Y = a \times (1 - \exp(-f(T) \times (DALA-c)^d)) \quad (2)$$

where: Y is the rescaled number of pycnidia per cm^2 of lesion; DALA is the number of days after lesion appearance; *a*, *c*, and *d* are the equation parameters; and f(T) is a function describing the effect of temperature as:

$$f(T)= e \times((h + 1)/h) \times h(1/h + 1)) \times (\exp((T-f) \times g/(h + 1))/(1 + \exp((T-f) \times g)))$$

where: T is temperature (°C); and *e*, *f*, *g*, and *h* are equation parameters.

Effect of each equation parameter on the shape of the response curve has been extensively explained by Duthie (1997). Briefly, *a* ($-\infty < a < +\infty$) represents the upper

limits of the response; c (c >0) represents the lag period before the response to wetness; *d* (*d* >0) is the fraction of the wetness period in which the response decelerates; *e* (*e* >0) represents the maximum response at the optimal temperature; *f* ($-\infty < f < +\infty$) locates the curve on the horizontal axis as a function of the optimal temperature; *g* (*g* >0) represents the intrinsic rate of increase in response to temperature; and *h* ($-\infty < h < +\infty$) characterizes the asymmetry of the curve with respect to the optimal temperature. Since the response variable was rescaled from 0 to 1, *a* and *e* were fixed to 1 (Duthie, 1997).

Goodness-of-fit of the equations was assessed by the adjusted R^2, the magnitude of the standard error of the parameter estimates, the root mean square error (RMSE), the coefficient of residual mass (CRM), the concordance correlation coefficient (CCC)(Lin, 1989; Nash and Sutcliffe, 1970). Briefly, RMSE represents the average distance of real data from the fitted line, and CRM is a measure of the tendency of the equation to overestimate or underestimate the observed values (a negative CRM indicates a tendency of the model toward overestimation) (Nash and Sutcliffe, 1970). CCC is the product of two terms: the Pearson correlation coefficient and the coefficient Cb, which is an indication of the difference between the best fitting line and the perfect agreement line (CCC = 1 means perfect agreement) (Madden *et al.*, 2007).

Field observations

A 3-year (2013 to 2015) long experiment was carried out in a vineyard of cv. Barbera at the University campus of Piacenza (Italy), in which no fungicide treatments were applied all season long. Details on the vineyard were indicated in Chapter 4. Briefly, plants were 7-year old in 2013 and were trained with a Guyot system.

At the end of February each year, metallic net boxes, each containing 20 g of grape berry mummies, were placed over the trellis of one vine row of 13 plants, 1.3 meter apart, to serve as primary inoculum source. Berry mummies were collected from grape bunches of 3 to 5 commercial vineyards in northern Italy, which have been severely affected by black-rot in the previous season. Rotted berries were detached from these bunches and included in a unique bulk sample, from which sub-samples of 20 g of random mummies were collected.

All the leaves of vines of the row with berry mummies were carefully observed every two or three days from bud break until berry ripening to detect: (i) the onset of black-rot lesions; and (ii) the time first pycnidia appeared on each lesion. Groups of lesions appearing in the same day were tagged with a permanent mark and considered as a coeval cohort of lesions (hereinafter simply named "cohort"). Only the 50 cohorts in which all the lesions produced pycnidia were considered in this work, which were the 5.5% of the total cohorts formed. There were 12 cohorts in 2013 (formed between May 20 and July 3) having a total of 178 black-rot lesions, 19 cohorts in 2014 (formed between May 14 and

July 16) and 2015 (formed between May 09 and June 3) having 194 and 274 lesions, respectively; 646 lesions were considered in aggregate.

A weather station (MeteoSense 2.0, Netsens s.r.l., Firenze, Italy) located into the vineyard provided hourly records of temperature, relative humidity, rainfall, and wetness duration.

Field data analysis. For each of the 646 lesions, the number of days elapsed between lesion appearance and the production of first pycnidia (DALA) was calculated, and used as proxy of the latency period (LP).

To study the relationships between weather conditions and length of latency under field conditions, the following variables were calculated between the day of appearance of a lesion cohort and the day when 50% of the lesions of the cohort have formed pycnidia (named LP50): average temperature, average RH, numbers of hours with RH >80% or >90%, numbers of wet hours, total rainfall, number of days with rain >0.2 mm. Both Pearson and Spearman correlation coefficients (r and ρ, respectively) were then calculated between pairs of observations of LP50 and the above weather variables. The Spearman rank correlation coefficient was calculated because it is less sensitive to strong outliers that are in the tails of both samples, because it limits the outlier to the value of its rank. For the variables showing significant correlation (e.g., average temperature), data were further analyzed by calculating averages and standard errors of LP50 for discrete intervals of the considered variable (e.g., 3°C intervals).

RESULTS

In vitro experiments

Effect of relative humidity on production of pycnidia and cirri. Pycnidia were produced between 90 and 100% RH, but not at 65 or 80% RH (Figure 1A). First pycnidia were produced at 2.0±0.3 and 5.6±0.6 DALA at 100 and 95% RH, respectively. At 90% RH, pycnidia were produced in only 21.4% of the lesions, and in low numbers (<10 pycnidia cm^{-2} lesion at 16 DALA). Approximately, 300 pycnidia cm^{-2} lesion were produced at 16 DALA at both 95 and 100% RH, but the production rate was faster at 100% RH than at 95% RH (Figure 1A).

At 100% RH, pycnidia started extruding cirri at 4.6±0.4 DALA, and 43.3 pycnidia cm^{-2} lesion (13.4% of the pycnidia) have extruded pycnidia at 16 DALA (Figure 1B). At 95% RH, extrusion of cirri started at 10.3±1.2 DALA in few lesions, and only 6.4 pycnidia cm^{-2} lesion (2.14% of the pycnidia) have extruded cirri at 16 DALA. No cirri were extruded between 90 and 65% RH (Figure 1B).

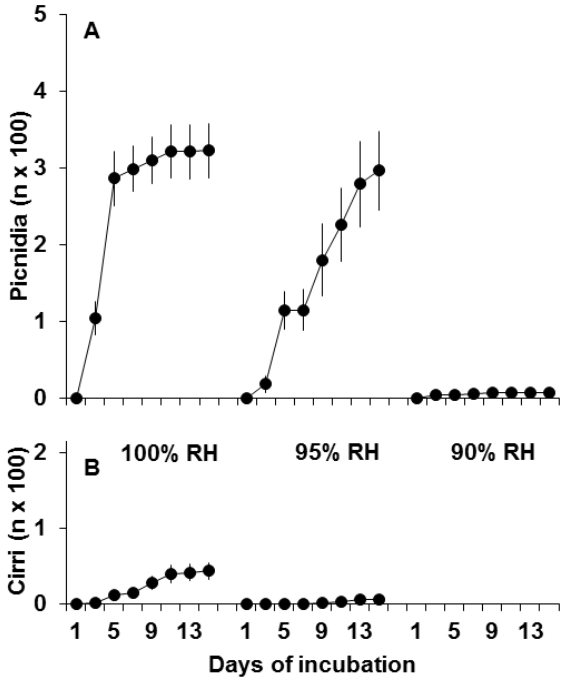

Figure 1. Effect of relative humidity (RH) on numbers of pycnidia (**A**) and of pycnidia with cirri (**B**) per cm^2 of black-rot lesion on grape leaves. No pycnidia were produced at 60% and 80% RH. Pycnidia were enumerated on lesions incubated at 25°C for 16 days. Each value represents the average of two repeated experiments, 5 lesions per experiment; whiskers represent the standard error.

Equation 1 provided a good fit of the rescaled production of pycnidia as a function of RH and time after lesion appearance. The equation parameters had low standard errors compared to the parameter estimates and the calculated indices indicate goodness-of-fit; negative CRM values indicated a slight overestimation (Table 1).

Effect of temperature on production of pycnidia and cirri. Production of pycnidia occurred between 5 and 35°C; no pycnidia were produced at 40°C within the 16 days of the experiment duration. Dynamic of pycnidium production and numbers of the pycnidia produced were both influenced by temperature (Figure 2A).

The time elapsed between the appearance of a black-rot lesion and the time when first pycnidia were observed on that lesion (the latency period) increased with temperature between 5 and 20°C, was almost similar between 20 and 30°C, and finally slightly increased at 35°C (Figure 3). For instance, approximately 13 days were necessary for the 90% of the total pycnidia to be produced at 5°C, 5 to 6 days were necessary at 20 to 30°C, and 7 days at 35°C (Figure 3). Between 5 and 15°C, production of new pycnidia continued for all the experiment duration (i.e., until 16 DALA), while at ≥20°C production of pycnidia reached a plateau after 5 to 7 DALA (Figure 2A). Total numbers of pycnidia increased as the temperature increased between 5 and 20°C, and then decreased at 30 and 35°C (Figure 2A).

Pycnidia did not extrude cirri at 5 and 10°C, and very few of them formed cirri at 15 and 35°C, precisely 1.1 and 5.5% of the pycnidia, respectively; 10.9, 23.5, and 20.9% of the pycnidia extruded cirri at 20, 25, and 30°C, respectively (Figure 2B). At 25°C, first cirri were extruded at 3 DALA and their number progressively increased until 16 DALA (Figure 2B).

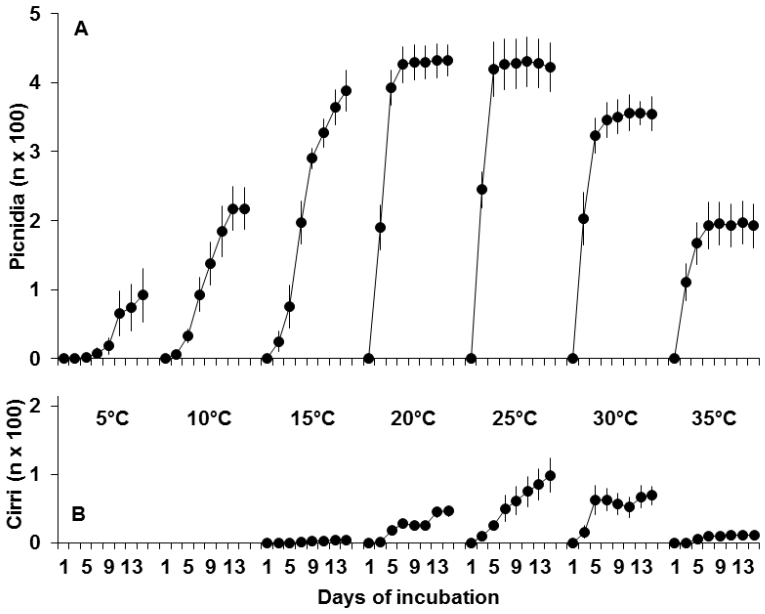

Figure 2. Effects of temperature on numbers of pycnidia (**A**) and of pycnidia with cirri (**B**) per cm^2 of black-rot lesion on grape leaves. No pycnidia were produced at 40°C. Pycnidia were enumerated on lesions incubated at 100% relative humidity for 16 days. Each value represents the average of two repeated experiments, 5 lesions per experiment; whiskers represent the standard error.

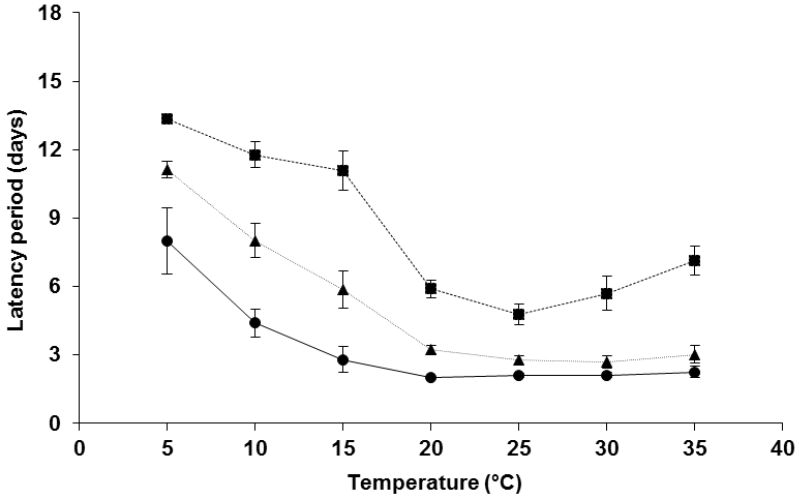

Figure 3. Effect of temperature on the length of latency period (LP), as numbers of days elapsed between appearance of a black-rot lesion on grape leaves and production of pycnidia on that lesion. Dots (solid line), triangles (dotted line), and squares (dashed line) represent the LP for first pycinida, 50% and 90% of the total pycnidia to be produced, respectively. Each value represents the average of two repeated experiments, 5 lesions per experiment; whiskers represent the standard error. No pycnidia were produced at 40°C.

Equation 2 provided a good fit of the rescaled numbers of the total pycnidia at different temperatures and times after lesion appearance (Table 1). The equation parameters had low standard errors compared to the parameter estimates, RMSE were low, R^2 and CCC were >0.94; CRM value was negative but very low (Table 1) indicating substantial no overestimation (Figure 4).

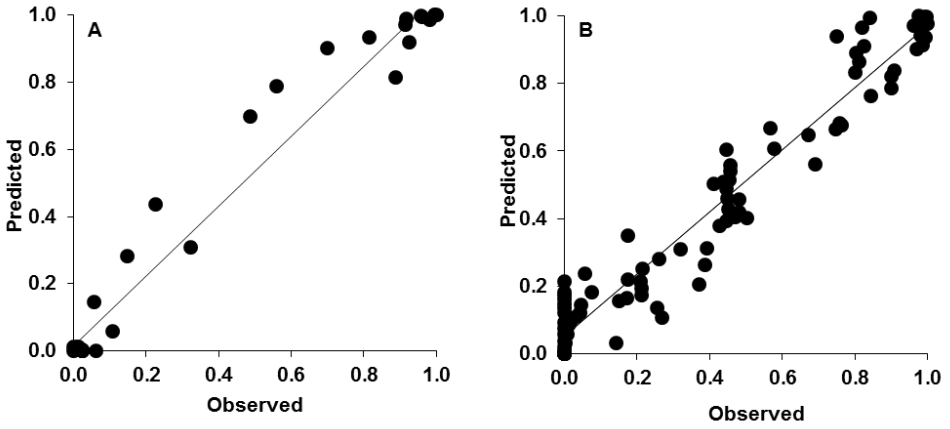

Figure 4. Comparison between observed and predicted production of pycnidia on black-rot lesions in grape leaves at different times and either relative humidities (**A**) or temperatures (**B**). Numbers of pycnidia are shown in Figure 1 and 2, respectively, and were rescaled by dividing each value by the maximum found at optimal relative humidity or temperature, respectively; predictions were generated by equations 1 and 2, respectively (see Table 1).

The estimates for parameter *c* of the Weibull equation was 1.85±0.06 for pycnidium production indicating there was a delay between lesion appearance and formation of pycnidia. Estimated optimal temperature (parameter *f)* was 25.0±0.2°C and parameter *h* was >1, indicating a degree of asymmetry (i.e., the intrinsic rate of acceleration in the response until optimal temperature is higher than those of decline after this temperature) (Table 1; Figure 5).

Table 1. Parameters, statistics and goodness-of-fit indexes of the equations used to describe the effect of time and relative humidity (equation 1) or temperature (equation 2) on the production of *Guignardia bidwellii* pycnidia on black rot lesions in grape leaves.

Equation[a]	Estimated parameters					R^2	RMSE	CRM	CCC
	a	***b***	***c***	***d***					
1	1.25 (0.26)[b]	-109.4 (24.2)	0.12 (0.01)	-11.0 (0.63)		0.97[c]	0.086	-0.082	0.98
	c	***d***	***f***	***g***	***h***				
2	1.85 (0.06)	0.74 (0.05)	24.98 (0.19)	0.48 (0.02)	1.30 (0.05)	0.95	0.087	-0.049	0.97

[a] Equation 1 has the following formula Y = exp[(-*a* × RH + *b*) × exp(-(*c* × RH + *d*) × DALA)], where: Y is the rescaled number of pycnidia per cm^2 of lesion; DALA is the number of days after lesion appearance; *a*, *b*, *c* and *d* are the equation parameters; and RH is the relative humidity (in %); equation 2 has the following formula: $Y = a \times (1-\exp(-f(T) \times (DALA-c)^d))$; where: Y is the rescaled number of pycnidia per cm^2 of lesion; DALA is the number of days after lesion appearance; *a*, *c*, and *d* are the equation parameters (with *a*=1); and f(T) is a function describing the effect of temperature as: $f(T) = e \times ((h+1)/h) \times h(1/h+1)) \times (\exp((T-f) \times g/(h+1))/(1+\exp((T-f) \times g)))$, where: T is temperature (°C); and *e*, *f*, *g*, and *h* are equation parameters (with *e*=1).

[b] In brackets, the standard errors of the estimated parameters.

[c] R^2, coefficient of determination; RMSE, root mean square error; CRM, coefficient of residual mass; CCC, concordance correlation coefficient.

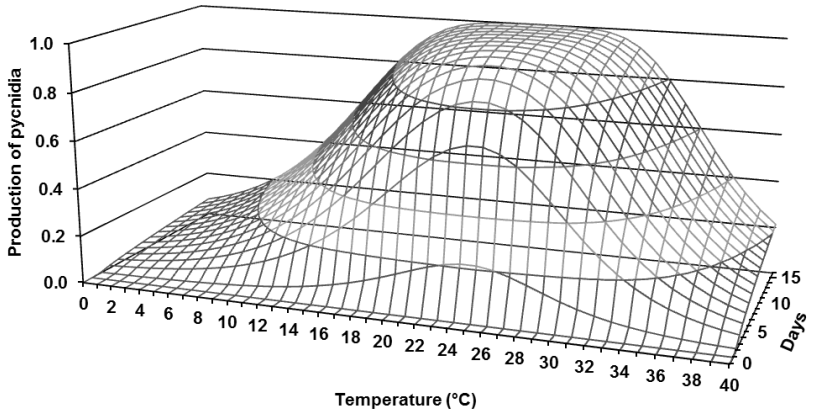

Figure 5. Relationship between temperature, incubation time (in days) and rescaled production of *Guignardia bidwellii* pycnidia in grape leaf lesion as predicted by equation 2 (see Table 1). Rescaled values were obtained by dividing each value of Figure 2 by the maximum found at optimal temperature.

Field observations

Effect of temperature on production and germination of conidia. Numbers of conidia present in the cirri formed at the different temperatures were higher at 15 and 20°C, and progressively lower at 25 to 35°C. Very few conidia were found in the cirri extruded at 35°C (Figure 6). No cirri were extruded at 5 and 10°C (Figure 2). Germination of the conidia produced at 20 to 30°C showed similar patterns, while conidia produced at 15°C showed lower germination rate (Figure 7).

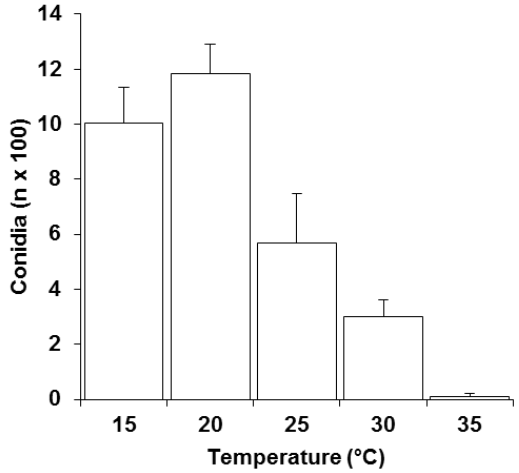

Figure 6. Effect of temperature on numbers of *Guignardia bidwellii* conidia extruded in cirri by the pycnidia produced on grape leaf lesions, after 16 days at 100% relative humidity. No cirri were extruded at 5, 10 and 40°C. Bars represent the average of 3 experiments, 50 cirri per experiment; whiskers represent the standard error.

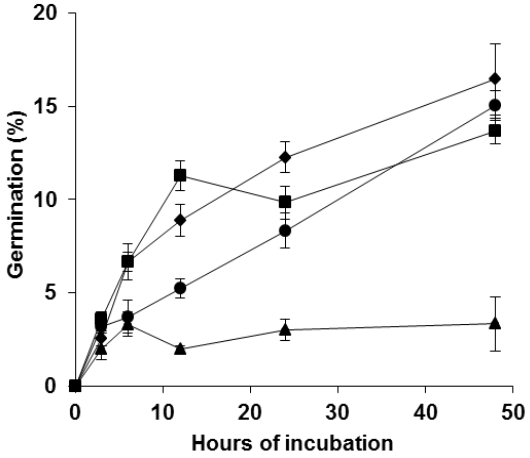

Figure 7. Effect of temperature at which *Guignardia bidwellii* pycnidia have been produced in grape leaf lesions on the germination of conidia. Conidia were collected from cirri extruded from the lesions incubated for 16 days at 100% relative humidity and 15 (▲), 20 (♦), 25 (●) and 30°C (■). No cirri were extruded at 5, 10, and 40°C. Dots represent the average of 2 experiments, 100 conidia assessed per experiment; whiskers represent the standard error.

Length of latency period in the field. The latency period for first pycnidia to be produced on lesions is shown in Figure 8, for the 50 cohorts considered in 2013, 2014 and 2015. Figure 9 shows the frequency distribution of the latency period for the 646 lesions forming these 50 cohorts.

The latency period was highly variable. About 22% of the lesions started producing pycnidia within 2 days after the lesion appearance (DALA) (Figure 9); in additional two days, 56% of lesions have started producing pycnidia. At 12 and 24 DALA, 87% and 91% of lesions have produced pycnidia. Few lesions (6% of total) started producing pycnidia between 19 and 24 DALA, and another few (<5% of total lesions) between 35 and 40 days after lesion appearance (Figure 9).

Long latency was observed for the cohorts formed in the last decade of May 2013 (Figure 8B). Some lesions of these cohorts started producing pycnidia in few days, during a rainy and humid period in the last days of May (Figure 8A). The number of lesions forming new pycnidia diminished in the first decade of June (which was dry), and increased again with the rainfall on May 9 and the correspondent wet period. Some lesions of one of these cohorts started producing pycnidia later on, with the rain fell at the end of June. Other lesions with long latency were observed for a cohort formed on June 11, 2014 (Figure 8D). In this cohort, first lesions started producing pycnidia on June 16, after 3 days of rain (Figure 8C). In the following dry period only few lesions produced pycnidia, but most of them did produce at the end of June, after a rainy period.

The relationship between rain and formation of pycnidia was confirmed for other lesion cohorts, like those formed in early June 2014 (Figure 8A and B), between late June and the first decade of July 2014 (Figure 8C and D), and in May 2015 (Figure 8E and F), but not for all the cohorts. For instance, lesions of the cohorts formed at the end of May 2015 produced pycnidia in 7 to 8 DALA (Figure 8F) even though the weather was hot, with no rain and few hours of wetness (Figure 8E). The same occurred for the cohorts formed at the end of June, same year (Figure 8E and F).

As a consequence, no significant correlation was found between the time 50% of lesion of a cohort formed pycnidia (LP50) and any of the weather variables related to rain, relative humidity or leaf wetness in that a period. A significant, negative correlation was found between LP50 and average temperature ($r = -0.31$, $P = 0.03$; $\rho = -0.45$, $P = 0.001$; $n = 50$), so that the length of LP50 diminished as average temperature increased (Figure 10).

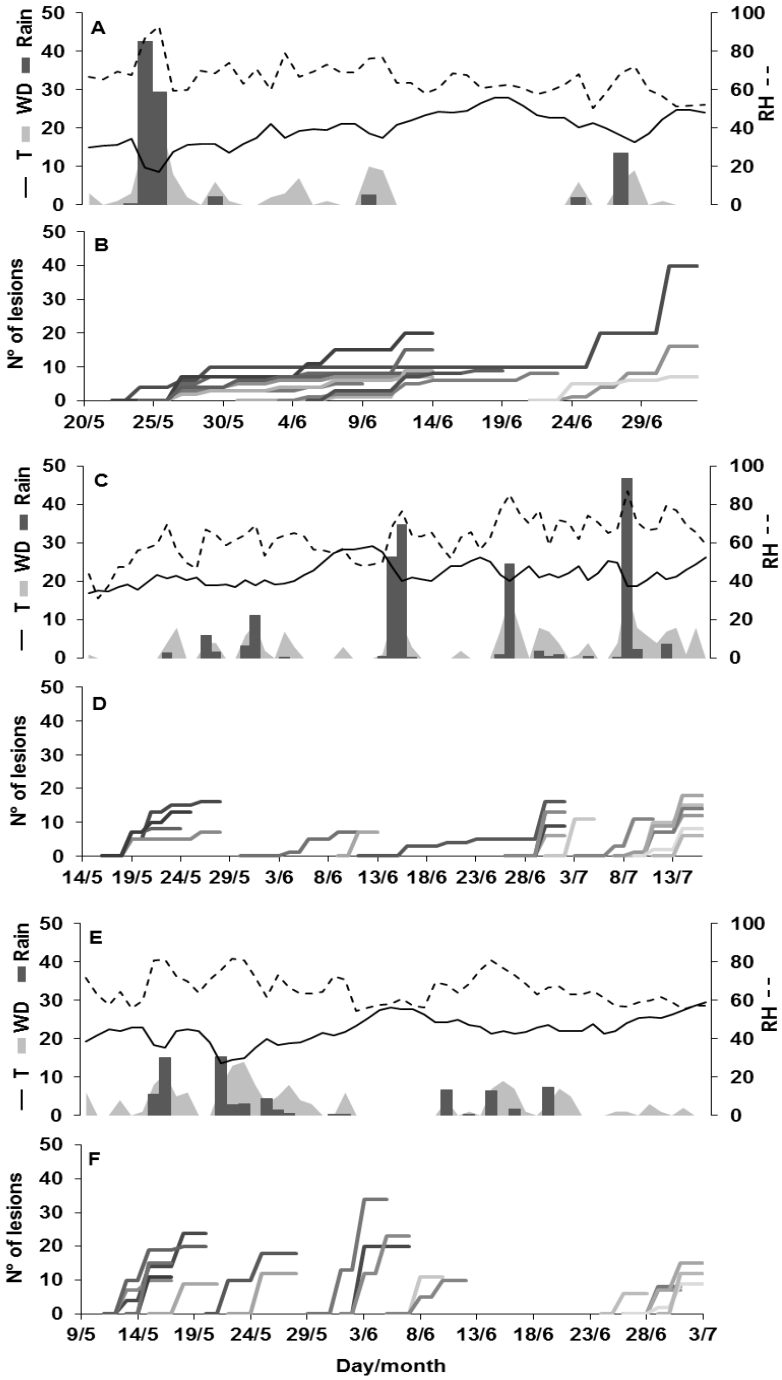
A
B
C
D
E
F
— T WD Rain
RH --
N° of lesions
20/5 25/5 30/5 4/6 9/6 14/6 19/6 24/6 29/6
14/5 19/5 24/5 29/5 3/6 8/6 13/6 18/6 23/6 28/6 3/7 8/7 13/7
9/5 14/5 19/5 24/5 29/5 3/6 8/6 13/6 18/6 23/6 28/6 3/7
Day/month

◄**Figure 8.** Data of temperature (in °C; solid line), relative humidity (in %; dashed line), rainfall (in mm; dark grey bars), and wetness duration (in hours; light grey area) measured in the experimental vineyard in 2013 (**A**), 2014 (**C**), and 2015 (**E**), during the period when different coeval cohorts of black-rot lesions (lines in **B**, **D**, and **F**) were observed every 2 to 3 days to determine the time when single lesions of each cohort started producing *Guignardia bidwellii* pycnidia. Each line refers to a cohort, from the time of lesion appearance until when all the lesions of the cohort have produced pycnidia.

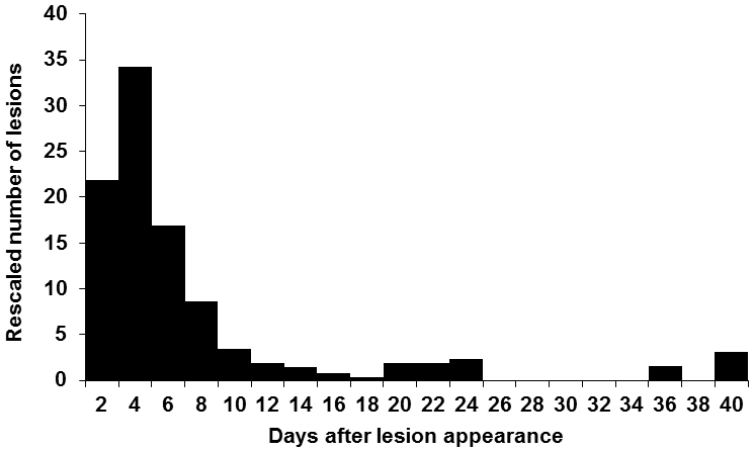

Figure 9. Frequency distribution of numbers of days elapsed between black-rot lesion appearance in grape leaves and the formation of first pycnidia (latency period), for the 646 lesions observed in the vineyard in 2013 to 2015. Lesions are those shown in Figure 8.

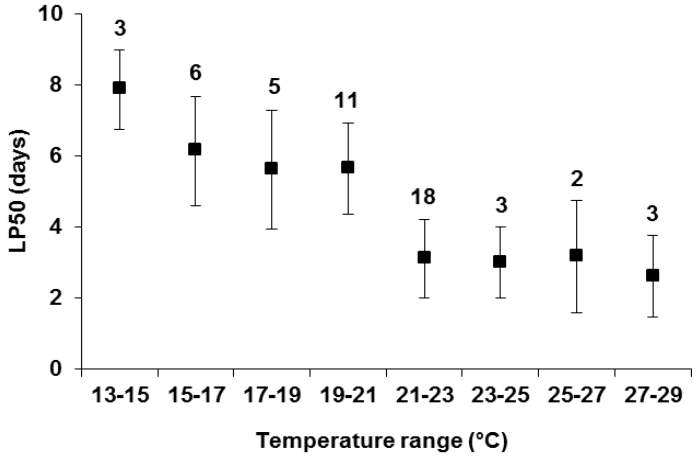

Figure 10. Numbers of days elapsed between the appearance of a black-rot lesion cohort in grape leaves and the time when 50% of the cohort lesions have formed pycnidia (latency period, LP50) at different temperature ranges. Cohorts are those shown in Figure 8. Dots represent the average LP50, whiskers the standard error, and the number is the number of cohorts for each temperature range.

DISCUSSION

To our knowledge, this is the first published study regarding the effect of time, temperature and relative humidity on production of pycnidia and extrusion of cirri in *Guignardia bidwellii* lesions on grape leaves.

Pycnidia of *G. bidwellii* were produced in a wide range of temperatures (5 to 35°C) and at 90 to 100% RH, but numbers of pycnidia were higher, and their production faster, between 20 and 30°C. Consistently with these results, Caltrider (1961) and Spotts (1977) found optimal temperature for production of *G. bidwellii* pycnidia at 25°C. Spotts (1977) found pycnidia in grape leaf lesions at all the temperatures tested (15, 21 and 26.5°C), but Caltrider (1961) did not observe pycnidia at 10, 15 and 35°C. These inconsistencies between results of the present study and Caltrider (1961) observations may be caused by different experimental conditions: Caltrider (1961) observed production of pycnidia in fungal colonies growing for 15 days in a glucose-yeast-extract agar. It may be postulated that 15-day old colonies did not have time enough for producing pycnidia at sub-optimal temperatures, as demonstrated by the fact that production rate of pycnidia in grape leaf lesions at these temperatures is slower than at optimal temperature (Figure 2). This is also the case of other pycnidial fungi. In *Stagonospora meliloti* fungal colonies grown on an artificial medium for 15 days produced pycnidia in a narrow temperature range, i.e., 15 to

30°C (Erwin *et al.*, 1987). However, in *Phomopsis viticola* (Anco *et al.*, 2013) infecting grapes, *Phomopsis amygdaly* (Lalancette *et al.*, 2003) infecting peaches, and *Diaporthe citri* (Mondal *et al.*, 2007) infecting citrus, production of pycnidia on host tissues occurred in a wide temperature interval (1-5°C to 35-38°C).

The latency period for the appearance of pycnidia on leaf lesions was also influenced by temperature, first pycnidia being produced in approximately 2 days after lesion appearance at temperature ≥20°C, and in 8 days at 5°C. This result is in full agreement with that of Spotts (1980) at 15 to 26.5°C, but it enlarges the range of the temperatures investigated. Pycnidia continued to be produced on the same lesion for 5 to 16 days after lesion appearance, depending on temperature (Figure 2). The fact that pycnidia are produced for several days on a leaf lesion, and that time is temperature dependent, was also confirmed under field conditions with fluctuating temperatures. In our knowledge, there is no previous published information on the effect of temperature on length of latency period in *G. bidwelii*. In *Septoria tritici*, the latent period for production of pycnidia in wheat leaf lesions shortened as temperature increased from 5 to 20°C (Shaw, 1990; Shearer and Zadoks, 1972); in a field experiment, the latent period shortened by 3 days when the temperature increased from 10 to 16°C (Shaw, 1990). In *S. tritici*, spaced appearance of pycnidia in lesions has been interpreted as an important epidemiological parameter, making an epidemic resulting from a single infection event into an apparently continuous epidemic (Royle *et al.*, 1986; Shaw, 1990). Based on our results, the same may be for *G. bidwellii*.

Temperature at which pycnidia were produced influenced the numbers of conidia yielded by individual pycnidia as well as conidial germination. More conidia were produced in the pycnidia developed at 15 and 20°C than at 25 to 35°C. Considering that optimal temperature for pycnidial production was between 20 and 25°C, the highest production of inoculum (as combination of number of pycnidia per lesion and number of conidia per pycnidium) occurred at 20°C. In other pycnidial fungi, such as *Phomopsis amygdaly* (Lalancette *et al.*, 2003) and *Phomopsis viticola* (Anco *et al.*, 2013), favorable temperatures for production of conidia were similar to that of *G. bidwelii*, being 17 and 21°C, respectively.

In this work, the germination rate of conidia was lower than that found by (Caltrider, 1961), but similar to the germination rate we repeatedly found for conidia extruded by pycnidia developed under field conditions (data not shown).

Concerning relative humidity, no pycnidia were produced on grape leaf lesions when RH was constantly kept at ≤80%. High relative humidity is also requested for other pycnidial fungi; minimum RH for pycnidia production was 86% for *Didymella rabiei* affecting chickpea (Navas-Cortes *et al.*, 1998), 74% for *Diaporthe citri* affecting citrus (Mondal *et al.*, 2007), and 90% for *Septoria nodorum* affecting wheat (Shearer and Zadoks, 1972). Spotts (1980) observed no differences in the time when pycnidial

production started in grape plants bearing leaf lesions of black-rot incubated in growth chambers kept at 90, 70 or 50% RH. No information was provided by Spotts (1980) on how RH was maintained in the growth chambers and the extent of the daily fluctuations in RH, except for saying that there was ±10% RH at any RH level. It may be supposed that in the growth chambers the RH during the period between lesion appearance and first pycnidium formed (which was approximately 4 days) reached a suitable RH level for a number of hours sufficient for starting producing pycnidia; based on results of this work, this level should be >80% RH. This hypothesis is supported by the works of Navas-Cortés *et al.* (1998) and Shearer and Zadoks (1972) on *Didymella rabiei* and *Septoria nodorum*, respectively. In *D. rabiei*, there was no pycnidial production at RH <87%; when incubated at alternate weekly intervals of 100 and 34% RH, production of pycnidia was similar to that found under continuous moist conditions. In *S. nodorum*, no pycnidia were produced at RH <90%; however, production of pycnidia under alternate 12-h periods at 80% and 100% RH or under continuous 100% RH was the same.

In the present work, no clear relationship was found between the production of pycnidia on leaf lesions in field and rainfall and humidity conditions between lesion appearance and pycnidial development. Overall, the findings from present work showed that high humidity is necessary for pycnidia to be produced (as demonstrated by no pycnidia produced at constant low humidities), but some hours at high humidity may be enough to provide sufficient moisture.

Extrusion of cirri only occurred between 15 and 35°C (being the optimal at 25°C), mainly at 100% RH; however, only a few of the pycnidia produced did extrude cirri. The fact that pycnidia need water for extrusion of cirri is well known; Janex-Favre *et al.* (1993) observed that mature pycnidia formed cirri some minutes after the deposit of a film of water. The discrepancy between the number of pycnidia produced and those able to extrude the cirrhus can be explained based on the pycnidial ontogeny.

Pycnidial formation in *G. bidwellii* goes through different developmental stages, which include the formation of a primordial within a stroma and the development of a fertile centre from which originate a conidiogenous layer covering the pycnidial cavity; the formation of the pycnidial neck can occur either before or after the development of the fertile centre. The formation of conidia and of the ostiole in the pycnidial neck occurs thereafter (Janex-Favre *et al.*, 1993). Therefore, pycnidia are visible before they mature the conidia and, consequently, are able to extrude them in the presence of water.

In a recent analysis of the existent literature, Rossi *et al.* (2014) identified the dynamic of pycnidial production on black-rot leaf lesions as one of the main gaps in the disease knowledge. In the absence of this information, the authors used the results from previous works on both *G. bidwellii* and on other pycnidial fungi to develop a model of the life cycle. The results obtained in the present work can be then incorporated in that model; the mechanistic approach used to develop the model makes this incorporation

easy (De Wolf and Isard, 2007; Rossi *et al.*, 2010). In detail, the non-linear equations developed to describe the production patterns of pycnidia as affected by time, relative humidity (with a modified Gompertz equation) and temperature (with a Weibull equation) could be used to estimate the inoculum potential for secondary infections. Both equations have parameters with relevant biological meaning (Duthie, 1997; Madden *et al.*, 2007), and have been previously used for other plant pathogens (Anco *et al.*, 2013; Arauz *et al.*, 2010; González-Domínguez *et al.*, 2013).

LITTERATURE CITED

Anco, D.J., Madden, L. V, Ellis, M.A., 2013. Effects of temperature and wetness duration on the sporulation rate of *Phomopsis viticola* on infected grape canes. Plant Disease 97, 579–589.

Arauz, L.F., Neufeld, K.N., Lloyd, a L., Ojiambo, P.S., 2010. Quantitative models for germination and infection of *Pseudoperonospora cubensis* in response to temperature and duration of leaf wetness. Phytopathology 100, 959–67. doi:10.1094/PHYTO-100-9-0959

Bottura, M., 2011. Black-rot o marciume nero della vite. In: Manuale Di Viticoltura. Fondazione Edmund Mach, San Michele all'Adige (TN), pp. 43–45.

Burnham, K.P., Anderson, D., 2002. Model selection and multimodel interference. Springer, New York.

Caltrider, P., 1961. Growth and sporulation of *Guignardia bidwellii*. Phytopathology 51, 860–863.

Coldiretti, 2013. Attenzione al black-rot della vite: le abbondanti precipitazioni favoriscono il "marciume nero". News Coldiretti (http://www.asti.coldiretti.it/tenzione-al-black-rot-della-vite.aspx?KeyPub=27004215%7C27015561&Cod_Oggetto=52440666&subskintype=Detail).

Dallyn, H., Fox, A., 1980. Spoilage of material of reduced water activity by xerophilic fungi. In: Society of Applied Bacteriology, Technical Series. Gould, J.E.L. and Corry, G.H. (Eds.), pp. 129–139.

De Wolf, E.D., Isard, S.A., 2007. Disease cycle approach to plant disease prediction. Annual Review of Phytopathology 45, 203–220. doi:10.1146/annurev.phyto.44.070505.143329

Duthie, J.A., 1997. Models of the response of foliar parasites to the combined effects of temperature and duration of wetness. Phytopathology 87, 1088–1095. doi:10.1094/PHYTO.1997.87.11.1088

Ellis, M.A., Madden, L. V, Wilson, L.L., 1986. Electronic grape black-rot predictor for scheduling fungicides with curative activity. Plant Disease 70, 938–940.

Erwin, D., Khan, R., Ribeiro, O., Lehman, W., 1987. Growth, sporulation, and pathogenicity of *Stagonospora meliloti* and selection for resistance to crown rot and leaf spot in alfalfa. Plant Disease 71, 181–185.

Ferrin, D.M., Ramsdell, D.C., 1978. Influence of conidia dispersal and environment on infection of grape by *Guignardia bidwellii*. Phytopathology 68, 892. doi:10.1094/Phyto-68-892

Ferrin, D.M., Ramsdell, D.C., 1977. Ascospore dispersal and infection of grapes by *Guignardia bidwellii*, the causal agent of grape black-rot disease. Phytopathology 67, 1501–1505.

Funt, R., Ellis, M., Madden, L., 1990. Economic analysis of protectant and disease-forescast-based fungicide spray programs for control of apple scab and grape black-rot in Ohio. Plant Disease 74, 638-642.

González-Domínguez, E., Rossi, V., Armengol, J., García-Jiménez, J., 2013. Effect of environmental factors on mycelial growth and conidial germination of of *Fusicladium eriobotryae*, and the infection of loquat leaves. Plant Disease 97, 1331–1338.

Hoffman, L.E., Wilcox, W.F., Gadoury, D.M., Seem, R.C., Riegel, D.G., 2004. Integrated control of grape black-rot: influence of host phenology, inoculum availability, sanitation, and spray timing. Phytopathology 94, 641–50. doi:10.1094/PHYTO.2004.94.6.641

Janex-Favre, M.C., Parguey-Leduc, A., Jailloux, F., 1993. The ontogeny of pycnidia of *Guignardia bidwellii* in culture. Mycological Researh 97, 1333–1339.

Jhorar, O.P., Butler, D.R., Mathauda, S.S., 1998. Effects of leaf wetness duration, relative humidity, light and dark on infection and sporulation by *Didymella rabiei*. Plant Pathology. 47, 586-594.

Kong, G., 2012. Diagnostic methods for black-rot of grapes - *Guignardia bidwellii*, PaDIL - Plant Biosecurity Toolbox. http://www.padil.gov.au/pbt.

Kuo, K., Hoch, H.C., 1996. The parasitic relationship between *Phyllosticta ampelicida* and *Vitis vinifera*. Mycologia 88, 626-634.

Lalancette, N., Foster, K. a, Robison, D.M., 2003. Quantitative models for describing temperature and moisture effects on sporulation of *Phomopsis amygdali* on peach. Phytopathology 93, 1165–72. doi:10.1094/PHYTO.2003.93.9.1165

Lin, L., 1989. A concordance correlation coefficient to evaluate reproducibility. Biometrics 45, 255–268.

Madden, L. V, Hughes, G., van den Bosch, F., 2007. The study of plant disease epidemics. APS-Press, St. Paul, MN, USA.

Magarey, R.D., Coffey, B.E., Emmett, R.W., 1993. Anthracnose of grapevines, a review. Plant Protection Quarterly 8, 106–110.

Mondal, S.N., Vicent, A., Reis, R.F., Timmer, L.W., 2007. Saprophytic colonization of citrus twigs by *Diaporthe citri* and factors affecting pycnidial production and conidial survival. Plant Disease 91, 387–392.

Nash, J., Sutcliffe, J., 1970. River flow forecasting through conceptual models part I. Journal of Hidrology 10, 282–290.

Navas-Cortes, J.A., Trapero-Casas, A., Jimenez-Diaz, R., 1998. Influence of relative humidity and temperature on development of *Didymella rabiei* on chickpea debris. Plant Pathology 47, 57–66. doi:10.1046/j.1365-3059.1998.00208.x

Northover, P., 2008. Factors influencing the infection of cultivated grape (*Vitis* spp. section Euvitis) shoot tissue by *Guignardia bidwellii* (Ellis) Viala and Ravaz. The Pennsylvania State University.

Ramsdell, D.C., Milholland, R., 1988. Black-rot. In: Compendium of Grape Diseases. Pearson, R., Goheen, A. (Eds.), APS Press, St. Paul, pp. 15–17.

Reddick, D., 1911. The black-rot disease of grapes. Cornell University Agricultural Experiment Station Bulletin 293, 289-364.

Rinaldi, P.A., Mugnai, L., 2012. Marciume nero degli acini, potenziale pericolo in viticoltura. Informatore Agrario 15, 68–71.

Rossi, V., Giosuè, S., Caffi, T., 2010. Modelling plant diseases for decision making in crop protection. In: Precision Crop Protection - the Challenge and Use of Heterogeneity. Oerke, E.-C., Gerhards, R., Menz, G., Sikora, R.A. (Eds.), Springer Netherlands, Dordrecht, pp. 241–258. doi:10.1007/978-90-481-9277-9

Rossi, V., Onesti, G., Legler, S.E., Caffi T., 2014. Use of systems analysis to develop plant disease models based on literature data: grape black-rot as a case-study. European Journal of Plant Pathology 141, 427–444. doi:10.1007/s10658-014-0553-z

Royle D.J., Shaw M.W. Cook R.J., 1986. Patterns of development of *Septoria nodorum* and in some winter wheat crops in Western Europe, 1981–1983. Plant Pathology 35, 466–476

Rubboli, V., Ortugno, C., Coatti, C., Gualco, A., 2014. Dynali, nuovo fungicida a base di cyflufenamid e difenoconazolo per la protezione della vite da oidio e black-rot. Giornate Fitopatologiche 2, 289–298.

Scribner, F., 1886. Report on the fungus diseases of the grapevine. US Dep. Agric. Bot. Div. Sect. Plant Pathol. Bull. 2 GPO. Washington DC.

Shaw, M., 1990. Effects of temperature, leaf wetness and cultivar on the latent period of Mycosphaerella graminicola on winter wheat. Plant Pathology 39, 255–268.

Shearer, B., Zadoks, J., 1972. The latent period of *Septoria nodorum* in wheat I. The effect of temperature and moisture treatments under controlled conditions. European Journal of Plant Pathology 78, 231–241.

Sosnowski, M.R., Emmett, R.W., Wilcox, W.F., Wicks, T.J., 2012. Eradication of black-rot (*Guignardia bidwellii*) from grapevines by drastic pruning. Plant Pathology 61, 1093–1102. doi:10.1111/j.1365-3059.2012.02595.x

Spotts, R.A., 1980. Infection of grape by *Guignardia bidwellii*-factors affecting lesion development, conidial dispersal, and conidial populations on leaves. Phytopathology 70, 252–255.

Spotts, R.A., 1977. Effect of leaf wetness duration and temperature on the infectivity of *Guignardia bidwellii* on grape leaves. Phytopathology 77, 1378. doi:10.1094/Phyto-67-1378

Vanniasingham, V., Gilligan, C., 1989. Effects of host, pathogen and environmental factors on latent period and production of pycnidia of *Leptosphaeria maculans* on oil-seed rape leaves in controlled environments. Mycological Research. 93, 167–174.

Viala, P., Pacottet, P., 1904. Recherches sue les maldies de la vigne: “Black-rot II, Sur le développment du Black-rot”, réceptivité des fruits, influence de la temperature, de l’humidité et des milieux toxique. Paris: Bordeaux de la “Revue de viticulture.”

Chapter 6

Chapter 6

Production of *Guignardia bidwellii* conidia on grape leaf lesions is influenced by repeated washing events and by alternation of dry and wet periods

ABSTRACT

The ascomycete *Guignardia bidwellii* is an economically important pathogen in many grapevine areas. Primary infections are caused by ascospores and conidia produced in mummified berries and in cane lesions. Secondary infections are caused by the conidia produced by pycnidia formed in leaf lesions and, in later season, in rotted berries. Environment-controlled experiments were conducted to study the production course of *G. bidwellii* conidia on grape leaf lesions as influenced by: (i) repeated washing events; and (ii) alternate dry and wet periods. Under optimal environmental conditions (25°C; 100% relative humidity), production of conidia declined over washings and was almost completely depleted after 4 washings. When pycnidia were incubated under low humidity conditions (i.e., average of 54% relative humidity) between successive washings, the production of conidia progressively diminished as the time at low humidity increased, and few conidia still produced after 87 days under low humidity conditions. This decline was faster at 29°C than at 20°C. This information is relevant in that it determines the potential of black-rot lesions to produce conidia along the grape-growing season and, therefore, their contribution to epidemic development.

Keywords: *Guignardia bidwellii*, sporulation, washing events, pycnidia cohort.

INTRODUCTION

The ascomycete *Guignardia bidwellii* (Ellis) Viala and Ravaz (anamorph: *Phyllosticta ampelicida* (Englem.) van der Aa), the causal agent of black-rot, is an economically important pathogen in some grapevines areas of North America and Europe (Ramsdell and Milholland, 1988; Reddick, 1911; Besselat and Bouchet, 1984; Mauri and Kobel, 1988; Corte, 1975; Rui, 1989) where yield loses can achieve 80% and the vine quality is lowered (Scribner, 1886; Ellis *et al.*, 1986; Ferrin and Ramsdell, 1977; Ferrin and Ramsdell, 1978; Ramsdell and Milholland, 1988; Funt *et al.*, 1990; Magarey *et al.*, 1993). These areas are characterized by mild and moist conditions in spring and early summer, which are conducive for black-rot epidemics (Harms *et al.*, 2005; Jermini and Gessler,

1996). In some Italian vine-growing areas, recrudescence of black-rot epidemics has been observed in recent years (Clabassi, 2000; Rinaldi and Mugnai, 2012; Rossi *et al.*, 2014).

Ascospores and conidia of *G. bidwellii* from rotted, mummified berries and canes are the primary inoculum for the disease (Reddick, 1911; Rousel and Bouard, 1971; Ferrin and Ramsdell, 1977; Becker and Pearson, 1992), causing infections on all green tissues, mainly between bud break and three weeks after full flowering (Kuo and Hoch, 1996; Ullrich *et al.*, 2009; Ferrin and Ramsdell, 1978; Hoffman *et al.*, 2002). These infections become visible as necrotic, circular, tan spots with a dark margin after approximately 1 to 2 weeks of incubation (Spotts, 1980). Pycnidia are produced on these lesions after a latency period, which is very variable in length (Chapter 5), and the conidia serve as inoculum for secondary infection cycles infecting both leaves and clusters (Molitor and Berkelmann-Loehnertz, 2011; EPPO, 2002). Once primary infection has established and pycnidia have formed, conidia produced in great numbers are responsible for rapid disease progression during the growing season (Ferrin and Ramsdell, 1978; Ramsdell and Milholland, 1988).

In spite of the epidemiological relevance of the secondary inoculum, it has received little attention (Rossi *et al.*, 2014) and important aspects regarding the production of pycnidia and conidia still remain unclear. One of these aspects has been recently addressed, exactly the effect of temperature and humidity on production of pycnidia and conidia on black-rot lesions, on the extrusion of cirri, and the duration of the latency period (Chapter 5).

A second aspect is addressed in this paper. Specifically, the objectives of this paper were to study the production course of *G. bidwellii* conidia on grape leaf lesions as influenced by: (i) repeated washing events; and (ii) alternate dry and wet periods. This information is relevant in that it determines the potential of black-rot lesions to produce conidia along the grape-growing season and, therefore, their contribution to epidemic development.

MATERIALS AND METHODS

Fungal material. The *G. bidwellii* strain G1.16 was used, provided by Prof. L. Mungnai of Università degli Studi di Firenze (Italy) and isolated in a vineyard of Colorino located in Quarrata (Tuscany, Italy). The strain was maintained at 5°C in glass tubes (5 ml) containing water-agar (WA; 20 gL^{-1} HIMEDIA, Mumbai, India). For the production of conidia, a small plug of the colonized water-agar was transferred from the glass tubes to Petri plates containing malt extract agar (MEA; 50 gL^{-1} HIMEDIA, Mumbai, India). Plates were incubated for three weeks at 25°C, 12-h photoperiod. Conidial suspensions were then obtained by flooding the plates with 10 ml of sterile distilled water and gently

scrapping the agar surface with a sterile spatula. The resulting suspension was filtered through a double gauze layer and adjusted to 10^4 conidia ml^{-1} with a haemocytometer.

Plant material and artificial inoculations. One year old *Vitis vinifera* plants cv. Barbera, which is susceptible to *G. bidwellii* (Rubboli *et al.*, 2014; Coldiretti 2013), were maintained in a greenhouse at the University campus of Piacenza (Italy). The plants were rooted in plastic pots (10 cm in diameter) containing a mixture of sand, peat moss and soil (20:50:30), and grown at temperatures between 18 and 26°C, 12-h photoperiod (provided by Philips Master Tl-D 90 Deluxe 18 W/950 lamps), until they developed shoots with 4 to 6 unfolded leaves. Shoots were positioned vertically and the adaxial surface of the second, third and fourth unfolded leaves from the shoot apex were inoculated with 10 µL drops of the conidial suspension prepared as described before (3 to 5 drops per leaf). After inoculation, the plants were covered with transparent plastic bags to ensure high humidity, and incubated at 25°C, 12-h photoperiod. After 48 h, the plastic bags were removed and the plants were kept under the same conditions of temperature and photoperiod, with 50 to 60% relative humidity (RH), until the onset of the typical black-rot lesions. Fresh lesions appeared after about 12 days and they did not bear pycnidia yet.

Influence of repeated washing events on production of conidia. Leaf pieces were cut from the leaves, one leaf piece incorporating a single black-rot lesion, disinfected with sodium hypochlorite (2%) for 2 minutes, rinsed with sterile water, and finally dried under a laminar flow. To keep the leaf tissue lying, each leaf piece was laid on a slip of sterile plastic net and then covered with another slip fixed to the previous one with sterile clips, the upper slip bearing a hole slightly larger than the disease lesion. These leaf pieces were then placed in Petri dishes (5 cm in diameter; one leaf piece per dish) containing two sterile blotting papers disks moistened with 1.5 mL of distilled sterile water. The dishes were finally sealed with Parafilm strips (Neenah, WI, USA) (Figure 1) and kept in an incubator at 25°C, 12-h photoperiod and 100% RH, for the whole duration of the experiment. Lesions were carefully observed for checking the formation of first pycnidia, which occurred in 2 days, and first cirri extruding from pycnidia, which occurred in 4 days.

To study the conidial production dynamics, the lesions were washed 7 times at 4, 7, 10, 13, 17, 20, and 24 days after the onset of pycnidia. At each of these timings, individual lesions were photographed, and the total numbers of pycnidia were counted by using Assess 2.0 (Image analysis software for plant diseases quantification, by Lanhdar Lamari, APS PRESS, Saint Paul, Minnesota). After the pictures have been taken, lesions were individually washed 3 times with a total of 0.5 mL of distilled sterile water with the aid of a brush to gently remove all the conidia extruded from the pycnidia. The resulting

suspension was collected in a vial (one vial per lesion) and the conidia were enumerated by using a haemocytometer. Production of conidia per pycnidium was finally determined by dividing the number of conidia washed off from a lesion by the number of pycnidia of that a lesion. The experiment was repeated twice and there were 13 lesions in each repetition.

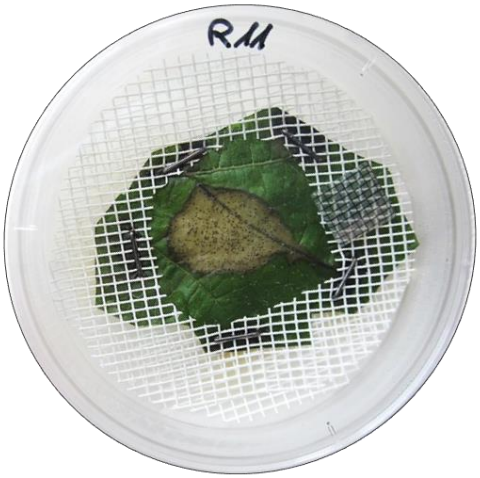

Figure 1. Example of the humid camber used to study the production of *Guignardia bidwellii* conidia in black-rot lesions on grape leaves.

Influence of alternate dry and wet periods on production of conidia. Six Barbera plants managed as previously described until the appearance of black-rot lesions were covered with transparent plastic bags to obtain a saturated atmosphere and kept at 25°C, 12-h photoperiod, for 5 days, to favour production of pycnidia and extrusion of cirri. Afterwards, all the lesions were washed with sterile water with the aid of a brush, as described before. Conidial suspensions of 5 random lesions from each plant were used to enumerate the conidia produced per pycnidium, as previously described. This counting was used as the conidial production at the time zero.

Plants were then split in 2 groups (3 plants per group) and placed in 2 growth chambers. The temperature ranged between 21 and 37°C (average 29°C) in the first growth chamber, and between 18 and 29°C (average 20°C) in the second one; average RH in the two growth chambers was kept at 54±0.2%. After 14, 28, 56, and 87 days of incubation, 5 random lesions were excised from each plant (15 lesions in aggregate) and managed as described in the previous experiment. Briefly, leaf pieces including lesions were: enclosed in the plastic net and arranged in Petri dishes (Figure 1); incubated at

25°C, 12-h photoperiod, 100% RH for 5 days; and finally managed until the determination of the numbers of conidia produced per pycnidium.

Data analysis. The numbers of conidia per pycnidium (x) were transformed by using the natural logarithm function [ln(x + 1)], to make variances uniform. The transformed data were used in an analysis of variance (ANOVA) to determine the effect of the number of washes (from 1 to 7) in the first experiment, and the combined effect low-humidity period length (from 14 to 87 days) and temperature (average of 20 or 29°C) in the second experiment. The Tukey HSD test was used at $P = 0.05$ to separate means.

RESULTS AND DISCUSSION

Influence of repeated washing events on production of conidia.

Production of conidia in *G. bidwellii* leaf lesions was significantly affected by the number of washing events ($P < 0.001$). Conidia production declined over washings and was almost completely depleted after 4 washings. At the first washing, 4 days after the lesion onset, 201.5±21.5 conidia were produced per pycnidium (Figure 2). In the following three washings, the production of conidia significantly diminished by 52, 80, and 88%, respectively. No significant differences were observed between the 5^{th}, 6^{th} and 7^{th} washing, when only 10.2±1.4 conidia were produced per pycnidium (95% reduction) (Figure 2).

Similar results were obtained for other pycnidial fungi. In *Septoria tritici*, conidial production was reduced by 40 to 60% after the first washing and few conidia were produced after the second one (Eyal *et al.*, 1987). In *Botryosphaeria dothiodea*, >90% reduction of conidia was observed between the pycnidia that have been previously irrigated by sprinkler irrigation three times and the pycnidia not subjected to washing by irrigation (Michailides and Morgan, 1993).

Pycnidial formation in *G. bidwellii* goes through different developmental stages. It is initiated by the formation of a primordial within a stroma and the development of a fertile centre, which originates a conidiogenous layer covering the pycnidial cavity. This conidiogenous cells start producing conidia, which accumulates in the cavity until they ooze in a cirrus through the ostiole (Janex-Favre *et al.*, 1993). Afterwards, rain (or sprinkler irrigation) washes off the conidia (Spotts, 1980; Ferrin and Ramsdell, 1978). Based on the results of this work, the capability of the pycnidia to produce conidia continues for some time (till 24 days in this work) and repeated cycles of conidial extrusion through cirri occur, even though the numbers of conidia progressively diminish.

Previous findings showed that the lesions originated by a single infection period continued to produce pycnidia for 2 to 40 days (Chapter 5), and that the *G. bidwellii* conidia were capable of germinating and causing infection for at least 60 days after being

formed (Kuo and Hoch, 1996). Overall, these findings show that the lesions formed by a single infection period continue to produce conidia and actively contribute to the epidemic development for a very long time.

The ability of *G. bidwellii* lesions of producing conidia for long time has been previously observed for the pycnidia formed in the lesions in overwintered canes and in bunch mummies (Becker and Pearson, 1992-1996; Northover, 2008; and chapter 4 of this Thesis), but not for single fresh, leaf lesions. Ferrin and Ramsdell (1978) caught conidia from rainwater runoff from pycnidia-bearing grape leaves immediately after lesions had appeared in the field and during each rainy period throughout the season until harvest. However, differently from the present work, the catching of Ferrin and Ramsdell (1978) did not refer to individual lesions, because the leaves were subjected to repeated infections.

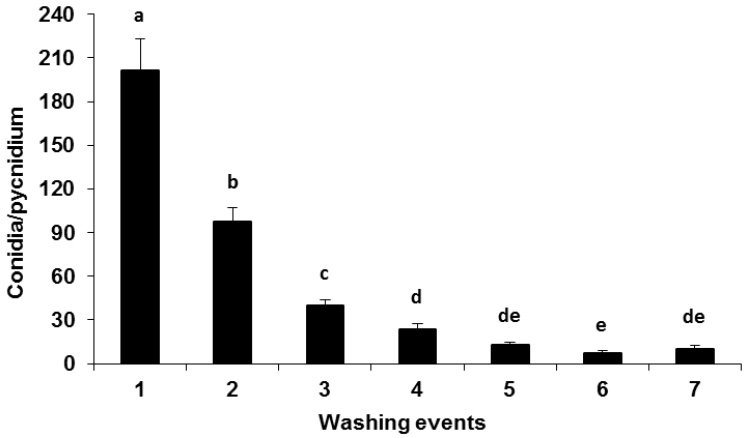

Figure 2. Effect of repeated washing events on the production of *Guignardia bidwellii* conidia in grape leaf lesions. The seven washings were performed at 4, 7, 10, 13, 17, 20 and 24 days after the lesion onset. Lesions were incubated in the humid chambers of Figure 1, at 25°C, in a saturated atmosphere, 12-h photoperiod. Bars show numbers of conidia washed off per pycnidium (average of two experiments, 13 lesions per experiment); whiskers represent the standard error. Values followed by the same letter are not significantly different at the Tukey HSD test at $\alpha = 0.05$.

Influence of alternate dry and wet periods on production of conidia.
Time the pycnidia were kept at approximately 54% RH significantly affected the numbers of conidia extruded by pycnidia in a subsequent wet period ($P<0.001$). Specifically, the production of conidia progressively diminished as the time at low humidity increased, and this reduction was faster when average temperature was 29°C than 20°C (Figure 3). After 87 days at either 20 or 29°C, few numbers of conidia were still produced.

In our knowledge, this is the first evidence of the capability of *G. bidwellii* pycnidia to produce conidia after even long periods with unfavorable conditions. This finding may have relevant implications in the disease epidemiology. Primary infections caused by both ascospores and conidia produced by overwintered fruiting bodies mainly occur in early grape-growing season (Ramsdell and Milholland, 1988), which is usually characterized by warm and moist weather. These conditions are conducive for infection (Spotts, 1977), appearance of black-rot lesions (Molitor and Berkelmann-Loehnertz, 2011; (Hoffman and Wilcox, 2002), production of pycnidia and extrusion of cirri (Chapter 5). Based on the present work, under high humidity conditions, pycnidia repeatedly produce conidia, which may be washed off by rain, so that they can cause secondary infections. This can lead to a rapid increase of the disease in the early grape-growing season (Chapter 3). Under many climate types where the disease develops, summer is characterized by warm and dry conditions, which are unfavorable for the disease development. The ability of the pycnidia of maintaining the capability of producing the conidia even after long periods (till 87 days in the present work) and low humidity (approximately 54% RH in the present work) makes it possible for the fungus to survive dry summer conditions, to recover under next moist conditions, and produce new inoculum that, possibly, originates new infections in the late season. Consistently with that, re-activation of the disease after dry summer periods has been observed in vineyards (Besselat and Bouchet, 1984; Rinaldi and Mugnai, 2012; Hoffman *et al.*, 2004; Ferrin and Ramsdell, 1978).

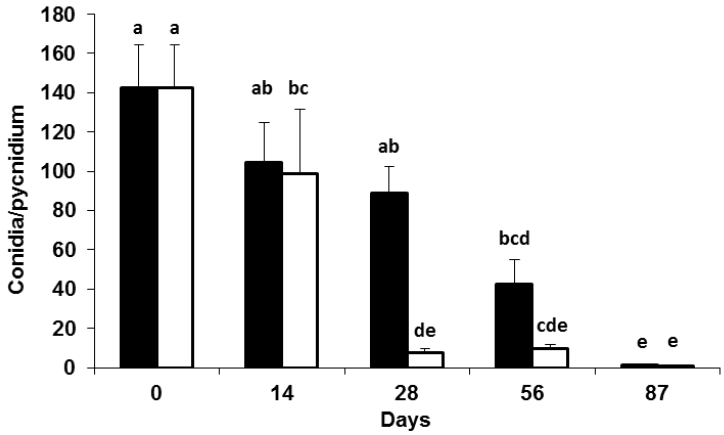

Figure 3. Effect of the time (in days) and temperature on the capability of the lesions to produce *Guignardia bidwellii* conidia. The lesions were incubated at approximately 54% RH, at either 20 (black bars) or 29°C (white bars). Prior the lesions were incubated for 5 days at 25°C, 100%RH, 12-h photoperiod (see Figure 1). Bars represent average of 15 lesions, and whiskers represent the standard error. Values followed by the same letter are not significantly different at the Tukey HSD test at $\alpha = 0.05$.

The new findings from the present work contribute to clarify some relevant aspects of the black-rot epidemiology, specifically: the possibility of the leaf lesions to repeatedly produce conidia under moist conditions, even after a long period at unfavorable, low humidity conditions. In the absence of specific information, the model previously developed (Rossi *et al.*, 2014) assumed that the pycnidia extrude conidia during four consecutive wet periods of at least 4 hours, at approximately equal rates (exactly, 29, 28, 22, and 21% of the conidia are extruded in the 1st to 4th wet period). However, results from the present work indicated that these rates should be modified, being 52, 24, 11, 7 and 4% of the conidia extruded in five washing events. Moreover, a reduction in conidial production rates should be considered when >14 days occur between consecutive washing events.

LITTERATURE CITED

Becker, C.M., Pearson, R., 1996. Black-rot lesions on overwintered canes of Euvitis supply conidia of *Guignardia bidwellii* for primary inoculum in spring. Plant Disease 80, 24–27.

Becker, C.M., Pearson, R.C., 1992. Patterns of spore release from black-rot (*Guignardia bidwellii*) infected grape mummies that overwintered on the ground or in the canopy. Phytopathology 82, 1084.

Besselat, B., Bouchet, J., 1984. Black-rot: situation inquiétante dans certains vignobles. Phytoma - défense des Cultures 33–35.

Clabassi, I., 2000. Black-rot, nouva ampelopatia in Friuli Venezia Giulia. In: L'agenda Del Viticultore. A. Morando, M. Morando, and D. Morando (Eds.), Vitenda 2000. Calosso, pp. 58–60.

Corte, A., 1975. Il marciume nero degli acini o "black-rot" della vite in provincia di La Spezia. Informatore Fitopatologico 8, 15–20.

Ellis, M.A., Madden, L. V, Wilson, L.L., 1986. Electronic grape black-rot predictor for scheduling fungicides with curative activity. Plant Disease 70, 938–940.

EPPO, 2002. EPPO Standards. Good plant protection practice. Bulletin OEPP/EPPO 23, 377.

Eyal, Z., Scharen, A.L., Prescott, J.M., Ginkel, M.V., 1987. The septoria disease of wheat: conceps and methods of disease mangment. CIMMYT, Mexico, D.F. 52pp.

Ferrin, D., Ramsdell, D., 1978. Influence of conidia dispersal and environment on infection of grape by *Guignardia bidwellii*. Phytopathology 68, 892. doi:10.1094/Phyto-68-892

Ferrin, D.M., Ramsdell, D.C., 1978. Influence of conidia dispersal and environment on infection of grape by *Guignardia bidwellii*. Phytopathology 68, 892. doi:10.1094/Phyto-68-892

Ferrin, D.M., Ramsdell, D.C., 1977. Ascospore dispersal and infection of grapes by *Guignardia bidwellii*, the causal agent of grape black-rot disease. Phytopathology 67, 1501–1505.

Funt, R., Ellis, M., Madden, L., 1990. Economic analysis of protectant and disease-forescast-based fungicide spray programs for control of apple scab and grape black-rot in Ohio. Plant Disease 74, 638–642.

Harms, M., Holz, G., Hoffmann, C., Lipps, H., Silvanus, W., 2005. Occurrence of *Guignardia bidwellii*, the causal fungus of black-rot on grapevine, in the vine growing areas of Rhineland-Palatinate, Germany. BCPC Symposium 81, 127–132.

Hoffman, L.E., Wilcox, W.F., 2002. Utilizing epidemiological investigations to optimize management of grape black-rot. Phytopathology 92, 676–680.

Hoffman, L.E., Wilcox, W.F., Gadoury, D.M., Seem, R.C., 2002. Influence of grape

berry age on susceptibility to *Guignardia bidwellii* and Its incubation period length. Phytopathology 92, 1068–76. doi:10.1094/PHYTO.2002.92.10.1068

Hoffman, L.E., Wilcox, W.F., Gadoury, D.M., Seem, R.C., Riegel, D.G., 2004. Integrated control of grape black-rot: influence of host phenology, inoculum availability, sanitation, and spray timing. Phytopathology 94, 641–50. doi:10.1094/PHYTO.2004.94.6.641

Janex-Favre, M.C., Parguey-Leduc, A., Jailloux, F., 1993. The ontogeny of pycnidia of *Guignardia bidwellii* in culture. Mycological Research 97, 1333–1339.

Jermini, M., Gessler, C., 1996. Epidemiology and control of grape black-rot in Southern Switzerland. Plant Disease 322–325.

Kuo, K., Hoch, H., 1996. Germination of *Phyllosticta ampelicida* pycnidiospores: prerequisite of adhesion to the substratum and the relationship of substratum wettability. Fungal Genetics and Biology 20, 18–29.

Kuo, K.C., Hoch, H.C., 1996. The parasitic relationship between *Phyllosticta ampelicida* and *Vitis vinifera*. Mycologia 88, 626–634.

Magarey, R.D., Coffey, B.E., Emmett, R.W., 1993. Anthracnose of grapevines, a review. Plant Protection Quarterly. 8, 106–110.

Mauri, G., Kobel, U., 1988. Black-rot – a new severe grape disease in Ticino. Schweizer Zeitschrift für Obsund Weinbau Wädenswil 124, 473–475.

Michailides, T.J., Morgan, D.P., 1993. Spore release by *Botryosphaeria dothidea* in pistacho orchards and disease control by altering the trajectory angle of sprinklers. Phytopathology 83, 145–152.

Molitor, D., Berkelmann-Loehnertz, B., 2011. Simulating the susceptibility of clusters to grape black-rot infections depending on their phenological development. Crop Protection 30, 1649–1654. doi:10.1016/j.cropro.2011.07.020

Northover, P., 2008. Factors influencing the infection of cultivated grape (*Vitis* spp. section Euvitis) shoot tissue by *Guignardia bidwellii* (Ellis) Viala and Ravaz. The Pennsylvania State University.

Ramsdell, D.C., Milholland, R., 1988. Black-rot. In: Compendium of Grape Diseases. Pearson, R., Goheen, A. (Eds.), APS Press, St. Paul, pp. 15–17.

Reddick, D., 1911. The black-rot disease of grapes. Cornell University Agricultural Experiment Station Bulletin 293, 289-364.

Rinaldi, P.A., Mugnai, L., 2012. Marciume nero degli acini, potenziale pericolo in viticoltura. Inf. Agrar. 15, 68–71.

Rossi, V., Onesti, G., Legler, S.E., 2014. Use of systems analysis to develop plant disease models based on literature data: grape black-rot as a case-study. European Journal of Plant Pathology 141, 427–444. doi:10.1007/s10658-014-0553-z

Rousel, N., Bouard, C., 1971. Black-rot,. In: Pathologie de La Vigne - Maldies Cryptomatiuas, pp. 239–251.

Rubboli, V., Ortugno, C., Coatti, C., Gualco, A., 2014. Dynali, nuovo fungicida a base di cyflufenamid e difenoconazolo per la protezione della vite da oidio e black-rot. Giornate Fitopatologiche. 2, 289–298.

Rui, D., 1989. "Ultimissime" sul black-rot della vite. Informatore Agrario 39, 67–69.

Scribner, F., 1886. Report on the fungus diseases of the grapevine. US Dep. Agric. Bot. Div. Sect. Plant Pathol. Bull. 2 GPO. Washington DC.

Spotts, R.A., 1980. Infection of grape by *Guignardia bidwellii*-factors affecting lesion development, conidial dispersal, and conidial populations on leaves. Phytopathology 70, 252–255.

Spotts, R.A., 1977. Effect of leaf wetness duration and temperature on the infectivity of *Guignardia bidwellii* on grape leaves. Phytopathology 77, 1378. doi:10.1094/Phyto-67-1378

Ullrich, C.I., Kleespies, R.G., Enders, M., Koch, E., 2009. Biology of the black-rot pathogen, *Guignardia bidwellii*, its development in susceptible leaves of grapevine *Vitis vinifera*. Journal Für Kulturflanzen 61, 82–90.

Chapter 7

Chapter 7

CONCLUSIONS

This Thesis covered a comprehensive study of *Guignardia bidwellii* affecting grapevines. In the second chapter, a system analysis of the literature data regarding epidemiology and biology of *G. bidwellii* was performed, and a mechanistic, weather driven model for (i) simulating all the relevant stages of the *G. bidwellii* life cycle and (ii) predicting the development black-rot epidemic was developed (Rossi *et al.*, 2014). A meta-analysis of the published data made it possible the development of mathematical equations operating within the model and describing the system quantitatively and dynamically. Gaps of knowledge were identified and bypassed by making plausible assumptions. In Chapter 2, the model outputs were compared with three typical black-rot epidemics; the model provided a reliable picture of the disease development (Rossi *et al.*, 2014). However, no detailed validation was performed there.

In the third chapter of this Thesis the model was evaluated by comparing model output with real disease development in a vineyard of north Italy, in 2013 to 2015. The disease was assessed on leaves (as lesion number per leaf) and bunches (as disease severity) 2 or 3 times per week between the first leaf unfolded and veraison. Leaf lesions in 2015 were more than 10 times higher than those in 2013 and 2014; the severity on clusters varied from 7% in 2013 to 47% in 2015. Disease assessments were compared with model output; exactly it was verified whether, on each disease assessment date, the model predicted or not the appearance of new disease symptoms. The model showed good accuracy in predicting disease onset; area under the ROC curve was 0.870 for leaves and 0.770 for clusters, and both were significantly >0.5. The probability to provide an unjustified alarm was ≤0.180, while the probability of missing real infections was 0.175 for leaves and 0.263 for bunches. Since in the 78% of these false negative predictions the difference between expected and real disease onset was ±2 days, most of these errors were caused by inaccuracies in calculating the incubation length rather than in predicting infection occurrence. Only one infection period was really missed by the model, which caused the appearance of few new leaf lesions (14 lesions) between end of July 27 and early-August 2013. When used to predict the epidemic development of black-rot, the model provided a slight overestimation of the disease severity, mainly on leaves, when the observed disease severity was >0.6. These discrepancies were likely caused by different patterns of inoculum availability in the considered vineyard compared to those used for model development. It was then concluded that further studies on the dynamics of both primary and secondary inoculum should be therefore useful for improving the model accuracy in predicting infection severity.

The inoculum availability was then studied in Chapters 4 to 6, specifically: (i) the dispersal of *G. bidwellii* ascospores and conidia from overwintered berry mummies

affected by black-rot in relation to weather conditions (Chapter 4); (ii) the effect of the weather variables on the production of pycnidia and cirri on leaf lesions, and on conidial germination (Chapter 5); and (iii) the production course of conidia, as influenced by repeated washing events and dry periods (Chapter 6). Globally, results from the experiments conducted in these chapters greatly increased our knowledge of the *G. bidwellii* inoculum dynamics. Due to the mechanistic structure of the model developed in Chapter 2, these new findings could be easily incorporated into the model. Modifications include:

(i) a threshold of infection severity (>0.001) for predicting the occurrence an infection period, specifically for reducing the probability of unjustified alarms;
(ii) new equations describing the effect of degree-days on the seasonal cumulative numbers of *G. bidwellii* ascospores and conidia produced in the overwintered berry mummies;
(iii) new cut-off values of rain for conidial and ascospore dispersal; specifically, >1 mm and >3 mm rain, respectively;
(iv) new equations describing the production patterns of pycnidia on leaf lesions as affected by time, relative humidity and temperature;
(v) new rates for describing the extrusion of conidia from pycnidia in the presence wet periods; specifically, 52, 24, 11, 7 and 4% of the total conidia produced by a pycnidium cohort are extruded in the first five washing events after pycnidium formation;
(vi) a reduction rate for the production of conidia by pycnidia when >14 days with low relative humidity occur between two consecutive washing events.

The model developed in this Thesis represents an improvement of the previous black-rot forecasters because considers not only infection periods, but also production, dispersal and survival of the inoculum; in addition, the model provides a quantification of the infection risk, while the previous methods only predict whether an infection can occur or not.

The model has proven to be highly accurate and robust in predicting infection periods and dynamics of black-rot epidemics. Possible improvements from the research conducted should contribute to further improve the model performances.

The model can be used for scheduling fungicide sprays in the vineyards. As illustrative information, applying the model output to schedule the application of fungicides in the vineyard of this work would result in 5 treatments in 2013 and 2014, and 4 in 2015; 9, 10 and 8 treatments should have been performed, respectively, by using a calendar-based timing. The model could be integrated into the decision-support system named vite.net (Rossi *et al.*, 2012) that already includes models for downy and powdery mildews. That should make it possible to schedule fungicide applications and to select the

most appropriate fungicides to be used taking into account the risk of the three main diseases at the same time.

Candidate’s pubblication

Candidate's pubblication

Onesti G., Legler S.E., Caffi T., Rossi V., 2013. A model for black-rot disease on grapevine. Proceedings of the 11th International Epidemiology Workshop, Beijing (China), August 22-25, pag.12.

Onesti G., Legler S.E., Caffi T., Rossi V., 2013. Systematic literature review for modeling black-rot disease of grapevine. Atti XIX Convegno Nazionale SIPAV, Padova, 23-25 settembre. In: Journal of Plant Pathology, 95, (4 suppl.), S4.55 (Poster).

Onesti G., Caffi T., Legler S.E., Rossi V., 2014. Un nuovo modello per il black-rot della vite, in: ATTI Giornate Fitopatologiche - Vol 1. pp. 501-508.

Rossi V., Onesti G., Legler S.E., Caffi T., 2015. Use of system analysis to develop plant disease models based on literature data: grape black-rot as a case-study. *European Journal of Plant Pathology* 141: 427–444. doi:10.1007/s10658-014-0553-z

Acknowledgements

Acknowledgements

Seems yesterday when I started this experience…but today are already past three years, and I have acquired a new great experience in the fitopathology field!!

Fisrt of all, I want thanks my advisor Prof. Vittorio Rossi, whose gave me the possibility to carried out the doctorate school. Thanks for the support, guidance, trust and for made the work of this Thesis very successful. I'm very grateful for the opportunity and his help in each step of this three doctorate years.

I am really grateful to Levente Kiss, Áron Horvát and his beautiful family, Zsolt Bereczky and all the colleagues of the Plant Protection Institute, Centre for Agricultural Research of the Hungarian Academy of Sciences. Thanks for hosting me in my research abroad experience, for the kind hospitality and for the life experience in Budapest!

Deepest gratitude is for Elisa González-Domínguez for her infinity patience, willingness and huge help in the data analysis, support and writing of the Thesis. Many thanks to Valentina Manstretta for her big patience, kindness and help both in office, laboratory and field during this three years. Them contribution to this Thesis has been essential.

Many thanks to the pathology team and colleagues for the help and support along these trhee years.

I am grateful to Prof. Nedeljko Latinovic (University of Montenegro Faculty of Biotechnology) and Prof. Isidre Llorente (Departament d'Enginyeria Química, Agrària I Tecnologia Agroalimentària Institut de Tecnologia Agroalimentària, Universitat de Girona) for accepting to review this Thesis and for providing valuable comments and suggestions, and also thanks to the members of the examiners board.

I am very grateful also to the Peoples who believed and supported me along this three years of doctorate school and were important for me and so for the realization of of this Thesis.

…finally thanks to this doctorate experience because thanks to its I met a lot of excellent people that now are my big, respectable friends and improved my little life!!

Piacenza, 17 March 2016